5-2019

By Proxy: A Radiocarbon Perspective on Prehistoric Mobility Using Summed Probability Distributions and Paleoenvironmental Reconstructions in Wyoming and Montana

Anastasia M. Lugo Mendez
Utah State University

BY PROXY: A RADIOCARBON PERSPECTIVE ON PREHISTORIC MOBILITY USING SUMMED PROBABILITY DISTRIBUTIONS AND PALEOENVIRONMENTAL RECONSTRUCTIONS IN WYOMING AND MONTANA

by

Anastasia M. Lugo Mendez

A thesis submitted in partial fulfillment
of the requirements for the degree

of

MASTER OF SCIENCE

in

Anthropology

Approved:

_____	_____
Judson Byrd Finley, Ph.D. Major Professor	Patricia Lambert, Ph.D. Committee Member
_____	_____
Molly Cannon, Ph.D. Committee Member	Richard S. Inouye, Ph.D. Vice Provost for Graduate Studies

UTAH STATE UNIVERSITY
Logan, Utah

2019

ABSTRACT

By Proxy: A Radiocarbon Perspective on Prehistoric Mobility Using Summed Probability Distributions and Paleoenvironmental Reconstructions in Wyoming and Montana

by

Anastasia M. Lugo Mendez

Utah State University, 2019

Major Professor: Dr. Judson Byrd Finley
Department: Sociology, Social Work, and Anthropology

Stone circles are among the most common and understudied archaeological features in the Rocky Mountains and High Plains. Their ubiquity coupled with increased archaeological research accompanying oil and natural gas exploration in the region has expanded the availability and size of the region's radiocarbon database. The dates as data approach uses radiocarbon ages as variables from a larger sample. This thesis compiles radiocarbon ages associated with tipi ring sites in Wyoming and Montana and creates a summed probability distribution from these ages to serve as a proxy for prehistoric mobility. The distribution is corrected for taphonomic bias and compared to two paleoenvironmental proxies from northwestern Wyoming lakes to determine whether prehistoric mobility meets the expectations of the patch choice model. Running correlation windows provide statistical

comparisons between datasets. Despite weak significant correlations between the overall mobility proxy and the paleoenvironmental reconstructions, no statistically significant correlations were identified at 150- or 200-year scales. Moderate strength correlations between the environmental data and mobility proxy when mobility is lagged suggest a delayed relationship between the datasets. Future research must include expanding the radiocarbon database and obtaining finer-scale paleoenvironmental reconstructions.

(129 pages)

PUBLIC ABSTRACT

By Proxy: A Radiocarbon Perspective on Prehistoric Mobility Using Summed Probability Distributions and Paleoenvironmental Reconstructions in Wyoming and Montana

Anastasia M. Lugo Mendez

Stone circles are among the most common and understudied archaeological features in the Rocky Mountains and High Plains. Their widespread availability coupled with increased archaeological research accompanying oil and natural gas exploration in the region has expanded the availability and size of the region's radiocarbon database. The dates as data approach uses radiocarbon ages as variables from a larger sample. This thesis compiles radiocarbon ages associated with tipi ring sites in Wyoming and Montana and creates a summed probability distribution from these ages to serve as a proxy for prehistoric mobility. The distribution is corrected for taphonomic bias, or data loss, and compared to two paleoenvironmental proxies from northwestern Wyoming lakes to determine whether prehistoric mobility meets the expectations of the patch choice model. Running correlation windows provide statistical comparisons between datasets. Although a weak statistical relationship is apparent between mobility and the paleoenvironmental reconstructions over the 5000-year study period, no statistically significant correlations were identified at 150- or 200-year scales. Moderate strength correlations between the environmental data and mobility proxy when mobility is lagged suggest a delayed relationship between the datasets. Future

research must include expanding the radiocarbon database and obtaining finer-scale paleoenvironmental reconstructions.

ACKNOWLEDGMENTS

To begin, I would like to thank Dr. Judson Finley who suggested this project and introduced me to the vast possibilities of tipi ring research and the promising applications of temporal frequency distributions. I am also grateful to Drs. Patricia Lambert and Molly Cannon for joining my supervisory committee and contributing their insight and expertise.

I would also like to thank Ross Hillman at the Wyoming State Historic Preservation Office and Damon Murdo at the Montana State Historic Preservation Office for their assistance in obtaining site records and radiocarbon ages from their respective state archives. This research would not have been possible without access to these repositories, a rich vein of data waiting to be mined.

My extended cohort and adopted USU family supported and sustained me throughout this process. They listened to my concerns, provided advice, allayed my fears, and pointed out the finish line when I couldn’t see it myself. I would not have made it this far alone.

Finally, an indelible gratitude to my friends and my family.

Anastasia M. Lugo Mendez

CONTENTS

LIST OF TABLES

LIST OF FIGURES

CHAPTER ONE:

INTRODUCTION

Tipi rings are among the most common and understudied archaeological features in the Rocky Mountains and High Plains (Banks and Snortland 1995; Frison 1983; Malouf 1961). As the remains of nomadic hunter-gatherer habitations (Kehoe 1958), they represent valuable evidence of ancient mobility patterns and domestic activities. In spite of their ubiquity (Frison 1983), tipi rings are rarely the focus of sustained or large-scale study (Davis 1983; Finnigan 1983; Gragson 1983). The paucity of associated material remains and excavation difficulties has resulted in a resounding silence regarding archaeological interpretations. In the last three decades, only a handful of researchers have studied tipi rings, although the available literature considers a breadth of subjects such as the social, symbolic, and monumental importance of tipi rings on the landscape (Oetelaar 2000; Scheiber and Finley 2009; Zedeño et al. 2014). In the proper context, tipi rings and their dated associated features allow archaeologists to question prehistoric behaviors that have so far gone unexplored, including considerations of gendered, symbolic, and quotidian use of domestic space (Banks and Snortland 1995; Oetelaar 2000; Scheiber and Finley 2009), development of hunter-gatherer persistent places and monumental landscapes (Dooley 2004; Zedeño et al. 2014) or, as in this this study, relationships between mobility and climatic variability.

Identifying these relationships requires a proxy for mobility. Using tipi ring sites in Wyoming and Montana as indicators of past mobility events, I use radiocarbon samples associated with these features to construct a database. This database allows for general analysis of tipi ring site characteristics and research patterns in the region. It also serves as the foundation for a summed probability distribution (SPD) that approximates continuous

prehistoric mobility trends. Taking into account SPD practices and critiques (Contreras and Meadows 2014; Shennan 2013; Williams 2012), I apply techniques that address overrepresentation and taphonomic bias in the distribution. Results indicate that neither overrepresentation nor taphonomic bias have strong effects on the tipi ring site SPD. I create artificial datasets and their summed probability distributions, as well as moving averages of the SPD, to assess calibration curve effects (Armit et al. 2013; French and Collins 2015:126, Zahid et al. 2016).

Comparisons of the tipi ring site SPD and a larger radiocarbon dataset obtained from the Canadian Archaeological Radiocarbon Record (Martindale et al. 2017) indicate that these are statistically distinct. With this assurance and necessary corrections applied, I can use the tipi ring site SPD as a proxy for prehistoric hunter-gatherer mobility to address the problem of how continuous climatic variability affects prehistoric mobility in the Rocky Mountains and adjacent High Plains.

I establish my predictions using the patch choice model and the marginal value theorem (Bird and O'Connell 2006; Charnov 1976; Kelly 1995:90), positing greater hunter-gatherer mobility along with improved patch density resulting from increasing moisture. I array the tipi ring site SPD against paleoclimatic reconstructions of temperature and moisture deficits obtained from northwestern Wyoming lakes (Shuman et al. 2010; Shuman 2012). I test my expectations using 150- and 200-year interval sliding correlation windows, as well as bootstrapped Pearson's correlations for the 5000-year study period. I also run the sliding correlation windows at 50- and 100-year lags.

Weak but significant correlations were identified between the tipi ring site SPD, temperature, and moisture deficit. These correlations remain consistent within bootstrapped

confidence intervals when the tipi ring site SPD was lagged 50 years against moisture deficit, and 100 years against temperature, suggesting that the mechanisms at play do not have immediate effects. Despite indications of a relationship at the 5000-year scale, significant correlations could not be identified within the finer-scale 150- and 200-year intervals at the appropriate α value. When the α value is increased, seven significant periods are identified between the tipi ring site SPD and temperature. However, there is no apparent underlying relationship between these.

The coarse-grained correlations between mobility and past temperature and moisture provide a jumping off point for additional study. Future research must expand the tipi ring site radiocarbon database, obtain additional proxy records, and refine the paleoenvironmental reconstructions such that fine-grained analyses may be attempted. Such studies may bring to bear an understudied aspect of the archaeological record to more nuanced understandings of human response to climate variability. These results may broaden our understanding of the effect of climatic variability on prehistoric peoples using data from cultural resource management studies in a research-oriented context. Clarifying and encouraging a better understanding of the archaeological value of tipi rings will ensure that one of the region's dominant archaeological features receives greater attention and consideration from cultural resource management practitioners who produce the lion's share of regional archaeological research.

CHAPTER TWO:

BACKGROUND

Tipi rings, or stone circles, represent the remains of nomadic hunter-gatherer houses (Banks and Snortland 1995), in which the stones were once anchors for canvas or skin lodges (Kehoe 1958). Tipi rings have a 5,000-year history in the Rocky Mountains and High Plains and represent one of the most visible regional archaeological features (Banks and Snortland 1995:126; Brasser 1983; Frison 1983; Loendorf 1970). Tipi rings first appear in the Middle Plains Archaic period, between 4500 and 500 years ago, becoming widespread in the Late Plains Archaic Period, between 2000 B.C. and A.D. 500, simultaneous with the rising importance of buffalo jumps (Frison 1991:21; Loendorf 1970;vVan West 1979).

Archaeological sites may have a single tipi ring or as many as hundreds, and ethnographic records indicate that on average tipis housed six to seven family members (Good and Loendorf 1974:120). Tipi rings may differ in size due to a camp's season, function, age, and the ethnicity of its inhabitants (Mobley 1983:106). They have been classified as single and multiple course, a variable thought to reflect season of occupation, and are characterized as containing limited artifacts and being located in favorable camping areas (Kehoe 1958; Malouf 1961). They occur in various ecozones and elevations, which are thought to reflect differences in use and seasonality (Loendorf 1974). Although ubiquitous, they have not been subject to much small- or large-scale research because of the dearth of material culture within the rings (Davis 1983; Finnigan 1983; Gragson 1983).

The challenges tipi rings present to researchers, such as their difficulty to date, the probability that stones from rings may have been reused and moved, and an inability to

distinguish whether multiple rings represent multiple occupations, have presented further obstacles to their study (Malouf 1961; Mobley 1983). Despite these purported setbacks, contemporary researchers have begun to ask questions of tipi rings that do not rely solely on lithic or zoological cultural remains, using these features to explore gender, symbolism, the use of domestic space, and hunter-gatherer construction of and mobility across monumental landscapes (Banks and Snortland 1995; Dooley 2004; Oetelaar 2000; Scheiber and Finley 2010; Zedeño et al. 2014). In this paper, mobility provides the framework for the study of tipi rings.

Mobility has long been acknowledged as a defining characteristic of hunter-gatherer lifeways, which has influenced researchers to study the link between mobility and the environment (Kelly 1995:111). Although researchers such as Beardsley et al. (1956) and Murdock (1967) developed mobility classifications, Binford's (1980) processualist system of residential and logistical mobility has endured as the fundamental framework. Binford's (1980) system classifies subsistence groups as foragers and collectors who practice residential and logistical mobility, respectively. Foragers exploit resource patches, gathering food daily, and returning to camp at night. They present high residential mobility, limited bulk procurement, and daily foraging strategies. Binford (1980) predicted that site variability will result from changes in seasonality and site occupation duration. In contrast, he noted that collectors store food and organize food-procurement task groups. Binford (1980) identified these subsistence strategies as mapping on and logistic systems, and expected more complexity in groups using both systems. Binford (1980) compared degrees of residential mobility and environmental variability, and found that foragers are the most mobile in areas of greatest and lowest production. He posited that logistical mobility will have greater importance with greater

seasonal temperature variability. Similarly, as mobility restrictions increase logistical organization must increase. Binford (1980) concluded that logistical and residential variability represent organizational alternatives, not opposing concepts.

The density and distance between various important resources influence residential and logistical mobility patterns (Binford 1980:13), and these environmental conditions have served as the basis for the development of the marginal value theorem and the patch choice model (Bird and O'Connell 2006; Charnov 1976; Kelly 1995:90). The patch choice model centers on resource distribution and hinges on a forager's decision to move from a patch or continue to exploit it (Charnov 1976). Foragers must consider not only the availability and density of resources available in each patch, but also take into account their travel time to and from or between the patch they are at and the next one (Bird and O'Connell 2006:147; Charnov 1976; Kelly 1995). The marginal value theorem (MVT) predicts that when the return rate for a particular patch falls below the average return rate for the region, with the cost of traveling to a new patch factored in, foragers will move on to another patch (Charnov 1976; Kelly 1995:91). The MVT also requires that patches be distributed homogenously across the landscape and that foragers have a precise knowledge of all patches and their productivity. As Binford (1980) predicted, environmental conditions affect mobility and foragers in highly patchy but dense environments may respond by increasing their residential mobility as they exploit new patches, or, in contexts of extreme patchiness and low density, rely on logistical mobility to meet their subsistence needs.

Predictions regarding hunter-gatherer mobility patterns based on the theoretical framework of the patch choice model and MVT may be adapted to archaeological sites comprising tipi rings. As the remains of nomadic hunter-gatherer homes, I expect that the

location and duration of tipi ring camps were influenced by local environmental conditions. Under favorable environmental conditions, in which resource patches would be resource-rich and dense on the landscape, I predict that hunter-gatherers would increase movement between patches and increase the number of tipi rings on the archaeological landscape. Conversely, under environmental conditions that result in greater travel time between patches and select for longer stays at resource patches, traces of tipi ring sites should decrease as communities spend longer periods in these structures. It follows that during periods of increasing precipitation and resource density, I expect hunter-gatherer mobility in this region to increase, while during periods of decreasing precipitation and increasingly scattered resources, I expect hunter-gatherer mobility to decrease. Changes in hunter-gatherer mobility should directly affect cultural carbon frequencies, which radiocarbon dating allows us to translate into a temporal frequency record. I propose to test this hypothesis by searching out chronological patterns in tipi ring site frequency on the landscape, and in particular to search for correlations between these data and periods of wetter and drier conditions as documented in a regional record of Holocene precipitation.

The Northwestern Plains have evidence of human occupation for the last 13,000 years (Loendorf 1970). Frison's (1991:20) chronology, widely used today, established the Paleoindian period (10,000-6,000 BC); the Early (6,000-3,000 BC), Middle (3,000-1,000 BC) and Late Plains Archaic (1,000 BC to AD 0) periods; and Late Prehistoric period (A.D. 0-1800). The Northwestern Plains area has prehistorically and historically served as territory for the Crow, the Shoshoni-Comanche, the Kiowa, Blackfeet, and Cheyenne tribes and their ancestors (Loendorf 1969).

The study area extends over the entirety of Wyoming and one Montana county, Bighorn County, covering slightly over 100,000 mi^2 (Figure 1).

Figure 1. Map of study area.

CHAPTER THREE:

METHODS

In this study I test whether a relationship exists between tipi ring site frequencies and climatic variability, identified as periods of increased or decreased temperature and/or precipitation, by comparing a radiocarbon summed probability distribution to paleoenvironmental reconstructions. My primary datasets are a database of tipi ring site radiocarbon ages from the northwestern High Plains of Wyoming and Montana, a database of general archaeological radiocarbon ages from Wyoming and Montana obtained from the Canadian Archaeological Radiocarbon Record (Martindale et al. 2017), an environmental reconstruction from Lake of the Woods, Wyoming (Shuman et al. 2010a), and an environmental reconstruction from Yellowstone National Park and the Bighorn Mountains (Shuman 2012). I constructed the tipi ring site radiocarbon database from site records obtained from the Montana and Wyoming SHPOs, with the goal of creating a summed probability distribution from this database. In this section, I detail the databases and reconstructions used, explain the analyses in which these data are used, and identify and address constraints and uncertainties associated with each step.

The Datasets

This study uses two radiocarbon datasets and two paleoenvironmental reconstructions. The primary radiocarbon dataset consists of 313 radiocarbon ages obtained from the State

Historic Preservation Office (SHPO) records from Wyoming and Montana. For both Wyoming and Montana, I started with a list of tipi ring sites with radiocarbon ages provided by researchers at their respective SHPOs. I obtained site records for each listed site and collected reported radiocarbon ages from these records, as well as a variety of other site and contextual parameters. These include the date of the latest site visit, the site's geographic coordinates and elevation, the site's county, whether the site is multicomponent, any assigned cultural temporal period, the site type, the site's National Register eligibility, the presence and number of identified stone circles on site, whether the radiocarbon sample was obtained from a feature on site, the sample's analysis date and identifying information, and the sample's material and provenience. Not all parameters were available for each radiocarbon age.

Inclusion of reported ages in the database followed the chronometric hygiene guidelines and examples of other modern studies using large radiocarbon databases (Brown 2015; Naudinot et al. 2014; Williams 2012). At a minimum, radiocarbon ages included in the database must have a reported standard error ≤200 years, an association with tipi rings, and an age range between 5000 BP-100 BP. In general, the standard error may fluctuate depending on the sample size, following standards outlined in Williams (2012:581, Table 1), although other researchers have chosen arbitrary standard errors to maintain as large a sample size as possible (Naudinot et al. 2014:580). The decision to limit standard errors in this database to 200 years was arbitrary, but informed by Williams (2012).

After removal of any radiocarbon ages older than 5000 BP and younger than 100 BP, 313 radiocarbon ages remain, with an average standard error of 68.6 years. Williams (2012) states that any study using 200-500 samples should be considered provisional. However, Contreras and Meadows (2014:602) point out that data density is also critical, identifying

average data densities of 0.5-1.5 dates/year in many studies, decreasing to 0.1 dates/year when geographic divisions are removed. The resulting data density for this study is 0.6 samples/year, which is on the high end of average for similar studies, many of which cover much longer time periods than addressed in this study (Bradtmoller et al 2012; French and Collins 2015; Muscio and Lopez 2016; Zahid et al. 2016).

Table 1. Rejection Criteria Identified by Williams (2012)

Sample Size	Standard Error	Date Range
n = 200	≤ 115 years	≤ 5000 years B.P.
n = 500	≤ 170 years	≤ 5000 years B.P.

The secondary dataset consists of radiocarbon ages reported to the Canadian Archaeological Radiocarbon Database (Martindale et al. 2017). All available data for Montana and Wyoming were downloaded, producing 455 and 2567 ages, respectively. These were filtered using the same standards as the tipi ring site database, removing any ages younger than 100 years, older than 5000 years BP, or with standard errors greater than 200 years. This resulted in 2246 radiocarbon ages representing, in theory, a sample of all cultural radiocarbon activity in Montana and Wyoming.

The first paleoenvironmental reconstruction used was obtained from Shuman et al. (2010), in which the authors analyzed past sediment deposition at Lake of the Woods, Wyoming, using sediment cores and ground-penetrating radar to identity past shoreline

elevations. Sediment packets were temporally bracketed by radiocarbon analyses of sedimentary charcoal. Analyses of sedimentary deposition over time allowed Shuman et al. (2010) to estimate past precipitation and evapotranspiration rates, creating a temporal series measuring moisture deficits in the past.

The second paleoenvironmental reconstruction used was obtained from Shuman (2012). In this study the author used fossil pollen data from the North American Pollen Database for Yellowstone National Park and the Bighorn Mountains to create a temperature reconstruction for the past 15,000 years in Wyoming. Shuman (2012) created a temporal series measuring temperature deviating from the historic mean.

Both the Shuman et al. (2010) and Shuman (2012) reconstructions were used effectively by Kelly et al. (2013) in their study of population change in the Rocky Mountains, in which the reconstructions were compared to a radiocarbon summed probability distribution. These reconstructions will be similarly compared to a summed probability distribution calculated using the radiocarbon database that I assembled here.

Summed Probability Distributions

Summed probability distribution (SPD) models have recently emerged as a popular tool for analyzing trends in large radiocarbon age samples (Kerr and McCormick 2014; Rick 1987; Williams 2012; Zahid et al. 2016), although critics have identified multiple sources of bias in this method, ranging from data to interpretation (Bamforth and Grund 2012; Contreras and Meadows 2014). Nevertheless, the widespread use of radiocarbon dating within archaeology opens the door to new statistical analyses (Bronk Ramsey 2009:337), which when used with acknowledgement of and consideration for constraints and biases, provide a powerful avenue

for archaeological research. In this research, I use SPDs and paleoenvironmental reconstructions to answer questions about prehistoric hunter-gatherer mobility in the western Rockies and northern Plains.

The foundation for SPDs arose when Rick (1987) first advocated for the use of dates as data, suggesting that dates interpreted as a population could reveal regional human behavioral patterns. Rick (1987:55) used radiocarbon ages, but noted any dating method could be used in the same manner, and posited an explicit relationship between surviving radiocarbon ages and occupation.

SPD models are constructed from a series of single radiocarbon ages representing a self-dated event or activity. These represent the measurement of an isotope ratio interpreted through a calibration curve that results in probability density functions with non-normal distributions (Bronk Ramsey 2009:337). Each year of the non-normal calibrated radiocarbon-age distribution is assigned a value totaling 1.0 for that particular age. When multiple radiocarbon ages are combined, these individual ages are summed in bins for the full range of the sample sequence. Peaks in the distribution reflect greater representations in calibrated ages for that event, while troughs reflect decreased frequencies. This approach pools data as though radiocarbon samples from different sources are all part of the same temporal sequence, whether this is for a single site or an entire region (Cobb et al. 2015; Kerr and McCormick 2014:494). The result is a continuous time-series that can be independently correlated with other datasets like artifact frequencies or climate variables (Bradtmöller et al. 2012; Bronk Ramsey 2009; Riede and Edinborough 2012; Tallavaara et al. 2010; Zahid et al. 2016).

Recent research has used radiocarbon samples as proxies for demographic information (Bamforth and Grund 2012:1769; Kelly et al. 2013; Riede and Edinborough 2012; Shennan

2013; Tallavaara et al. 2010; Zahid et al. 2016). Rick (1987:56) emphasizes that this method provides information regarding *occupation magnitude,* not population size. Current research applying summed probability distributions to radiocarbon ages considers peaks and troughs in the distribution as instances of population highs and lows (Bamforth and Grund 2012:1769; Collard et al. 2010; Shennan 2013:757), although other factors may influence the shape of the SPD (Bamforth and Grund 2012; Contreras and Meadows 2014:592). Mobility patterns have been identified by some researchers as an alternate factor in studies focused on demographic change—although their purported role varies from a source of bias to an alternate hypothesis (Crombé and Robinson 2014; French and Collins 2015; Naudinot et al. 2014; Tallavaara et al. 2010).

Research has found that the ideal sample size for SPDs is linked to the mean of the standard deviations and the time span represented by the samples (Contreras and Meadows 2014; Williams 2012). Variability in SPDs has also been found to decrease significantly once a dataset has at least 200 to 500 samples (Williams 2012), although this is dependent on the sample time span, error, and age, since the calibration curve changes over time (Contreras and Meadows 2014). Dates as data is considered an ideal application in the context of a regional study of large-scale processes where typical material culture data are absent (Rick 1987:72), which is the exact context for this study.

In this study, I use Wyoming and Montana radiocarbon ages to create a summed probability distribution that examines the temporal frequency of tipi ring sites on the landscape. This SPD provides a landscape-scale perspective that strips out site-level variability (Williams 2012). I use Oxcal 4.2 to create summed probability distributions that are binned in single- and fifty-year intervals. These data are plotted to visualize the resulting probability of the frequency

of tipi ring sites on the landscape over time. Researchers advise that the calibration effects associated with radiocarbon samples be accounted for when creating summed probability distributions, which are necessary to ensure that the patterns in the distribution reflect changes in human behavior rather than sources of bias such as the calibration curve, research intensity, taphonomic loss, and deposition bias (Bamforth and Grund 2012; Contreras and Meadows 2014; Holdaway et al. 2008). The constraints of summed probability distributions also require that I consider sample size and representation within my database, as well as test and correct, where possible, the effects of the calibration curve and taphonomic loss (Bamforth and Grund 2012; Contreras and Meadows 2014; Surovell and Brantingham 2007; Surovell et al. 2009; Williams 2012).

Constraints and Biases

Due to their nature, SPDs cannot be separated from the biases and constraints of their individual dates (Kerr and McCormick 2014:493). Critical consideration and full acknowledgement of these quirks and idiosyncrasies, of limitations and sources of bias are necessary at each step of this endeavor. Williams (2012) notes five primary issues when constructing SPDs: intra-site sampling, sample size, calibration effects, taphonomic loss, and comparisons with other proxies. Crombé and Robinson (2014:565) add the caution that research intensity, research scale, archaeological feature density, and site taphonomy should also be considered. Based on the suggestions of these and other researchers (Naudinot et al. 2014), I address five broad issues relevant to this research: radiocarbon biases, research-

associated biases, taphonomic bias, calibration curve biases, and issues with proxy comparisons. Sources of uncertainty are outlined in Figure 2.

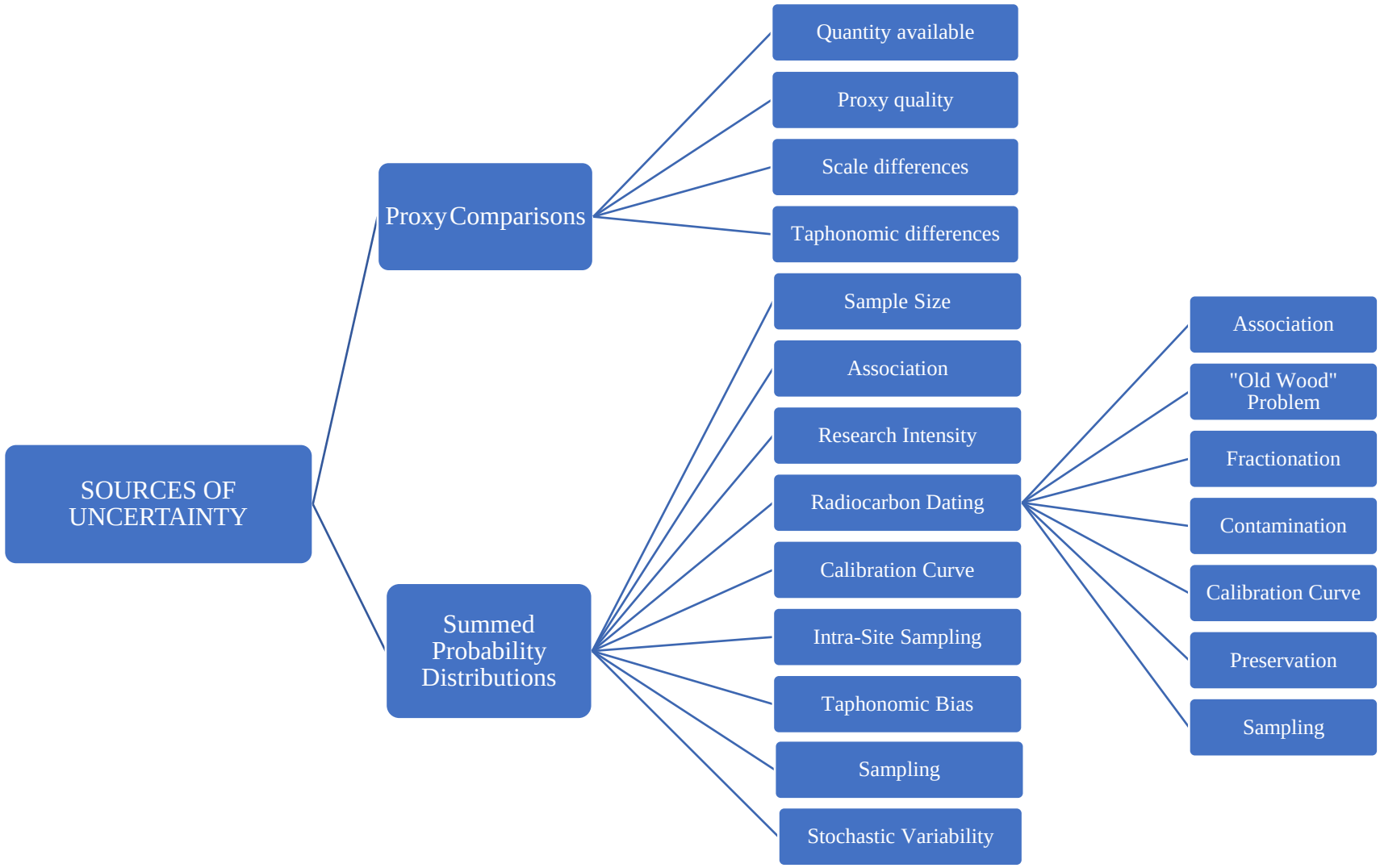

Figure 2. Sources of uncertainty

Radiocarbon Biases. In order to create a reliable database it is critical to consider the shortcomings and constraints of radiocarbon dating, as any analysis dependent on radiocarbon dates will be affected in turn by radiocarbon dating's inherent drawbacks (Bronk Ramsey 2009:358). I outline below the various sources of bias and uncertainty associated with radiocarbon dating, radiocarbon dating in archaeology, and radiocarbon summed probability distributions, along with the steps I will take to correct these issues, where possible.

Radiocarbon dating is a well-established practice common across scientific disciplines and one that is preferred within archaeology due to its relatively low cost and the widespread availability of cultural carbon at archaeological sites. When treating radiocarbon ages as a data class, it is important to note the potential sources of bias and issues associated with the radiocarbon dating process (Rick 1987), as these are magnified when compiling a radiocarbon database. Radiocarbon samples are differentially affected by preservation contamination, fractionation issues, reservoir effects, calibration effects, the "old wood" problem, in which the dated radiocarbon is not related to the context with which researchers associate it, and errors and discrepancies introduced by different laboratory processes and standards (Bronk Ramsey 2008; Waterbolk 1971).

The most critical question surrounding radiocarbon dating was raised by Waterbolk (1971) and has since been echoed by Bronk Ramsay (2008) and other archaeologists working with radiocarbon databases: namely, is the radiocarbon sample associated with the archaeological event in question? In this case, is the radiocarbon sample reflective of past tipi ring habitation events? I have evaluated the radiocarbon samples included in this database for association with tipi rings and cultural origins. In this study, this means that for each radiocarbon age I have noted its provenience within a site and its link to the feature, whether

direct or indirect. Cultural origins are considered confirmed for samples located within hearths, ovens, charcoal features within tipi rings, and other cultural features such as burial mounds or culturally-modified bone. Tipi ring association is considered direct for samples located within a tipi ring, generally in a hearth. However, most radiocarbon dates included in my sample have neither confirmed cultural origins nor a direct association with tipi rings.

In order to maintain the recommended sample size within the database, individual radiocarbon ages were only excluded if the site reports from which they were obtained expressed doubts about their viability or if the ages were in direct contradiction with material culture found within the same site. Constructing a sizable database that met provenience criteria, particularly when the site records I used often failed to specify sample origins, was simply not possible within the scope of this project. A future search of archaeological site records may obtain greater detail regarding radiocarbon sample materials and origins, allowing for better agreement between dated events and target events in the future.

Researchers must, but do not always, account for the aforementioned issues in their reports. It is an unfortunate but unavoidable fact that when compiling a radiocarbon database many of the included ages will have one or several of these problems. It is generally acknowledged that increasing sample size will minimize many of these effects (Smith 2016; Timpson et al. 2015:201; Williams 2012).

Research Biases. Radiocarbon databases are subject to additional issues arising from archaeological practice. These issues include sample size, sampling practice, and research intensity (Contreras and Meadows 2014; Williams 2012). These must be accounted for when attempting to analyze radiocarbon populations (Rick 1987:58).

Radiocarbon samples chosen for analysis, and available for compilation within archaeological literature, are the result of research intensity and sampling practices. Fluctuations in research intensity arise not only from differing research interests, but also from varying archaeological visibility, available datable materials, funding, and preservation (Contreras and Meadows 2014; French and Collins 2015; Kerr and McCormick 2014:494). Researchers are less likely to radiocarbon date more recent sites, as other diagnostic measures are available, leading to their underrepresentation within the radiocarbon record. Sites that are better preserved and visible on the landscape are more likely to be excavated, and in more recent decades, sites located in the path of oil and gas exploration may have produced more radiocarbon ages.

Researchers may also give preference to materials such as charcoal, which results in erasure of ages resulting from bone and other organic materials that may be more easily linked to cultural behaviors (French and Collins 2015). Certain archaeological sites may be revisited numerous times, or have a budget that allows for numerous radiocarbon assays, leading to overrepresentation of some sites over others. Thus, radiocarbon ages reported in academic and gray literature are neither geographically nor temporally representative samples of the underlying radiocarbon population.

Due to these biases, a one-to-one relationship between occupation events and dated radiocarbon tipi ring sites does not exist (Rick 1987:57). The assumption that radiocarbon data provides a representative sample across all archaeological periods is defined as cumulative archaeological pressure by French and Collins (2015:125). However, prehistoric practice and occupation trends need not have a linear relationship with cultural carbon produced (Rick

1987), which may result in the overrepresentation of a given time period within the radiocarbon population, with no actual correlation to past population size or mobility patterns.

Various methods are available to correct for the overrepresentation of radiocarbon samples in a site or site phase (Collard et al. 2010:867; French and Collins 2015:126; Kerr and McCormick 2014; Naudinot et al. 2014:580; Shennan 2013:301). Despite this, the inherent difficulty in distinguishing separate occupations at tipi ring sites (Dooley 2004:107) presents a complicating factor for consideration. In this study, radiocarbon samples are interpreted as resulting from independent occupations unless there is temporal overlap between dates or compelling provenience or depositional reasons to suspect radiocarbon samples originated during the same occupation, following a similar approach by Crombé and Robinson (2014:559), who also analyzed open-air sites. For samples suspected of representing the same occupation, dates were averaged using the Oxcal 4.2's R_combine function following Naudinot et al. (2014). This addressed overrepresentation within the database. Other issues arising from research intensity are assumed to be minimal, as the database does not attempt to consider all human activity on the landscape, but instead represents a specific prehistoric behavior in the form of tipi ring site occupations.

Ultimately, even while addressing each of these issues, stochastic variability will remain—no database can be fully adjusted such that it reflects the original underlying population. However, I rely on the law of large numbers to conduct analyses and make general determinations about patterns in prehistory (Rick 1987:59), and follow recommendations outlined in Williams (2012:582) to ensure a viable minimum sample size greater than 200 radiocarbon dates for provisional results. Despite the numerous biases encountered, this

research is ideal for the dates as data approach, which is well-suited to studies such as this, with its regional focus on nomadic hunter-gatherers (Rick 1987:72).

*Taphonomic Bias***.** Within archaeology, taphonomic bias refers to the forces of decay and differential preservation that affect material culture or, in this case, cultural carbon (Surovell and Brantingham 2007:1870; Surovell et al. 2009). The radiocarbon samples available to archaeologists are those that have survived taphonomic processes, samples that may not be representative of the original cultural carbon deposit (Rick 1987; Surovell and Brantingham 2007; Williams 2012). The primary evidence of taphonomic effects on a data set is a curvilinear increase in frequency over time (Surovell and Brantingham 2007:1896), which, interestingly, is not reflected by my tipi ring site data and may result from research biases toward earlier (older) sites (Rick 1987:61).

Taphonomic loss has been addressed by Surovell and Brantingham (2007) and Surovell et al. (2009), and numerous strategies have been devised to correct it. In one such study, Surovell et al. (2009:1717) determined that taphonomic effects are not constant, but decrease over time (Surovell et al. 2009:1723). In response to this finding, they developed an equation based on past volcanism to correct for taphonomic loss. They used a global and terrestrial database of volcanism spanning the past 40,000 years, which appeared to represent global taphonomic bias (Surovell et al. 2009). They used non-linear regression to fit a curve to their data, creating a best-fit model that adjusts the taphonomic rate as sites increase in age, with a site's probability of survival increasing the longer it has been on the landscape (Surovell et al. 2009).

This taphonomic equation depends on two assumptions: 1) the model is representative in each specific context; and 2) the data to undergo taphonomic correction have no change in

relative frequency (Surovell et al. 2009:1718). Surovell et al. (2009) tested their model against open-air and rockshelter sites in the Bighorn Basin, Wyoming, under the assumption that rockshelter sites would be less affected by taphonomic bias. Regional Wyoming results corresponded with the expectations of the globally derived taphonomic equation (Surovell et al. 2009), indicating its suitability in this context.

The premise of my research is that my radiocarbon data reflect change in relative frequency over time; additionally, my data have been affected by sources of bias distinct from taphonomy (Peros et al. 2010). Peros et al. (2010:661) presented their own taphonomic correction, but concluded that the correction led to underestimating past demographic estimates, and that factors beyond taphonomy must be considered when using SPDs. In this research, I use Surovell et al.'s (2009) corrections and compare the resulting dataset to the original to determine whether a taphonomic correction produces a statistically different dataset.

Calibration Bias. Radiocarbon ages are measurements of an isotope ratio that must be interpreted against a radiocarbon calibration curve to produce a calendar date (Bronk Ramsey 2009). Portions of the radiocarbon calibration curve have steps and plateaus, which may create non-representative peaks or smooth periods within SPDs (Bamforth and Grund 2012:1770; Kerr and McCormick 2014:497; Williams 2012:581). The effects of the calibration curve are dependent on the time period under consideration, and the peaks and plateaus present within it (Contreras and Meadows 2014:603). When operating with a large radiocarbon data set, it is imperative to determine if the peaks and troughs of an SPD reflect the underlying radiocarbon calibration curve, because without this determination we run the risk of interpreting effects of the calibration curve as the result of human activity (Bamforth and Grund 2012:1773).

Bamforth and Grund (2012:1773) propose a simple but limiting solution using coarse analytical scales to minimize the calibration curve's effects. However, we need a finer resolution to effectively study changes, such as those of demography and mobility, that take place over centuries rather than millennia (Shennan 2013:302). Numerous alternate methods to distinguish the signals created by the calibration curve have been developed (Armit et al. 2013; Contreras and Meadows 2014:593; French and Collins 2015; Kelly et al. 2014; Kerr and McCormick 2014; Shennan et al. 2013; Williams et al. 2012). I tested many of these in this study, as described below.

The artificial peaks and troughs in SPDs attributed to the underlying calibration curve may be resolved by creating a moving average (Kelly et al. 2014; Shennan et al. 2013; Williams 2012). Using R Studio's "zoo" package rollmean function (R Studio Team 2015), I created a rolling average of the taphonomically corrected tipi ring site SPD for both 150- and 250-year windows. For comparitive purposes, I produced an additional 500-year average after Williams (2012).

Another common method involves the creation of 'dummy' or artificial data, which may be fitted to random (Armit et al. 2013) or uniform models (French and Collins 2015; Zahid et al. 2016). Producing a simulated dataset may reveal the underlying calibration curve (Armit et al. 2013; French and Collins 2015:126, Zahid et al. 2016). This underlying curve can be compared to the SPD produced using the tipi ring ages, and the differences between the two should reveal which patterns result from calibration bias and which may represent patterns in human mobility.

To create a random distribution, I followed Armit et al.'s (2013:435) method, using Microsoft Excel's RANDBETWEEN function to create a dataset of 500 "radiocarbon" dates

between 5000 and 50 years BP with randomly assigned errors between 30 and 120 years set at 10 year intervals. For purposes of comparison, I created a second simulated dataset, separating 5000-50 years BP into uniform 100-year periods and assigning them random errors between 30 and 120 years at 10-year intervals following French and Collins (2015). Armit et al. (2013:435) also created a uniform distribution, but dismissed it as an unlikely reflection of human activity.

Following Kerr and McCormick (2014), I used Oxcal to create a summed probability distribution from the artificial datasets. The R_Simulate function turned the artificial datasets' calendar ages into radiocarbon probability curves, while the Sum function created the sum probability distribution. Oxcal's Markov Chain Monte Carlo (MCMC) function allowed me to run through this process for 10,000 iterations. Each iteration was constructed of slightly different R_Simulate frequency distributions for each date, and the end result was a frequency distribution reflecting the underlying radiocarbon distribution for both a random and uniform radiocarbon sample dating from 5000 BP to present. If the calibration curve is significantly affecting the tipi ring site SPD, I would also expect a significant correlation between the artificial datasets and the tipi ring site SPD.

I created line graphs comparing the artificial datasets and the tipi ring site SPD. For additional comparisons, I used IBM SPSS to create P-P plots for the datasets to determine normality. This test allowed me to determine whether to use a parametric Pearson's correlation or alternate nonparametric correlation tests for all datasets.

Finally, I compared the tipi ring distribution and the random distribution using running correlation analysis, which is often used in climate research (Robinson et al. 2007). In order to improve statistical results, these distributions were placed into one-year bins, whereas prior

analyses placed these distributions into 50-year bins. This increased our data to 5638 variables, which were compared in 100-year running Pearson's correlations.

Assumptions and Corrections

It is clear from the numerous confounding factors explored above that clarity is paramount; researchers working with SPDs treat nearly as gospel that all assumptions must be explicitly stated and supported (Tallavaara et al. 2010:253). A failure to understand and clarify the potential biases affecting SPDs can both create false patterns and obscure real ones (Bamforth and Grund 2012:1772). In this research, I assume that the radiocarbon dates represent occupation events, and that my database constitutes a representative sample of occupation events in Montana and Wyoming over the past 5000 years. The former assumption relies on cultural carbon as the source of the radiocarbon ages in use. Within this database, 11% (n= 35) of the samples were directly associated with a tipi ring. Slightly over half of the ages, 56% (n= 175), had very strong evidence for cultural origins, such as hearths. The remaining ages originated from excavations, with identified proveniences including block excavation, trenches, and cultural stains. In order to address the issue of sample size, I did not remove surface carbon finds from the database.

I compare my database against the radiocarbon date sample retrieved from the Canadian Archaeological Radiocarbon Database to test this assumption, running a one-sample Kolmogorov-Smirnov test. If the test does not reject the null hypothesis, I cannot assume that my database differs from a larger radiocarbon database representative of the Northwestern High Plains of Montana and Wyoming. In this case it may represent greater demographic

trends in the region, and the results of the tipi ring site SPD must be interpreted with this in mind.

Proxy Comparisons

The second stage of the analysis examines relationships between the frequency of tipi ring sites on the landscape and changes in effective moisture. I compare the tipi ring site SPD to a reconstruction of regional effective moisture from Lake of the Woods (LOW) in Wyoming's Wind River Range (Shuman et al. 2010), as well as to a reconstruction of prehistoric temperatures in Yellowstone National Park (YNP) (Shuman 2012). Tipi ring site frequency is an assumed proxy for mobility rates, which provides a test for hunter-gatherer response to late Holocene climate variability.

In order to compare my data with the LOW reconstruction, which is scaled to 50-year intervals for the last 12,000 years, I converted the Oxcal output into calibrated years BP (using AD 1950 as the cutoff) and aggregated the data into 50-year bins. The complete datasets are compared using bootstrapped nonparametric correlations, with additional 150- and 200-year interval pairwise Pearson's correlations run for finer-scale results. Bootstrapping provides a robust approach to non-parametric data by sampling, with replacement, from the available data, allowing the same statistical test to be run multiple times (Field 2013:199). In this research, bootstrapping is set to 1000 samples, the results of which allow for the creation of confidence intervals at the 95% level. The confidence interval values allow for interpretation of correlation coefficients. Values that cross zero indicate the potential for no actual effect, as well as the

potential for either a positive or negative correlation (Field 2013:275). In these instances, correlation coefficients and significance values with $p < .05$ still may not indicate a true relationship. Significance for the 150- and 200-year intervals is determined by calculating p values; the alpha value is set at $\alpha = 0.01$ or set at $\alpha = 0.01/n$, where n equals the number of statistics tests. This is known as the Bonferroni correction (Field 2013).

While one or even two paleoclimate proxies are not considered sufficient for robust results (Crombé and Robinson 2014:564; Robinson et al. 2013:758) adopting a multi-scale approach such as in Crema (2012), which also used a single paleoclimate proxy, can aid in identifying relationships otherwise obscured by issues of chronological variability between the radiocarbon database and paleoclimatic reconstruction. As other paleoclimatic proxies become available, finer resolution analyses will become possible.

Robinson et al. (2013) point out that relationships between human behavior and climatic variability may have leads and lags. For example, Robinson et al. (2013:759) point out that, "vegetation response times to abrupt climate change vary, and can be as rapid as a few decades or up to 200 years." In order to properly address the relationship between mobility and precipitation change, we must consider that the influence of precipitation change on vegetation and, in turn, on human mobility will not only not be immediate, but the temporal relationship between the two is also likely to change depending on the severity of precipitation change. Moving correlations applied at different lag levels will begin to identify non-linear relationships of this kind.

Although these calculations may make the strength or weakness of this relationship apparent, I must still define at which point a rate of change in a distribution becomes significant, a crucial distinction that Contreras and Meadows (2014:604) point out has often

been overlooked, since with amplitude between a peak and trough significance thresholds are hard to identify. In order to ensure that any observed relationship between the radiocarbon SPD for mobility and climate variables is significant rather than simply reflecting the cumulative uncertainties of sampling, measurement and calibration, I will use the methods outlined in Zahid et al. (2016:934) and Telford (2013). I will use my uniform and artificial datasets, creating 10,000 simulated SPDs in each case, from which the deviation in the original SPD may be measured. If these differ, the radiocarbon SPD can be judged to measure something beyond uncertainty. Researchers have recommended that SPDs be analyzed at different temporal resolutions (Crema 2012; Riede and Edinborough 2012:747; Shennan 2013); doing so will help determine significance levels. Analyzing the data sets using a running correlation at different bin-levels should reveal the temporal scale at which a significant relationship exists and the temporal lag between precipitation and its effects on mobility.

In future research, ethnographic data on mobility patterns among hunter-gatherers in similar geographic and climatic settings may help provide a basis for this definition, providing a model of what a proportional change in mobility may look like in the cultural carbon record. Perhaps these data will provide distinct significance thresholds, which can serve as hypotheses and be tested against a radiocarbon sample from the same population.

CHAPTER FOUR:

RESULTS

The ready availability of cultural carbon and the increasing accuracy and affordability of radiocarbon dating have yielded a massive archaeological data source over the last half-century. Efforts to make use of these dates began in earnest with Rick's (1987) dates as data concept, and research compiling radiocarbon dates into a comprehensive sample has been widely used throughout Europe, Australia, and the Americas. The Canadian Archaeological Radiocarbon Database (CARD) represents the largest current radiocarbon project in North America, with over 90,000 radiocarbon ages spanning the last 50,000 years from over 23,000 sites worldwide (Martindale et al. 2017). Canada has 8,749 reported ages from 2,689 sites, while the United States has 41,116 reported ages from 10,121 sites (Martindale et al. 2017). Despite the diligent effort of researchers at CARD and elsewhere, these still likely represent only a fraction of all available radiocarbon data. Some of the data available from CARD is incomplete and/or inaccurate (Martindale et al. 2017). I encountered this same issue while creating my own radiocarbon database representing tipi ring ages throughout Wyoming and Montana.

I built this radiocarbon database with assistance from Ross Hillman at the Wyoming SHPO and Damon Murdo from the Montana SHPO. Hillman provided 122 sites throughout Wyoming with tipi rings and available radiocarbon ages, while Murdo provided reports for Bighorn, Custer, Rosebud, and Powder River counties in Montana, yielding 4 sites. I compiled additional ages from articles and reports within a *Plains Archaeologist* (Davis 1983) memoir dedicated to tipi ring research. This yielded 313 radiocarbon ages from 97 sites (table 2).

Table 2. Data per State

State	Sites	^{14}C Ages
Montana	6	90
Wyoming	91	223
Total	97	313

Site Characteristics

Prior to manipulating the database or undergoing complex statistical tests, I determined what contextual data were available within the tipi ring database. The supplementary information I collected provides general information not only about prehistoric patterns but about recent research patterns as well.

Of 97 sites, 86 specified cultural periods within their reports. These temporal determinations arose not only from radiocarbon dating, but also from diagnostic artifacts located within these sites. I noted these data in order to conduct a general comparison against the tipi ring radiocarbon ages. The same nomenclature was not used for all reports, resulting in differing temporal scales. However, for the most part researchers used terminology adapted from Frison (1991), which serves as this work's primary cultural chronology.

Of 86 sites, many identified multiple cultural periods resulting in 142 data points, which I then reduced to 125. I eliminated the broad category "Prehistoric," and removed data from the Paleoindian and Historic periods, which fall outside of the limits of the tipi ring radiocarbon database. Seven periods identified only as "Archaic" were averaged throughout the Archaic's three divisions. I used the original radiocarbon ages, as well as the minimum and maximum

ages determined from their standard errors, binned into the same cultural periods, for comparison. A bar graph comparing the two standardized datasets reveals that the diagnostically derived cultural periods and the radiocarbon data have similar patterns with a discrepancy during the Late Archaic and Late Prehistoric periods (Figure 2).

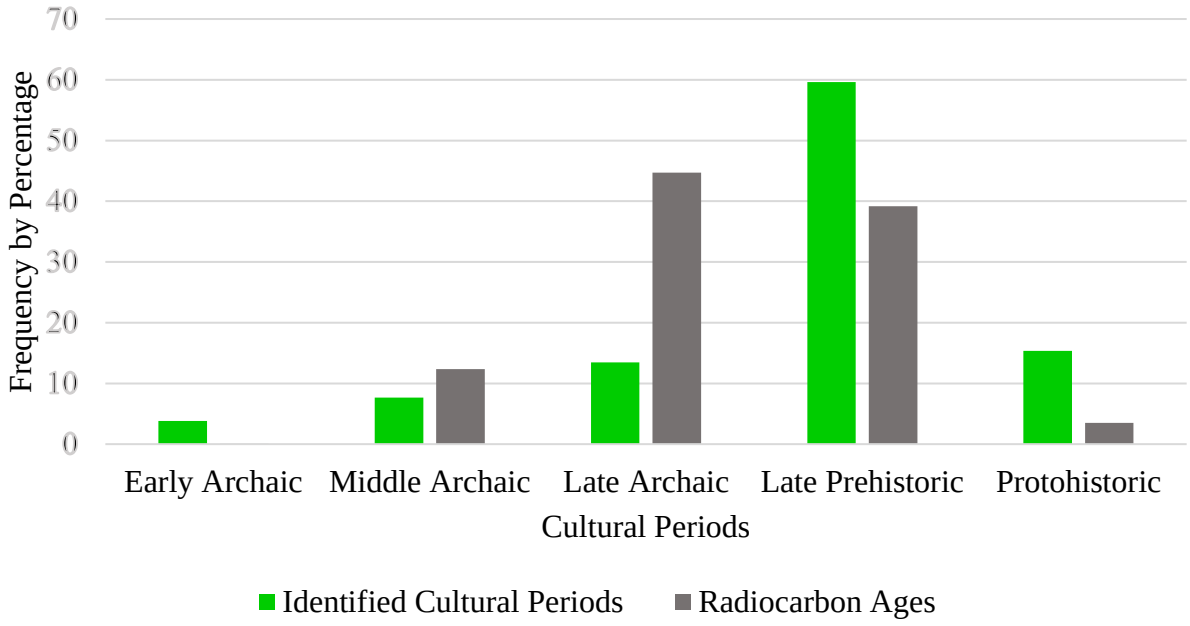

Figure 3. Relative frequency per cultural period

In addition to temporal data, I also collected elevation data. Eighty-three site records included elevation data. A correlation test of ages and elevation returned a weak correlation coefficient of $r = 0.091$, not significant at $p = 0.414$. A scatterplot also failed to identify any visual relationships within the data. Despite this, I calculated descriptive statistics and binned the elevation data in 500 feet bins, creating a histogram to ascertain the elevation thresholds at which tipi ring sites are most common (Table 3; Figure 3). Tipi rings sites are most prevalent between 4000-6000 ft.

Table 3. Descriptive Statistics for Elevation

Elevation (ft)	
Mean	5640
Standard Error	125
Median	5660
Mode	4600
Minimum	2800
Maximum	8020
Count	83

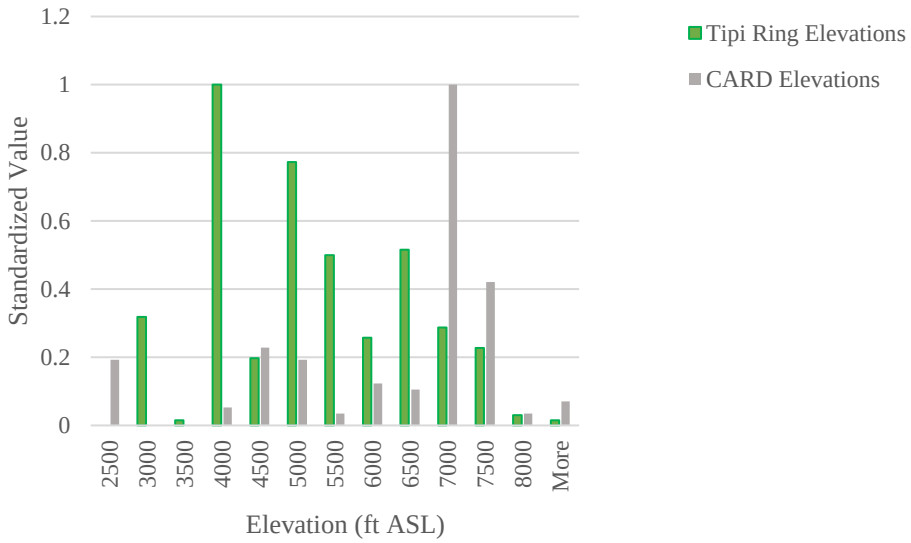

Figure 4. Elevations at tipi ring sites versus all sites

In order to further explore these data, I compared them to elevations for Wyoming sites located in the same counties and dating to the same 5000-100 cal year BP time period, using the data I obtained from CARD. Frequencies appear to descend across both categories between 4000 and 7000 feet, but the proportions across elevation bins vary significantly. CARD has significantly more sites between 2500-3000 feet, as well as above 7000 feet.

Research Biases

The tipi ring database provides a glimpse not only of prehistoric behaviors and decisions, but also of archaeological research trends and practices, and their influence on the data sample ultimately available to archaeologists. The tipi ring database includes the analysis dates for each radiocarbon age. This analysis was cut off at 2009, as only six years of data from the 2010s were available at the time of data collection. Notably, tipi ring radiocarbon dating appears to have peaked in the 1980s, decreasing slightly in the 1990s and 2000s (Figure 4). Unfortunately, I could not compare my data with CARD's, as the dates associated with each radiocarbon age in their database were publication dates from references rather than dates of the analysis.

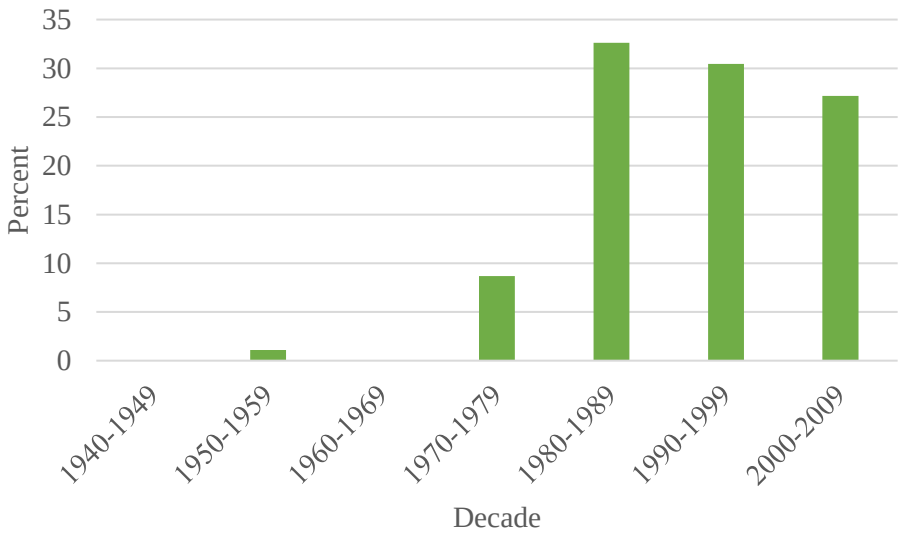

Figure 5. Radiocarbon age analyses by decade

CARD, however, does provide information on the materials available to and chosen by researchers for dating, data that I also collected for the tipi ring database. Within my database, "charred material" is by far the most popular material type used by researchers, followed by bone and bulk sediment samples. It is apparent from Table 4 that the distribution of radiocarbon dating materials is quite similar between the two databases.

Table 4. Radiocarbon Sample Materials

Material Type	Tipi Ring Radiocarbon (%)	CARD Radiocarbon (%)
Charred material	61	65
Bone	9	2
Sediment	4	8
Unknown	25	23
Wood	0	2

Correcting the Radiocarbon Database

Overrepresentation. The first task necessary to begin unpacking and analyzing these radiocarbon ages lies in dealing with the possibility that certain sites were overrepresented within the database. This did not appear to be a prevalent issue within the database: 49% of sites had only one radiocarbon sample, while a full 87% of sites had 5 or fewer radiocarbon samples (Figure 5). However, the remaining 11% had anywhere from 6 to 35 radiocarbon samples. A simple solution to overrepresentation is to use OxCal's R_Combine function for samples from the same cultural layer (Naudinot et al. 2014), however, the prevalence of multicomponent tipi ring sites warrants caution in the application of this technique.

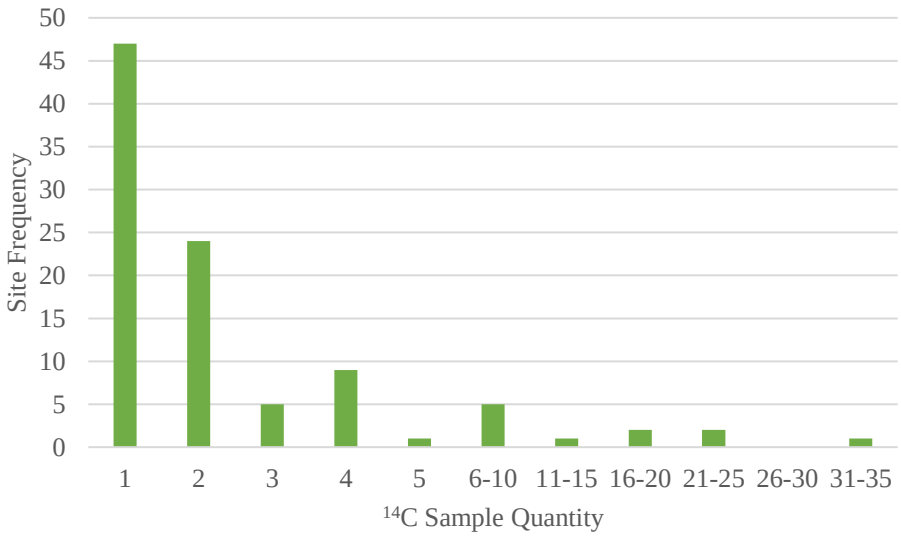

Figure 6. ^{14}C Samples per site

The number of recorded tipi rings at a site was noted within the database (Figure 6). If the researcher classified a site as multicomponent, this was also noted. Over half of the sites

(n=54) were multicomponent, while 20 had no classification, and 25 were classified as single episodes. I ran a correlation test to determine whether the number of tipi rings at a site bore any relation to the number of radiocarbon samples collected. The correlation coefficient of tipi ring frequency at a site and radiocarbon ages obtained is 0.16, indicating no statistically significant correlation. Overrepresentation does not appear to be a direct result of the number of tipi rings at a site.

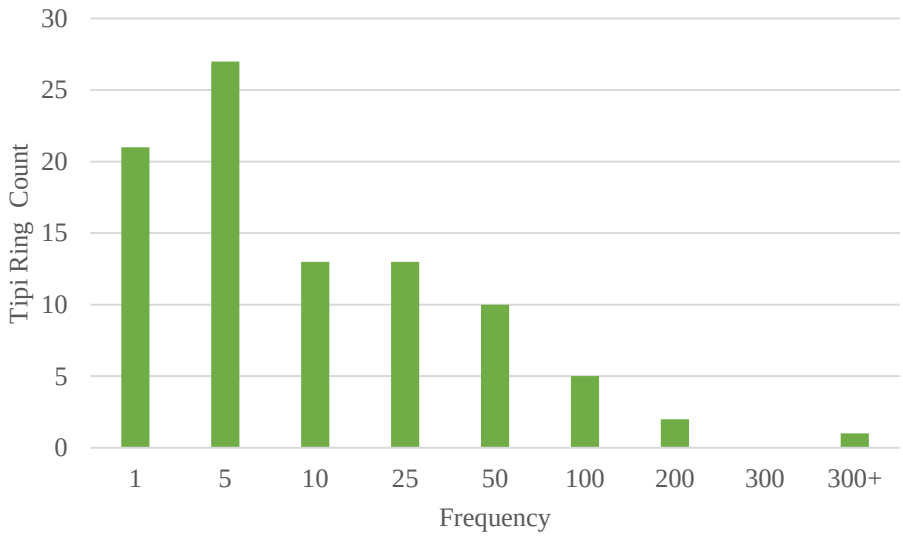

Figure 7. Site frequency of tipi ring counts

I addressed overrepresentation one site at a time, constructing high-value plots to determine visually whether multiple radiocarbon ages overlapped. Sites with a clear temporal distinction between radiocarbon samples were not analyzed. Radiocarbon ages within a single site that were identical were simply reduced to a single data point. In the case of a more than 50-year overlap of standard errors, radiocarbon ages were averaged using R_Combine, using the general assumption that these ages represented the same occupation event. I used this

technique sparingly, as radiocarbon ages are far too coarse to represent the short-term seasonal use of tipi ring sites, and overlap between ages could just as easily represent multiple occupations as it could multiple radiocarbon samples from the same temporal event. This ultimately resulted in 234 radiocarbon ages for analysis, reducing 79 ages. Most combinations averaged two ages, although in some cases up to four samples were averaged through R_Combine.

Averaging ages to remove overrepresentation within the dataset, an inconclusive issue to begin with, removed a quarter of the original database. It is central to the use of dates as data, as well as general statistics, that larger samples are better approximations of the original population (Rick 1987, Williams 2012).

In order to test whether combining dates had a discernible effect on the dataset, I compared a summed probability distribution (SPD) of the original dataset with 313 ages and the corrected dataset with 234 ages both visually (Figure 8) and using significance tests, running non-parametric tests comparing independent samples in IBM SPSS Statistics v. 24. A visual examination shows that the distributions retain the same shape, but that the uncorrected SPD has greater frequencies between 2500-500 years BP. Both the Mann-Whitney U test and Kolmogorov-Smirnov test determined that I should retain the null hypothesis that these samples originate from the same distribution (Figure 9). One possible reason for this result is the process of creating SPDs in the first place, in which the underlying radiocarbon calibration curve may affect each dataset enough that they appear to originate from the same distribution.

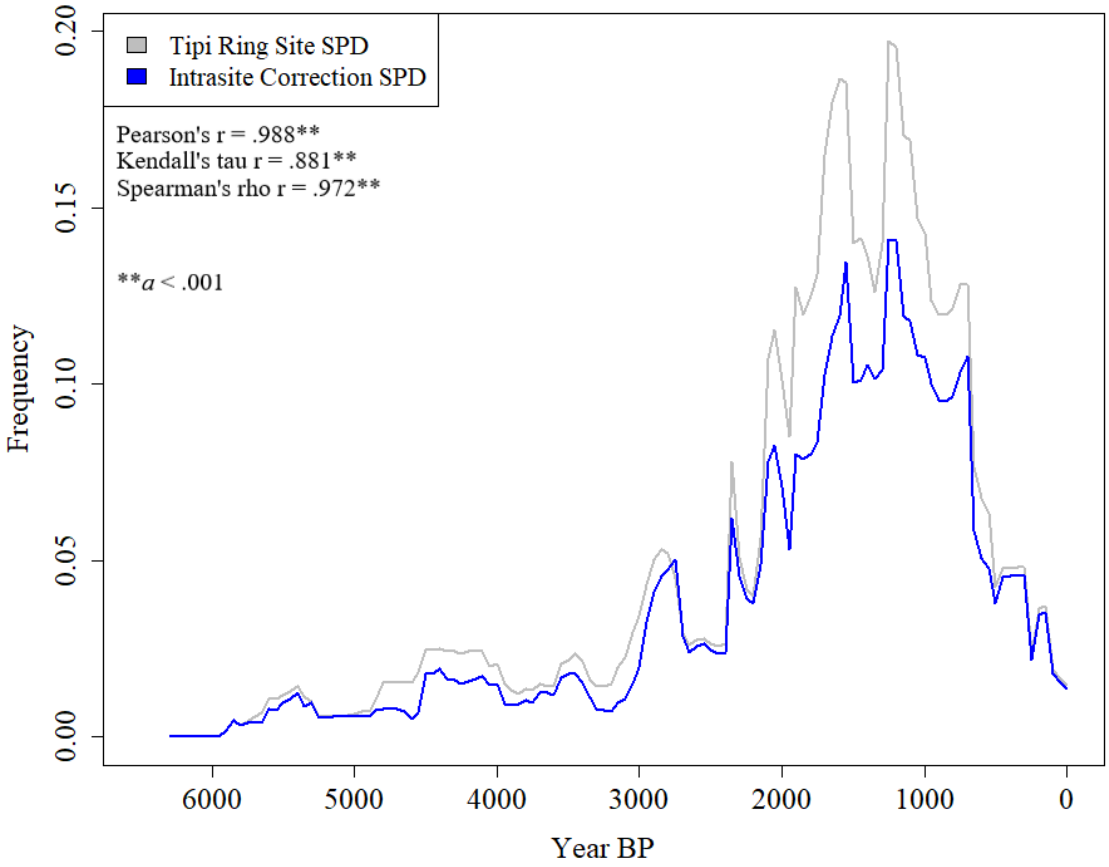

Figure 8. Comparison between R_Combine SPD and Uncorrected SPD

Hypothesis Test Summary

	Null Hypothesis	Test	Sig.	Decision
1	The distribution of data is the same across categories of group.	Independent-Samples Mann-Whitney U Test	.972	Retain the null hypothesis.
2	The distribution of data is the same across categories of group.	Independent-Samples Kolmogorov-Smirnov Test	1.000	Retain the null hypothesis.

Asymptotic significances are displayed. The significance level is .05.

Figure 9. Independent samples test of SPDs of original and corrected datasets

To determine whether this was the case, I also compared the datasets prior to conversion into SPDs. Each dataset was built from the original radiocarbon ages as well as the minimum and maximum age values calculated from their standard error. This comparison yielded the same results from Mann-Whitney U and Kolmogorov-Smirnov tests (Figure 10). I conclude from these results that overrepresentation is not a statistically significant issue within my original dataset, and will continue to use the original, larger, dataset for my subsequent analyses, in order to maintain as representative a dataset as possible. However, I will run some analyses on the R_Combine data, to determine whether results are consistent between the original dataset and the dataset corrected for intrasite errors, with a particular eye toward the 2500-500 years BP period.

Hypothesis Test Summary

	Null Hypothesis	Test	Sig.	Decision
1	The distribution of data is the same across categories of group.	Independent-Samples Mann-Whitney U Test	.442	Retain the null hypothesis.
2	The distribution of data is the same across categories of group.	Independent-Samples Kolmogorov-Smirnov Test	.864	Retain the null hypothesis.

Asymptotic significances are displayed. The significance level is .05.

Figure 10. Independent samples test of SPDs of original and corrected datasets

Taphonomic Correction. In addition to determining the effects of overrepresentation within the database, it was essential that I correct for potential taphonomic loss. The effects of taphonomic bias on the database should "produce a positive curvilinear frequency distribution through time" (Surovell and Brantingham 2007:1869). I created a histogram representing the radiocarbon ages as well as the ranges represented by the addition and subtraction of their

standard error. I placed these data in bins of 50, 100, 150 and 500 years to study the frequency patterns visible at different scales (Figure 9). The patterns do not appear to represent direct exponential growth at these scales, but they do show growth and a drop off roughly 1000 years BP that corresponds with Surovell and Brantingham's (2007) expectations and Surovell et al.'s (2009:5) Bighorn Basin data. Alternate explanations to taphonomic loss may also result from research bias against more recent sites, the availability of alternate dating methods for more recent sites, or changes in tipi ring construction favoring alternatives to stones for canvas weights. Due to these patterns, I opted to apply the Surovell et al. (2009) taphonomic correction.

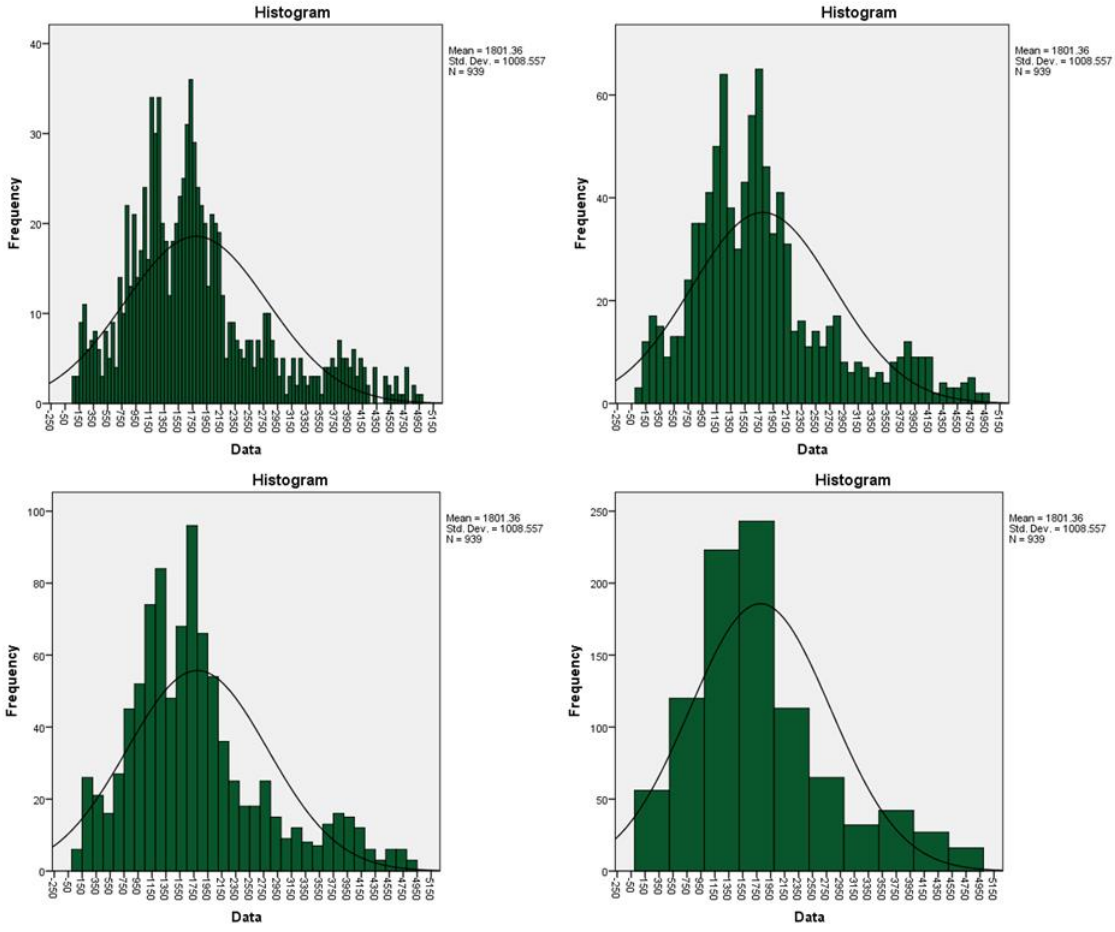

Figure 11. Radiocarbon ages at different bins. Top left: 50 years, top right: 100 years, bottom left: 150 years, bottom right: 500 years.

Surovell et al. (2009) developed Equation 1 to correct for taphonomic bias using a radiocarbon-dated volcanic eruption frequency distribution. They interpret the volcanic eruptions as proxy data for global sedimentation events, and successfully used Eq. 1 as a taphonomic correction in Wyoming's Bighorn Basin (Surovell et al. 2009).

$$n_t = 5.726442 * 10^6(t + 2176.4)^{-1.3925309}$$

Following the methods outlined in Surovell et al. (2009), I used Eq. 1 to apply a taphonomic correction to my complete database SPD, as well as the smaller SPD I created while using R_Combine. I used visual and statistical tests to compare these two taphonomic corrections, as well as to correct the complete SPD's taphonomic correction to the original, uncorrected database. Scatterplots comparing the taphonomic corrections and the corrected vs. original data revealed a near one-to-one relationship between the data, with a strong trendline in each case (Figures 12 and 13).

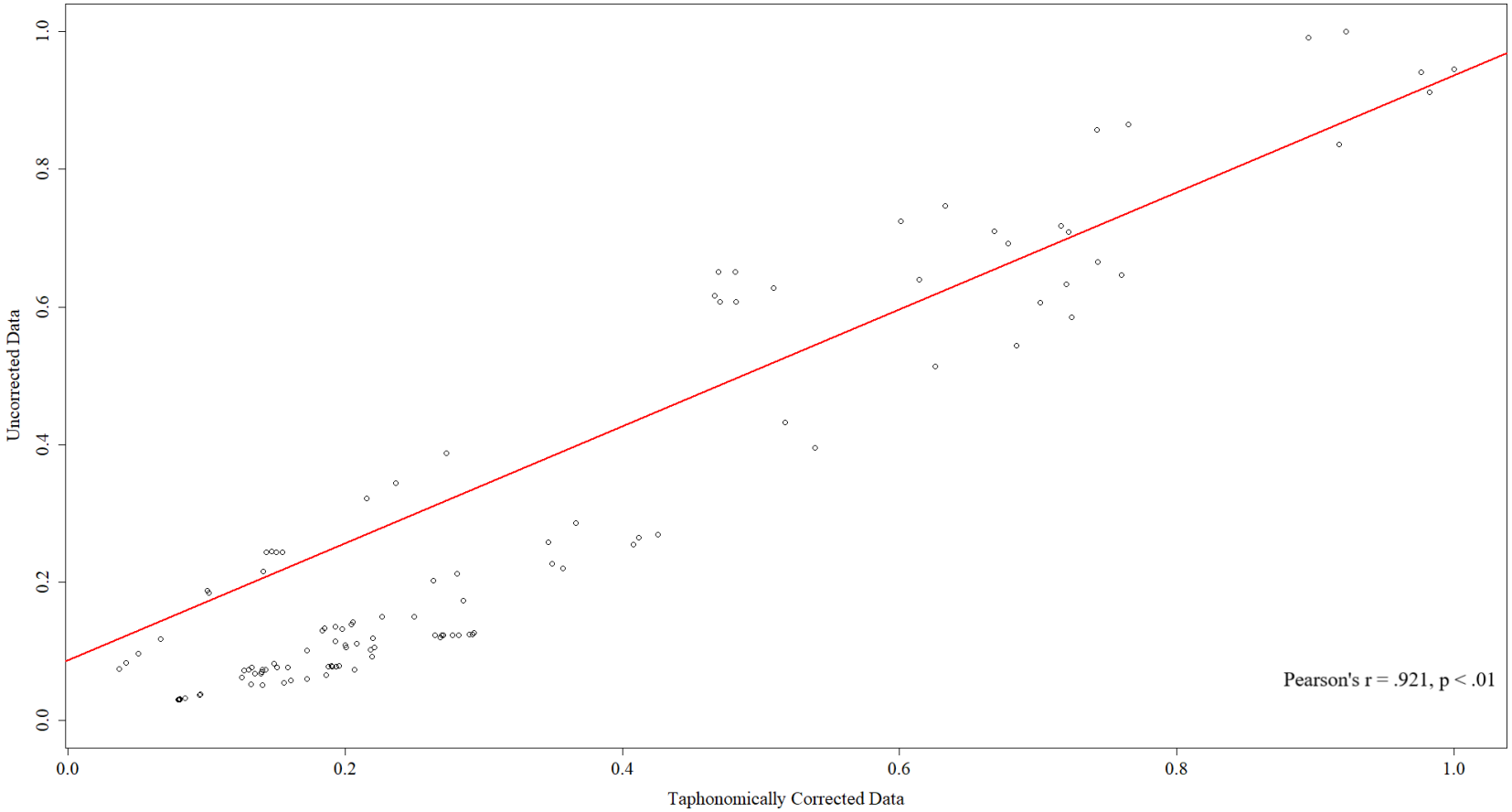

Figure 12. Scatterplot of taphonomically corrected and uncorrected SPDs

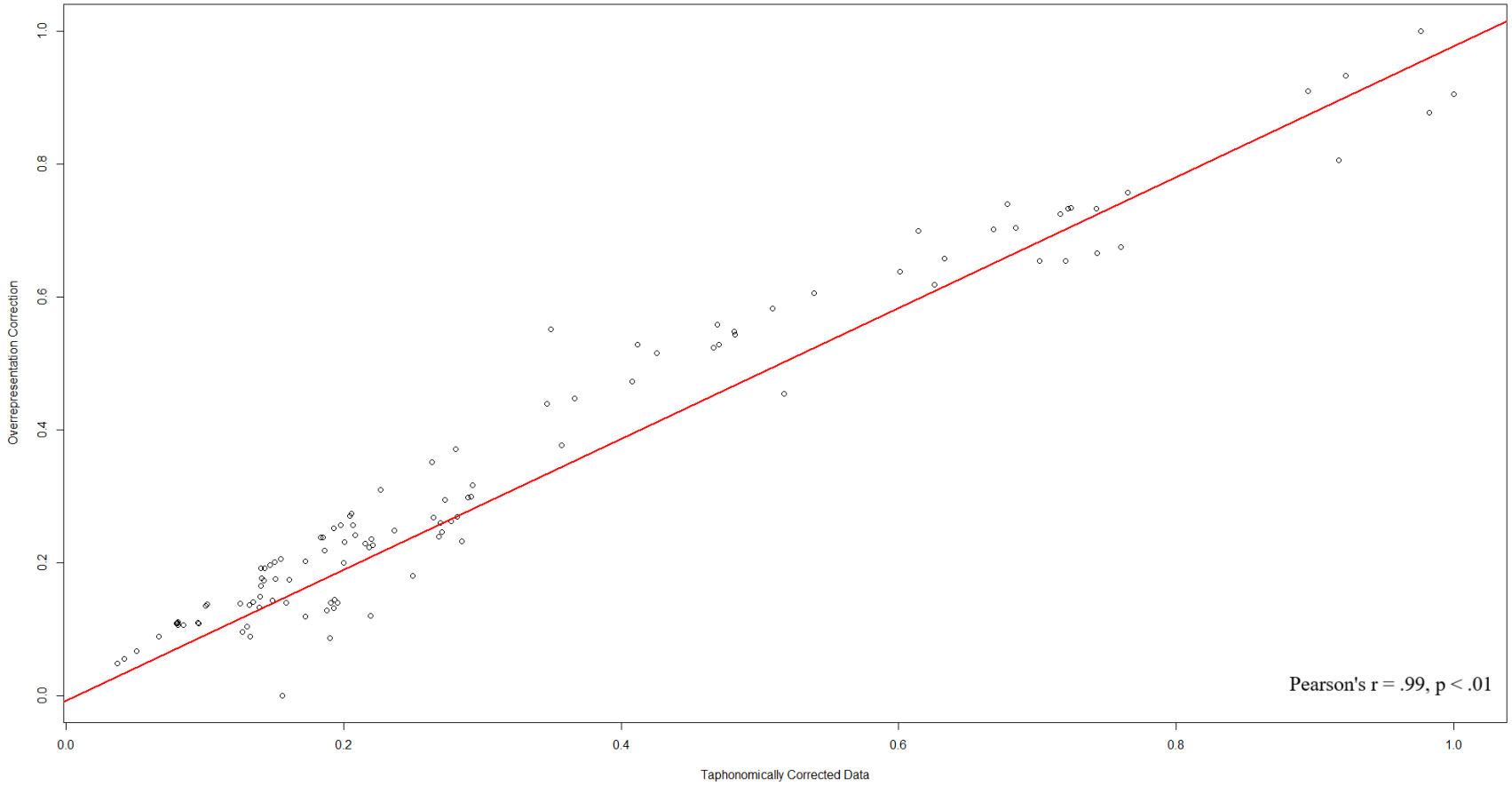

Figure 13. Scatterplot of taphonomically corrected overrepresentation correction SPD and original SPD

A correlation test of the corrected complete database and the original, uncorrected database yielded a very strong correlation coefficient of $r = 0.921$, with $p < .01$, suggesting the taphonomic correction does not create a significantly different frequency distribution. Similarly, a correlation test of the corrected complete and R_Combine databases also had a correlation coefficient of $r = 0.99$, with $p < .01$, providing further evidence that the correction for overrepresentation is unnecessary in this case.

Calibration Curve Bias. The final correction suggested by researchers utilizing radiocarbon summed probability distributions is to account for variability introduced by the underlying radiocarbon calibration curve. For visual purposes, I created a moving average at 150-, 250-, and 500-year intervals. This smoothed peaks and troughs, theoretically reducing noisy patterns introduced by the underlying calibration curve (Figure 14).

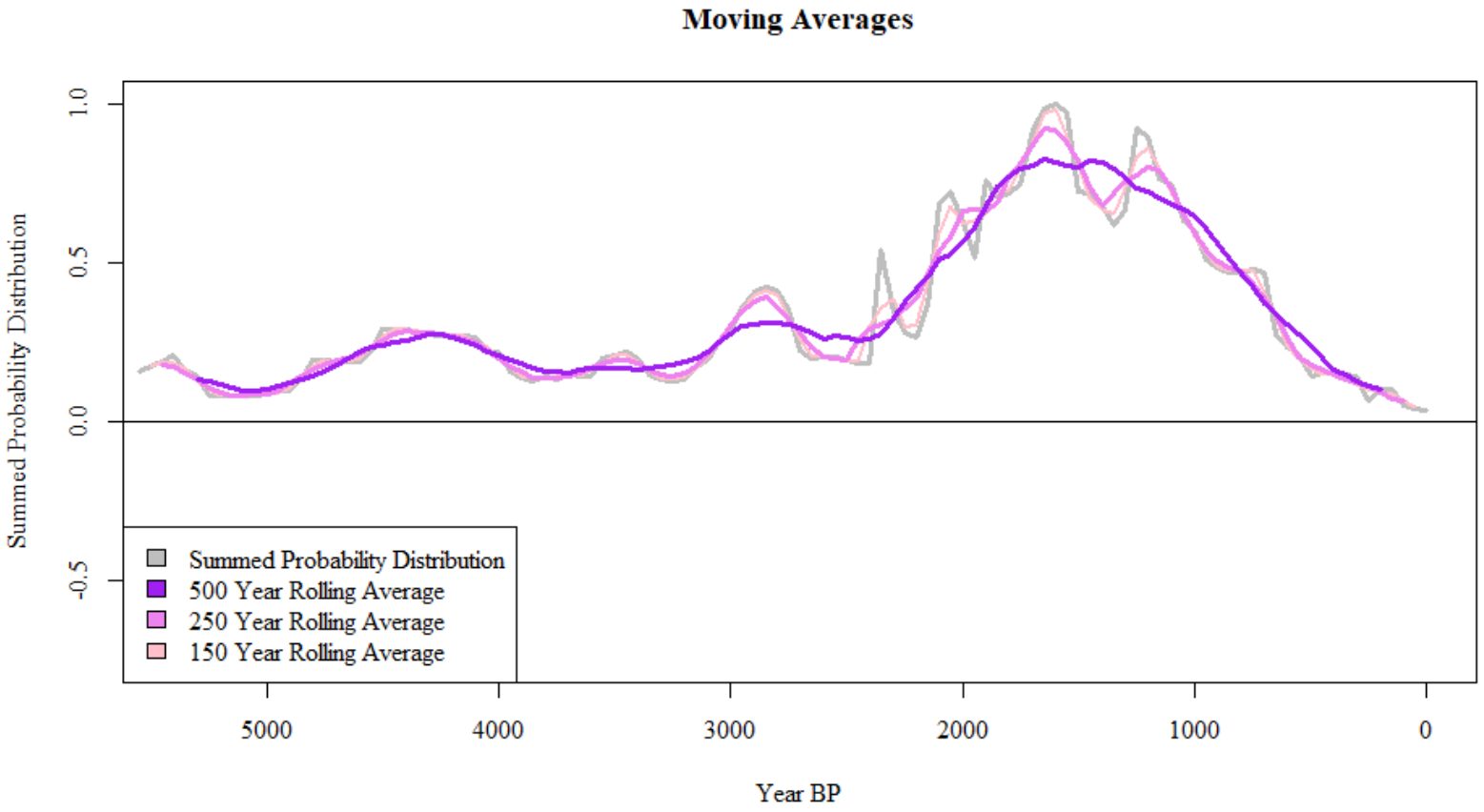

Figure 14. Tipi ring site SPD rolling averages at multiple intervals.

For a statistical approach to the calibration curve, I created both a uniform and a random radiocarbon dataset spanning 5000-50 years BP, n = 500, with random standard errors between 30 and 120 years. I used Oxcal 4.2 to turn these dates into simulated radiocarbon ages for use in a summed probability distribution. I used the MCMC function to run the SPD 1000 times for a more robust distribution. Radiocarbon smear (Baillie 1991) leads to edge effects issues (Contreras and Meadows 2014:605) resulting in distributions extending past 5700 BP and prior to 50 BP from an original 5000-50 years BP sample. Analyses limited the distributions to their original 5000-50 year BP time span. The differences between these distributions are visible below in Figures 15 and 16.

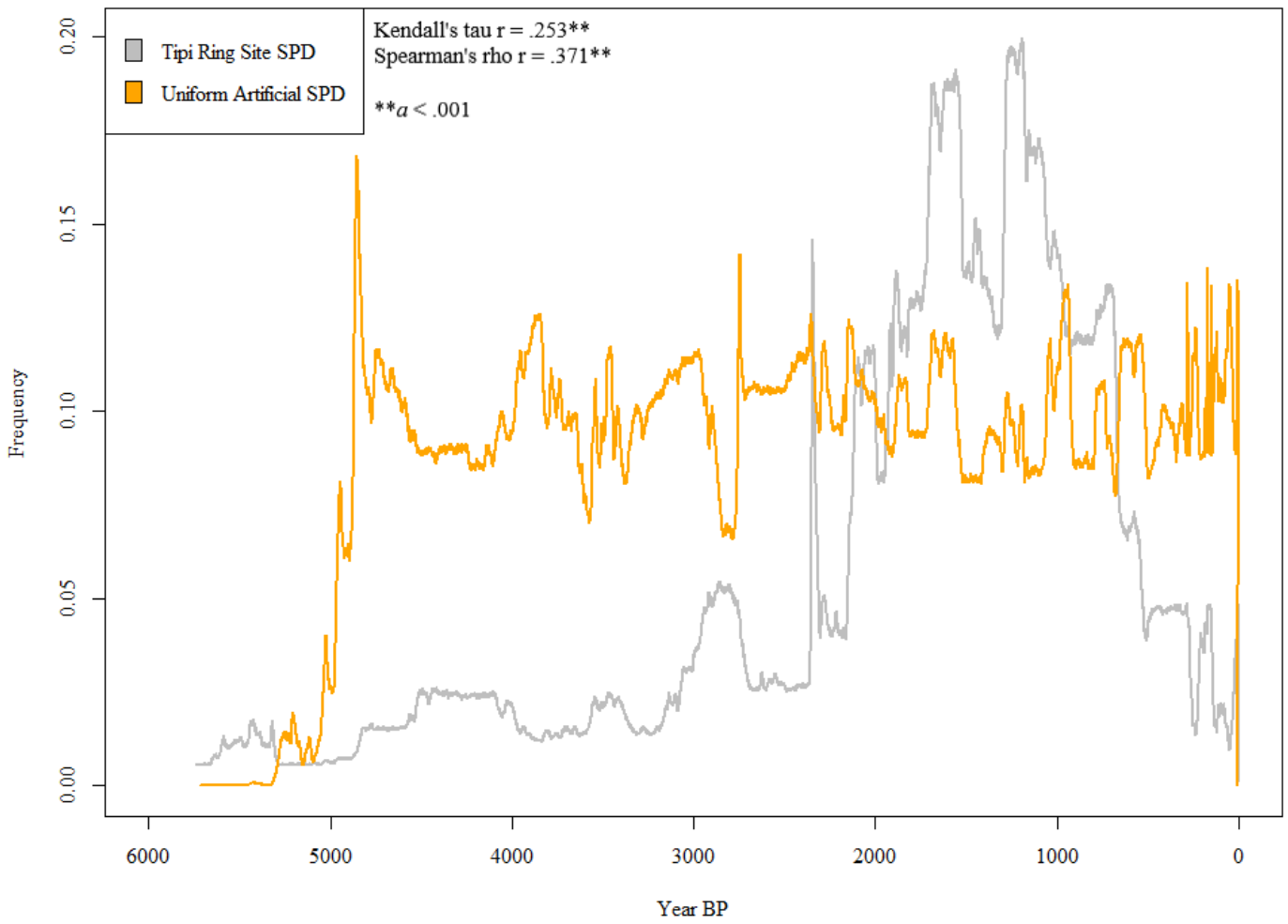

Figure 15. Line graph comparisons of tipi ring and uniform artificial SPD

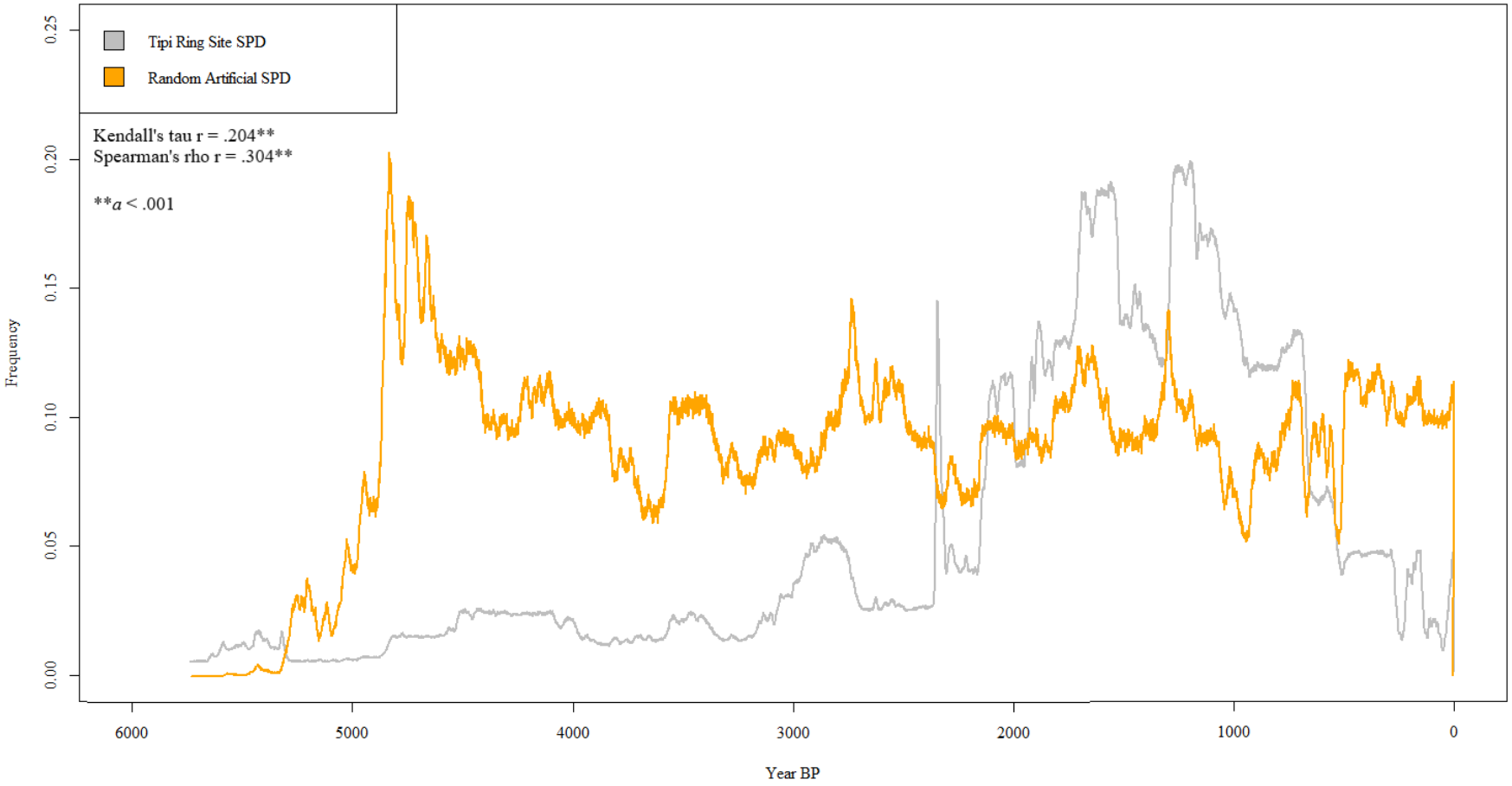

Figure 16. Line graph comparisons of tipi ring and random artificial SPD

Visually comparing the tipi ring site SPD and artificial dataset SPDs in Figures 15 and 16 reveals that decisions regarding the null distribution have a tremendous impact. Since these artificial datasets are used to determine whether a signal in the target SPD is significant, the choice of method, such as Armit et al.'s (2013) random distribution as opposed to French and Collins's (2015), will lead to different interpretations of significance. Although the same methods were applied to models meant to approximate a null distribution, these resulted in contradicting indications of the underlying calibration curve's influence on the tipi ring site SPD. I ran correlations between these artificial datasets and the tipi ring site SPD to determine which had a higher correspondence. As a conservative choice, I posit that using the distribution with the stronger correlation may minimize Type II interpretation errors, as fewer deviations will be interpreted as significant.

Prior to the correlations, I used IBM SPSS to create P-P plots for the datasets to determine normality. Only the randomly distributed artificial dataset approximated normality. I ran two-tailed non-parametric Kendall's tau and Spearman's rho correlation tests, bootstrapping the tests for 1000 iterations with a 95% bias-corrected and accelerated confidence interval. All distributions are significantly correlated at the 0.01 level. In the Kendall's tau test, the artificial datasets are correlated with $r = .376$, while the tipi ring dataset has a weaker correlation with the randomly distributed dataset at $r = .204$ and $r = .252$ with the evenly distributed dataset. It is encouraging that although the datasets have a significant correlation, as would be expected, the correlation is weak, indicating deviations in the tipi ring site SPD from both approximations of null distributions that may reflect the underlying calibration curve.

The Spearman's rho test resulted in a stronger correlation between the evenly and randomly distributed artificial data sets, r = 0.527 and significance at the 0.01 level. Correlations between the tipi ring site dataset and the artificial data sets were also significant at the 0.01 level and stronger than in the Kendall's tau test, with r = .304 for the randomly distributed data and r = .371 for the evenly distributed data. It is interesting to note that the evenly distributed data has a stronger correlation with the tipi ring site dataset than the truly random data. Although the potential reasons for this relationship are unknown, the uniform distribution was chosen for interpretations of significance.

To further determine correspondence, I calculated running Pearson's correlations over 100 year windows between the tipi ring site and uniform SPDs. This resulted in 5006 variables representing 100-year sliding window correlations between 50-5000 years BP. The correlation coefficients resulted in a bimodal distribution, with 42% representing strong negative correlations ($r \leq$ - 0.05) and 28% representing strong positive correlations ($r \geq 0.05$) (Figure 17). Correlations with $p < .01$ were present across 85.5% of the sliding correlations. There are n = 3997 strong ($0.05 \geq r \leq$ - 0.05) and significant ($p < .01$) correlations, representing 80% of all sliding correlations. The proportions here remain bimodal, similar to the overall distribution (Figure 18).

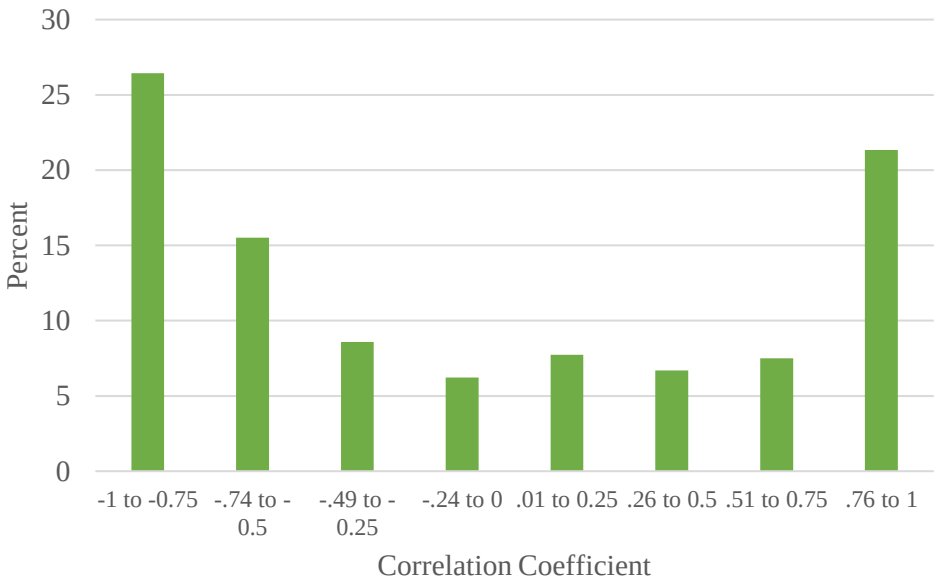

Figure 17. Tipi ring and uniform artificial SPD correlations

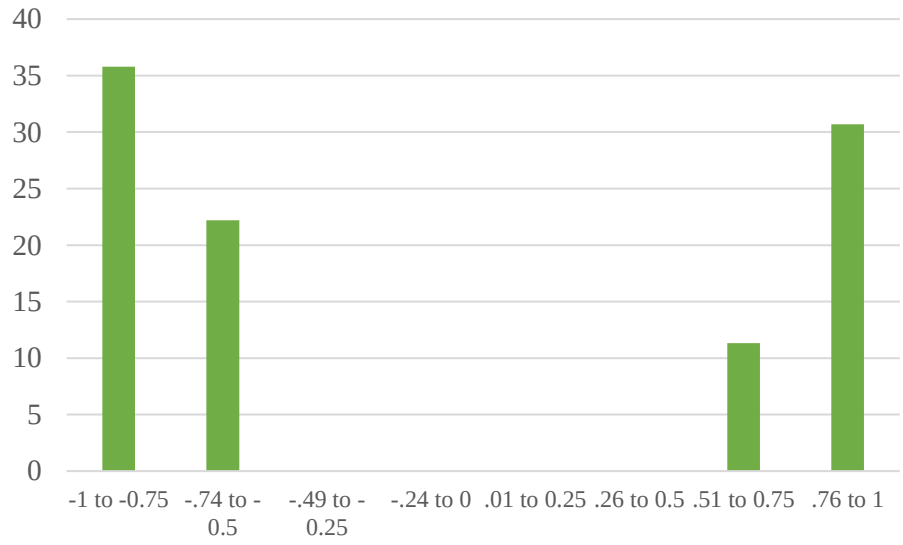

Figure 18. Strong and significant correlations

An immediate problem with sliding window correlations, however, is the problem of multiple comparisons and the increasing potential for Type I and Type II errors (Field 2013).

One solution is the Bonferroni correction, in which our desired α = 0.01 is divided by the number of tests—in this case, 5006, resulting in α = 1.9976E-06. However, all significant *p* values less than 0.01 are also less than 1.9976E-06, resolving the problem in this scenario. This means that of the 5006 sliding correlations, roughly 20% of the tipi ring site SPD does not have a statistically significant correlation with the uniform probability distribution. This will be important when determining whether correlations with paleoenvironmental reconstructions are significant.

Kerr and McCormick (2014) outline an alternate ratio method that allows comparison between the underlying calibration curve and a radiocarbon dataset's SPD. The ratio is constructed by dividing the tipi ring frequency by the artificial dataset frequency for each bin. The closer a value is to 1, the greater the correspondence between the tipi ring and artificial datasets. Values greater than 1 reflect a greater frequency than expected, and values less than one reflect fewer radiocarbon ages than expected. I binned the ratios in 0.25 intervals and created a histogram to view the ratio distribution (Figure 19).

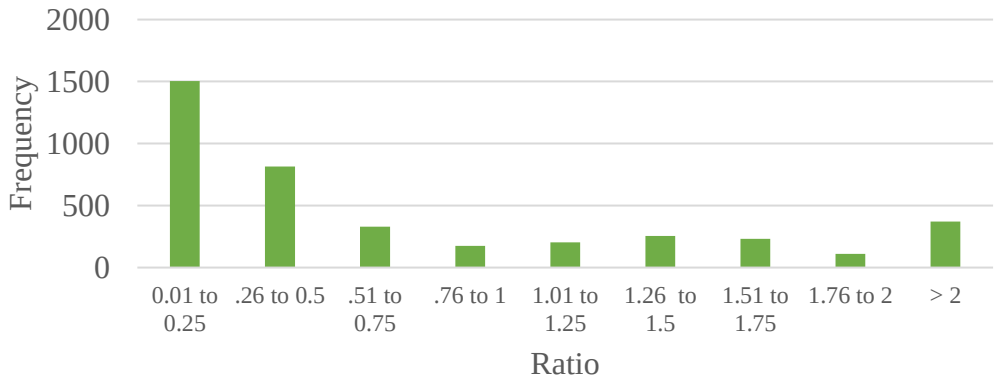

Figure 19. Kerr and McCormick ratio method

Approximately 9.5% of the ratios were between .76 and 1.25, or within the range of expected radiocarbon frequencies. Most of the data is less than 1, with 66% of the ratios between .01-.75, suggesting fewer radiocarbon ages than expected, and the remaining 24% suggesting greater radiocarbon ages than expected. This method indicates a much stronger archaeological signal in the tipi ring site data than suggested by Armit et al.'s (2013) method, in which only 20% of the tipi ring site data deviate from the expectations of the artificial dataset. Once again, to be conservative and minimize the possibility of interpreting significant signals where there are none, the results of the sliding correlations will be used over those of the ratio method. When significant relationships are identified between the tipi ring site data and paleoenvironmental reconstructions, the same period can be identified in the running correlations to determine whether the calibration curve has unduly influenced the tipi ring site distribution at this point.

Proxy Comparisons

The preceding analyses corrected or addressed issues with my dataset and with SPDs in general. These determined that overrepresentation did not present a major source of bias and introduced a method by which relationships can be tested for significance despite calibration curve effects. I applied a taphonomic correction to account for taphonomic loss and increase compatibility with my proxy comparisons. Completing these analyses allowed me to proceed to comparisons between the tipi ring dataset, my mobility proxy, and past temperature and precipitation reconstructions.

My primary analysis consists of identifying relationships between the tipi ring site SPD and the paleoenvironmental reconstructions from Lake of the Woods and Yellowstone, such as through correlations and running correlations. Field (2013:263) suggests using scatterplots to assess visually apparent relationships prior to running correlations.

The tipi ring site SPD and temperature scatterplot shows a promising visual relationship, with a negative linear trend (Figure 20). The bootstrapped Pearson correlation test between the two datasets returns a correlation coefficient of r = -.707, with a significance of p < .01, and confidence intervals of -*.785* and -*.609*. The Kendall's tau correlation resulted in r = -.301, with a significance of p < .01, and confidence intervals of -*.419* and - *162*. The Spearman's rho correlation resulted in r = -.468, with a significance of p < .01, and confidence intervals of -*.610* and -*.278*. All results reject the null hypothesis that the datasets have no correlation, and the confidence intervals indicate consistent results across 1000 bootstrapped tests.

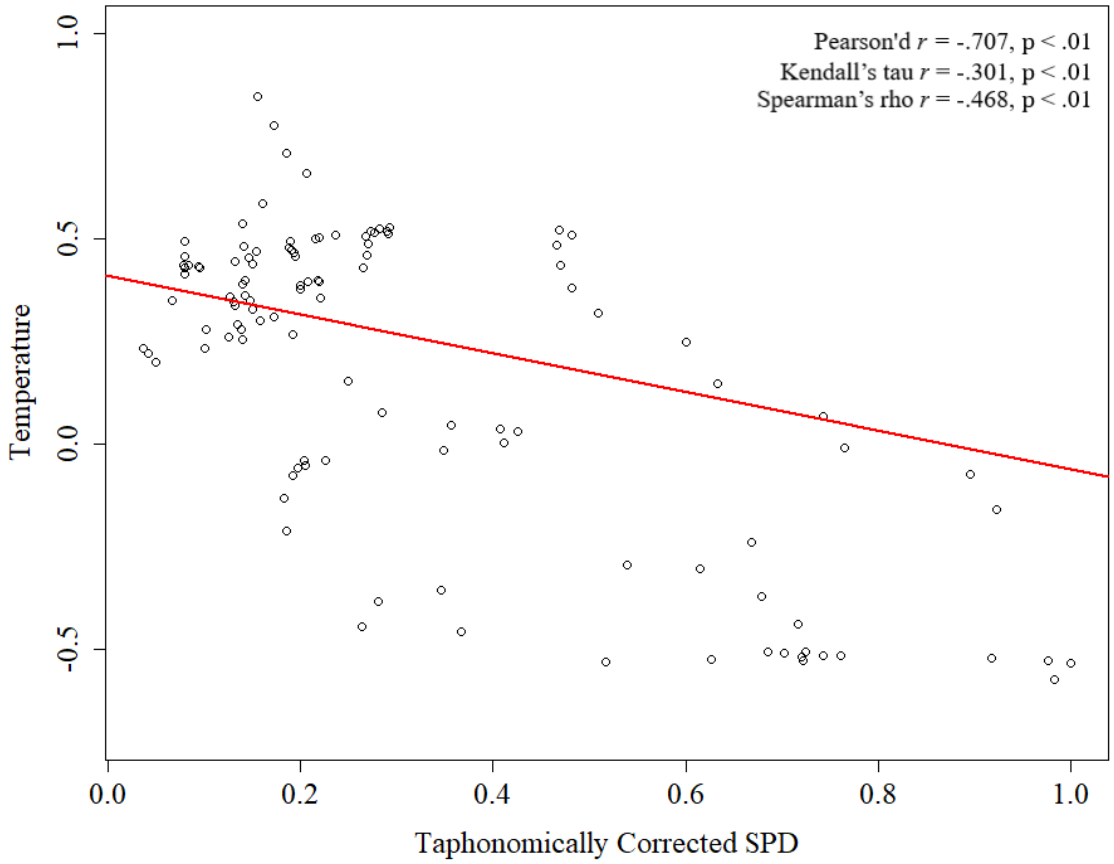

Figure 20. Tipi ring site SPD and temperature scatterplot

The tipi ring site SPD and moisture deficit scatterplot also appear to have a visual relationship (Figure 21), with a positive linear trend. The bootstrapped Pearson correlation test between the two datasets returns a correlation coefficient of $r = .398$, with a significance of $p < .01$, and confidence intervals of *.265* and *.509*. The Kendall's tau correlation resulted in $r = .202$, with a significance of $p < .01$, and confidence intervals of *.062* and *.338*. The Spearman's rho correlation resulted in $r = .271$, with a significance of $p < .01$, and confidence intervals of *.053* and *.467*. All results reject the null hypothesis that the datasets have no correlation, and the confidence intervals indicate consistent results across 1000 bootstrapped tests.

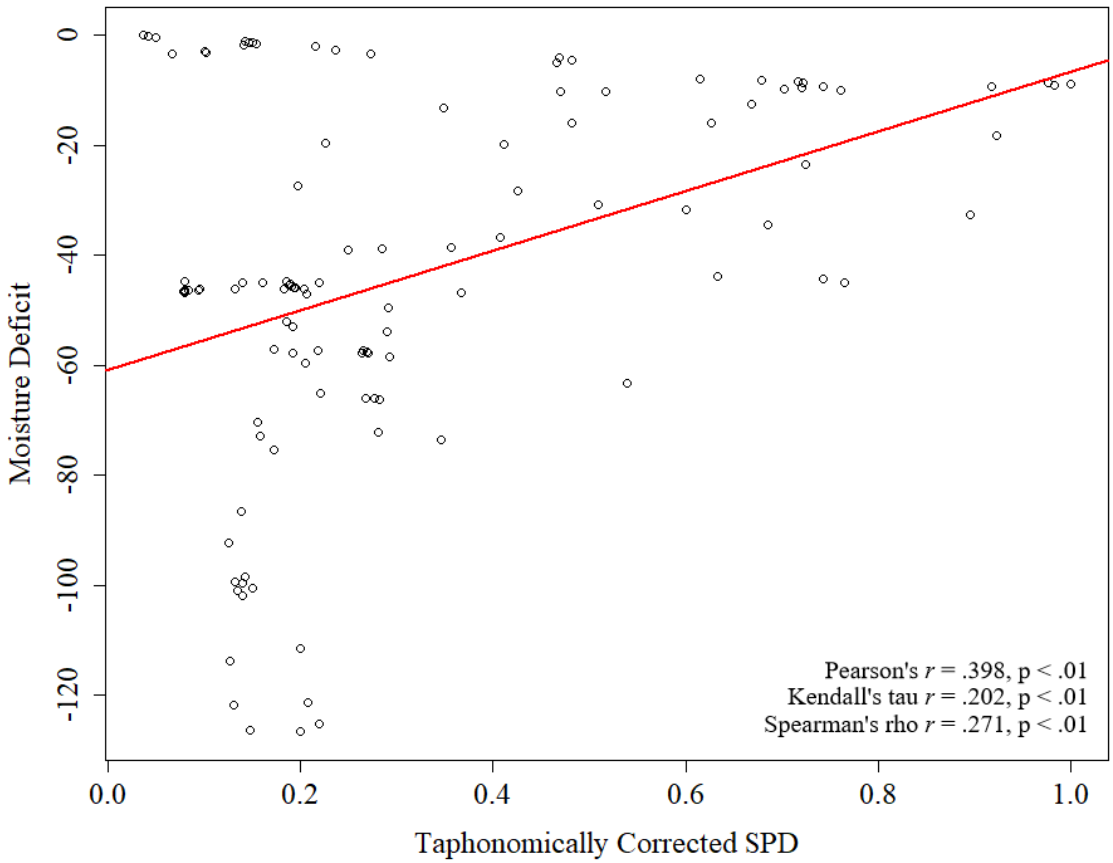

Figure 21. Tipi ring site SPD and moisture deficit scatterplot

I ran the same tests between the environmental datasets and the artificial SPDs to determine whether significant correlations might also occur with arbitrary data.

Scatterplots for the random artificial SPD and temperature and moisture deficit revealed no apparent visual relationship (Figures 22, 23). The Pearson correlation between the random SPD and moisture deficit was weak at r = .138, and non-significant at p = .146. However, the nonparametric correlations found significant, albeit weak, correlations at the α= 0.05 level, with a Kendall's tau of r = .144, p = .025, and a Spearman's rho of r = .238, p = .011. For temperature, the Pearson correlation resulted in r = - .266, significant with p = .005.

These results are corroborated by the nonparametric tests, with a Kendall's tau of *r* = - .187, p = .003, and a Spearman's rho of *r* = - .251, p = .008.

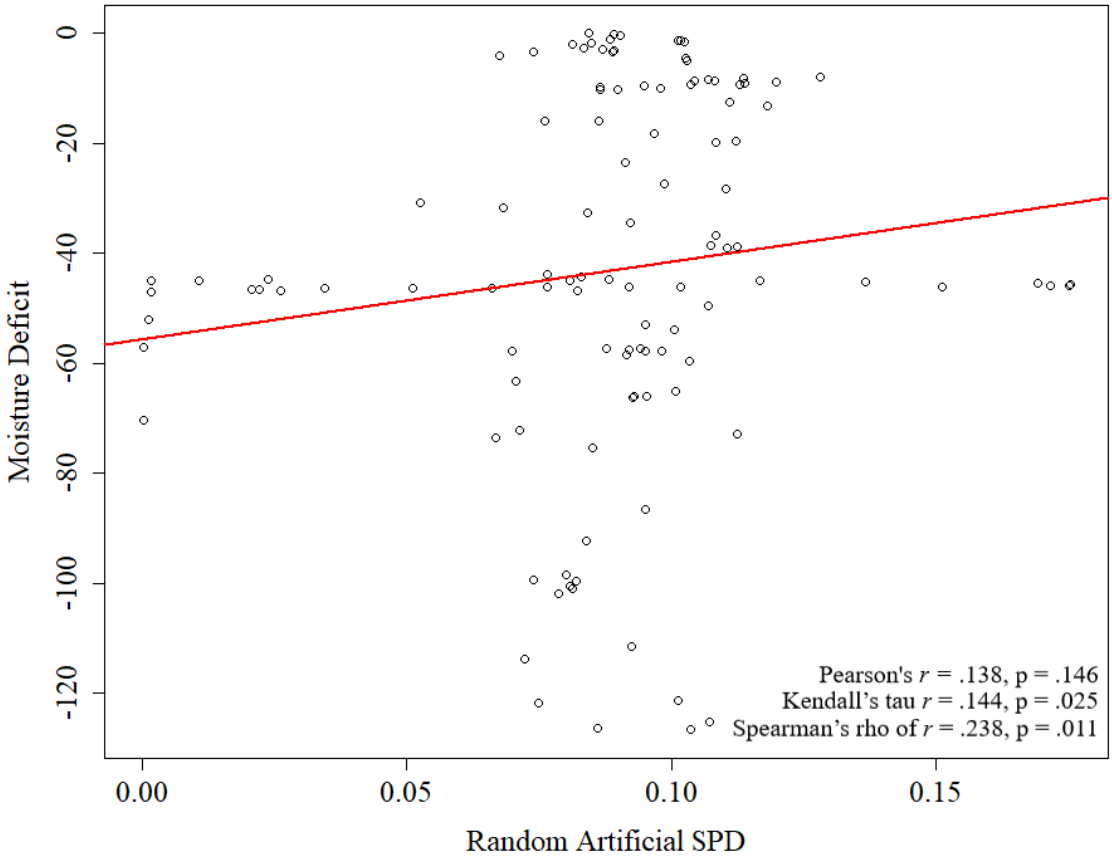

Figure 22. Randomly distributed artificial dataset and moisture deficit scatterplot

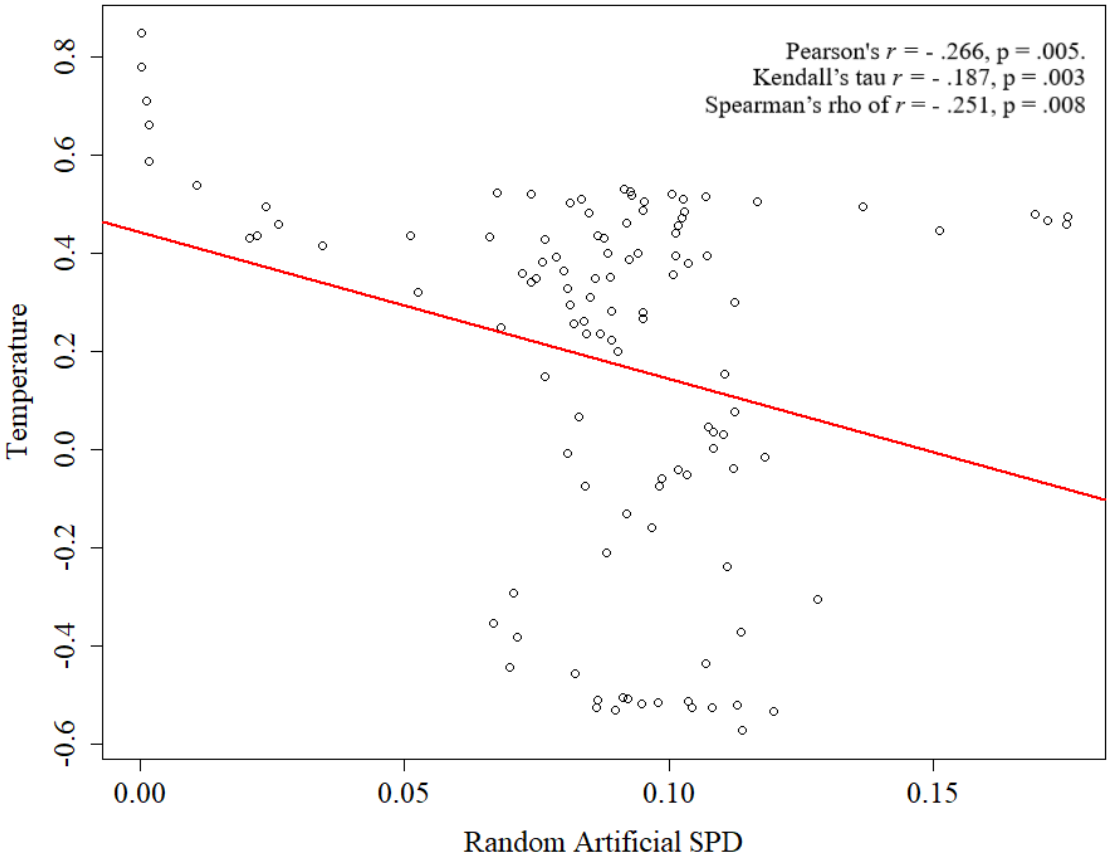

Figure 23. Randomly distributed artificial dataset and temperature scatterplot.

The uniform artificial dataset also lacked a visual relationship with the environmental reconstructions (Figures 24, 25). The Pearson correlation between the uniform SPD and moisture deficit was very weak at r = .007, and nonsignificant at p = .941. This result was consistent across the nonparametric tests, with a Kendall's tau of r = .034, p = .595, and a Spearman's rho of r = 0.47, p = .625. For temperature, the Pearson correlation resulted in r = - .398, p < .01. The nonparametric tests were also significant, with a Kendall's tau of r = - .227, p < .01, and a Spearman's rho of r = -.332, p < .01.

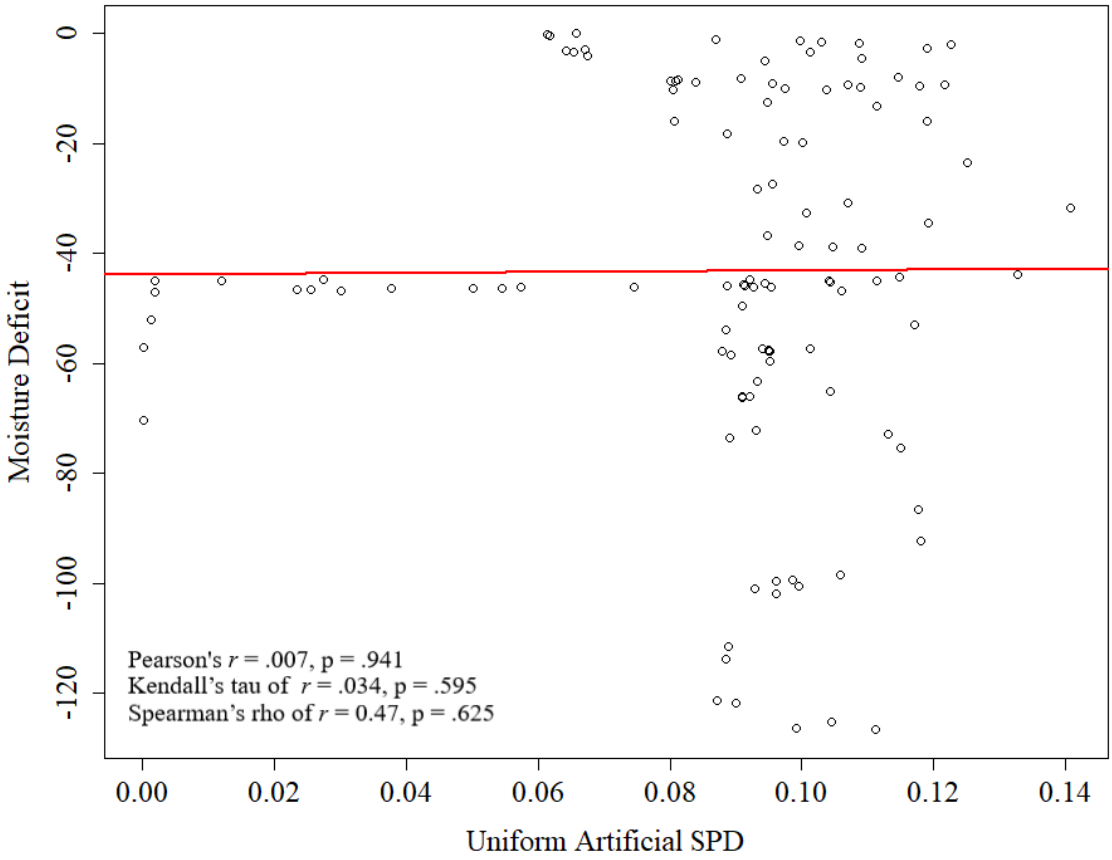

Figure 24. Uniformly distributed artificial dataset and moisture deficit scatterplot

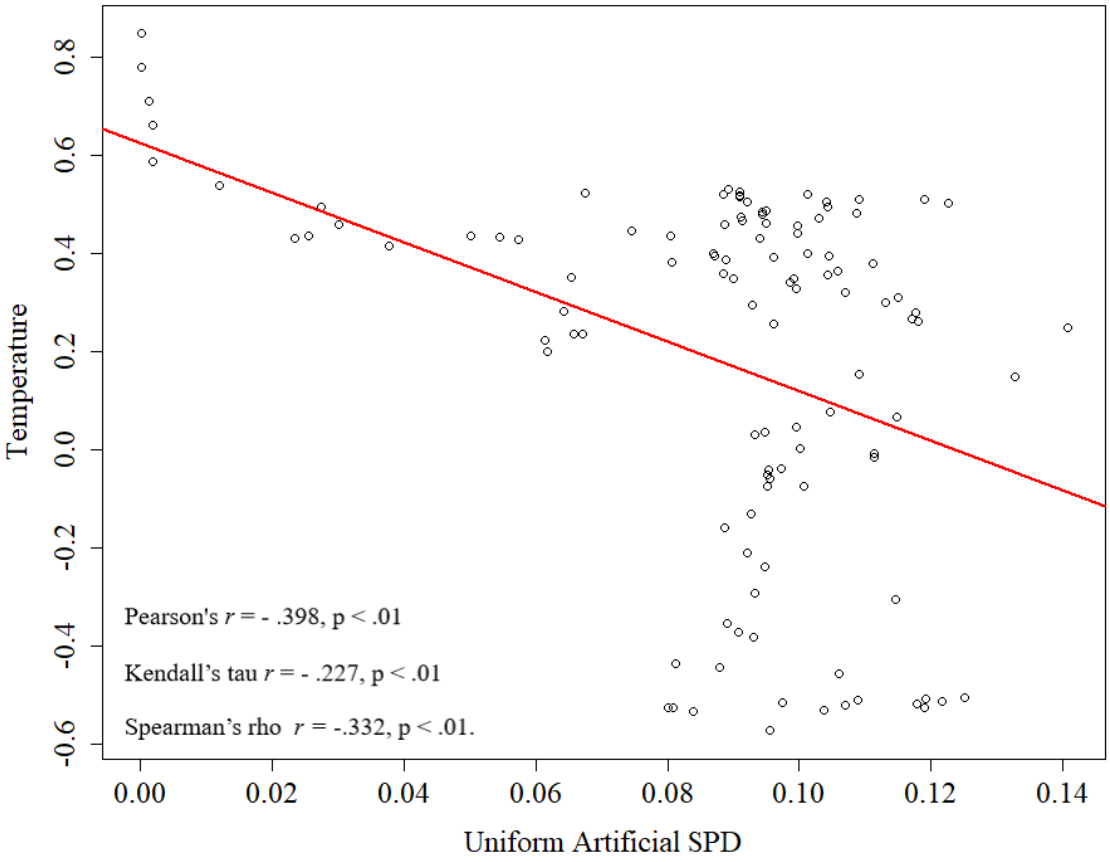

Figure 25. Uniformly distributed artificial dataset and temperature scatterplot

Finally, I ran parametric and non-parametric correlations between moisture deficit, temperature, and the tipi ring site SPD lagged at 50 and 100 years. All correlations were significant at $p < .01$. These test results, as well as the direct correlations previously noted, are listed below in table 5. The test results including the bootstrapped confidence intervals are attached in Appendix A.

Table 5. Tipi ring site SPD Correlation Results

	Moisture			Temperature		
	Pearson's	Kendall's tau	Spearman's rho	Pearson's	Kendall's tau	Spearman's rho
Tipi ring site SPD	.398**	.202**	.271**	-0.707**	-.301**	-.468**
50-year lag	.516**	.371*	.578**	-.660**	-.395**	-.574**
100-year lag	.511**	.371**	.569**	-.706**	-.417**	-.603**
Uniform artificial data	.007	.034	.47	-.398**	-.227**	-.332**
Random artificial data	0.138	.144*	.238*	-0.266**	-.187**	-.251**

*$\alpha < 0.05$

** $\alpha < 0.01$

Despite my previous tests determining overrepresentation is not a significant issue in this dataset, I opted to run these correlations with the SPD created from the dataset corrected for radiocarbon sample overrepresentation. These relationships were also analyzed at 50- and 100-year lags; as above, the datasets merited nonparametric correlation analyses. These correlations were run with the same parameters as the uncorrected tipi ring site SPD to allow comparisons. The correlation results are listed below in Table 6, while the bootstrapped confidence intervals are visualized in Figures 26 and 27.

Table 6. Overrepresentation Correction Correlation Results

	Moisture			Temperature		
	Pearson's	Kendall's tau	Spearman's rho	Pearson's	Kendall's tau	Spearman's rho
Overrepresentation	.543**	.357**	.580**	-.586**	-.390**	-.547**
50-year lag	.552**	.364*	.598**	-.538**	-.376**	-.529**
100-year lag	.565**	.373**	.612**	-.489**	-.373**	-.517**
Uniform artificial data	.007	.034	.047	-.398**	-.227**	-.332**
Random artificial data	0.138	.144*	.238*	-0.266**	-.187**	-.251**

* $\alpha < 0.05$

** $\alpha < 0.01$

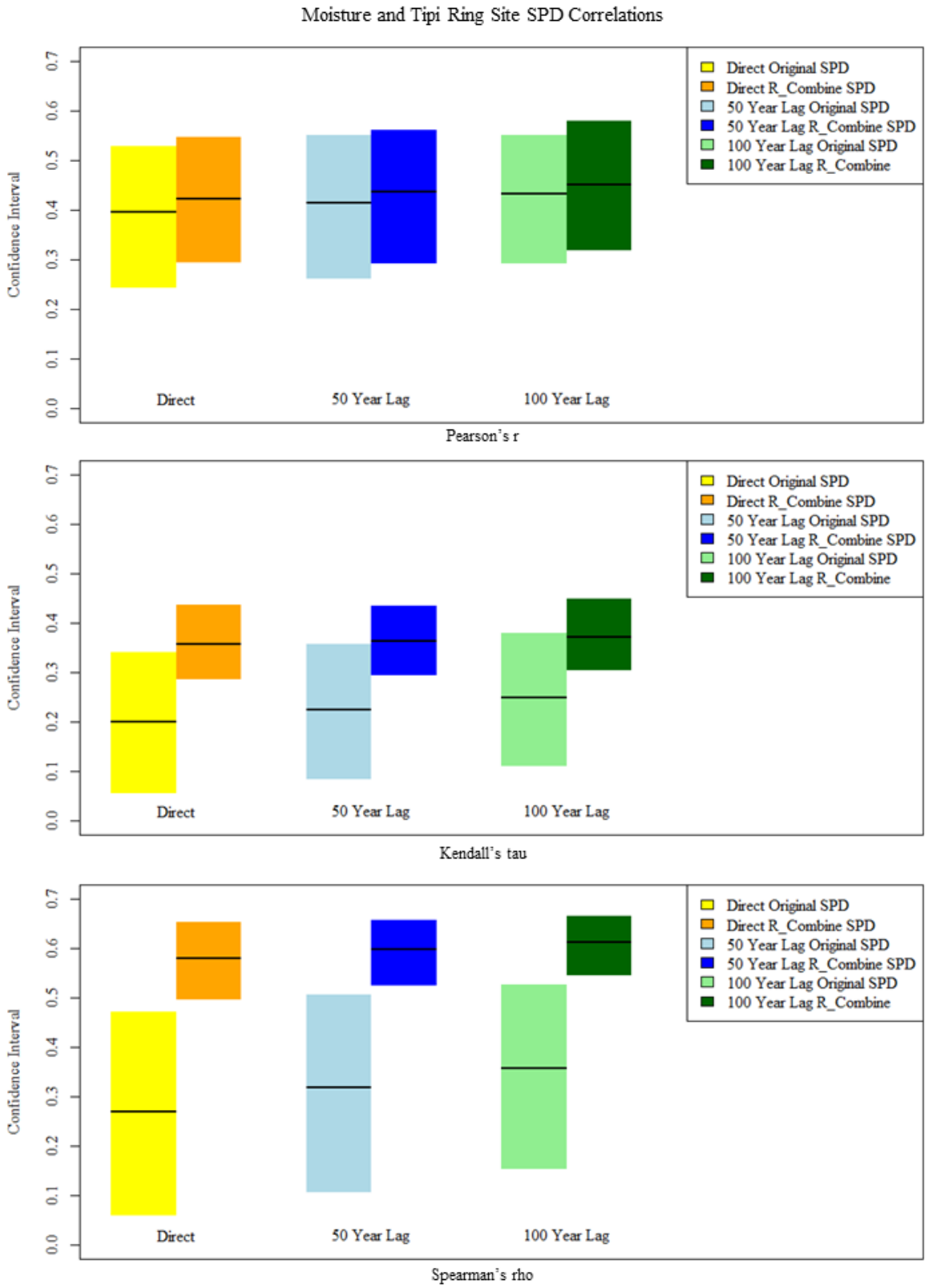

Figure 26. Moisture and tipi ring site SPD correlations - original and corrected. The r value is identified by a black line, while the confidence intervals are identified by color blocks.

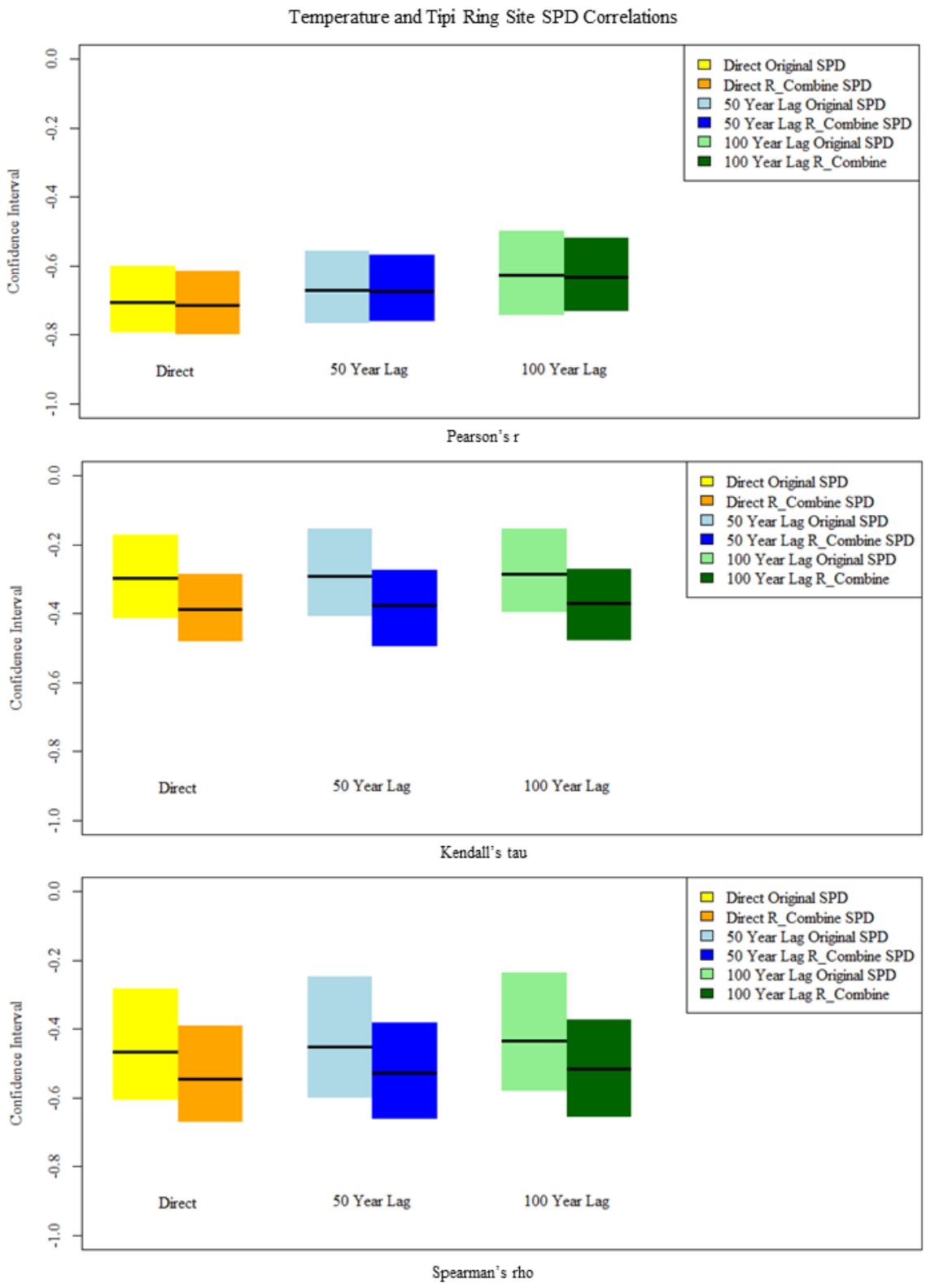

Figure 27. Temperature and tipi ring site SPD correlations - original and corrected. The r value is identified by a black line, while the confidence intervals are identified by color blocks.

Although these correlations provide us with a broad sense of possible relationships between these datasets, the actual relationship necessitates further investigation. Are there periods during which strong and/or significant correlations occur? I used a sliding correlation analysis for a deeper look at the relationship between environment and mobility. I calculated the Pearson's correlations at 150- and 200-year scales at one-to-one and lagged 50- and 100-year intervals, to account for possible delays between environmental and behavioral changes (Robinson et al. 2013). At such small sample sizes (n= 3 and n=4), it is unclear whether nonparametric correlation tests would improve accuracy. Ideally, I would assess these relationships at 50- or 100-year intervals using 1-year bins; however, the paleoenvironmental reconstructions have been reported at 50-year intervals and represent the smallest bins in these correlations.

When assessing whether significant correlations may be found within specific temporal periods, additional tests may be beneficial, since tests of significance are necessary. P-P plots for the three datasets determined that none fits a normal correlation. A lack of normality does not affect the correlation tests used, but it does affect confidence intervals and significance tests (Field 2013:271). These parameters are crucial to these analyses. When comparing multiple correlations across time periods, it is not enough to simply determine that a correlation is strong because the coefficient is closer to 1, but one must also determine whether a correlation is significant. I calculated the *p* values for each test, and compared these to the appropriate α value. Once again, I applied the Bonferroni correction—the 150-year intervals result in 110 tests, therefore $\alpha = 9.09091E\text{-}05$. The 200-year intervals result in 109 tests, therefore $\alpha = 9.17431E\text{-}05$. These results are included in Appendix B.

At these α values, there are no significant correlations for either environmental proxy at any time interval or lag. Due to these results, I revisited the correlation values at the more forgiving $\alpha = 0.01$ level. The tipi ring site SPD and moisture deficit correlation resulted in six significant periods. These periods all have strong correlations of $-.99 \geq r \geq .99$, with positive and negative correlations resulting within the same lag period. For the temperature reconstruction, eight significant periods were identified. These periods all have strong correlations of $-.99 \geq r \geq .99$ at the 150-year interval level, with consistent $r \leq -.99$ results at the 200-year interval level. The significant periods are listed below in tables 7 and 8.

Table 7. Sliding Window Correlation Results, 150-Year Period

150-Year Intervals												
Significance			Moisture					Temperature				
Level	Direct	r =	Lagged 50 Years	r =	Lagged 100 Years	r =	Direct	r =	Lagged 50 Years	r =	Lagged 100 Years	r =
Bonferroni	None		None		None		None		None		None	
0.01	None		900-1049	-0.99	2650-2799	0.99	550-699	0.99	2850-2999	0.99	4700-4849	0.99
			3100-3249	0.99	2950-3099	-0.99	3050-3199	-0.99	2950-3099	-0.99	4850-4999	-0.99
					3500-3649	0.99						

Table 8. Sliding Windows Correlation Results, 200-Year Period

	200-Year Intervals									
Significance	Moisture					Temperature				
Level	Direct	r =	Lagged 50 Years	r =	Lagged 100 Years	r =	Direct	r =	Lagged 50 Years	r =	Lagged 100 Years	r =
Bonferroni	None		None		None		None		None		None	
0.01	None		None		4850-5049	-0.99	2950-3199	.-99	None		3050-3249	.-99

These periods were then assessed against the uniform probability distribution for possible independence from the calibration curve. The uniform SPD was calculated using 1-year bins, therefore rather than simply assessing the exact period identified in tables 7 and 8, correlations in the 50 years prior and after in the uniform SPD are compared for potential significance, resulting in 250-350 year comparison windows.

I identified nonsignificant correlations between the tipi ring site SPD and the uniform artificial SPD using alpha values modified using the Bonferroni correction. The more non-significant correlations, the greater chance of independence from the underlying calibration curve. Within each 150 to 200 year period with a significant correlation to moisture and temperature, however, I was able to identify very few time periods in which the calibration curve's effect could be discounted.

Table 9. Significant Correlation Windows

Number of Correlation Windows	Time Period Years BP	Number of Non-Significant Correlations	Non-significant Correlation Period Years BP
250	500-749	69	515-528, 644-681, 697-713
250	850-1099	43	850-858, 887-916, 1083-1086
250	2600-2849	57	2628-2638, 2662-2683, 2758-2766, 2776-2790
250	2800-3049	8	2949-2956
250	2900-3149	8	2949-2956
350	2900-3249	35	2949-2956, 3171-3196
250	3000-3249	26	3171-3196
250	3049-3299	26	3171-3196
250	3449-3699	50	3545-3586, 3629-3636
250	4650-4899	53	4650-4675, 4780-4806
250	4800-5049	18	4800-4806, 5034-5044
300	4800-5099	18	4800-4806, 5034-5044

* α Value for 250 is .0004. α Value for 300 is .0000334. α Value for 350 is .0000286.

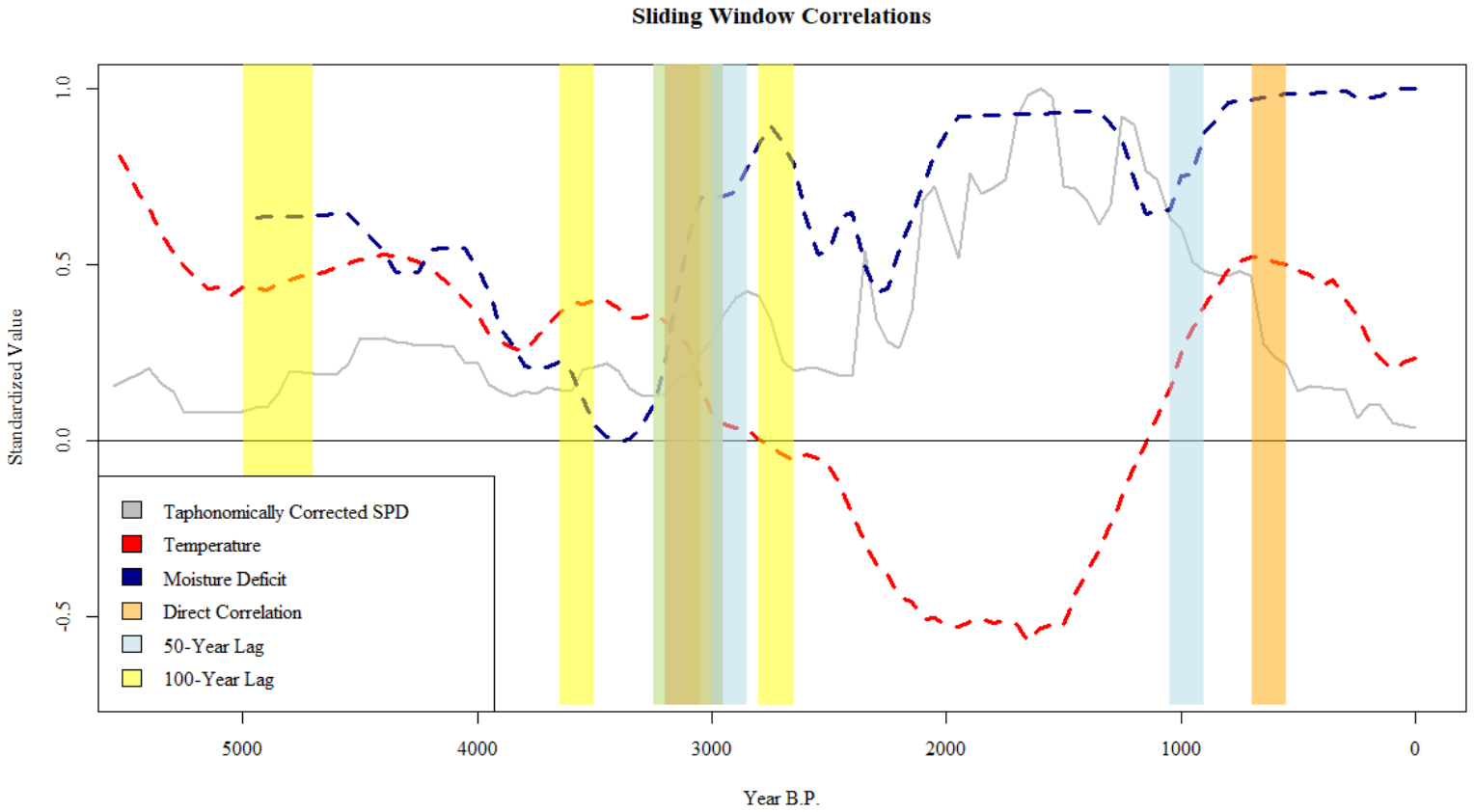

Figure 28. Significant correlation windows

CHAPTER FIVE:

DISCUSSION

Although the primary goal of this research was to identify whether prehistoric mobility in the Northwestern Plains and Central Rockies meets the expectations of the patch choice model by comparing a tipi ring site SPD to paleoenvironmental reconstructions, the journey to this comparison produced a significant amount of data. In addition to data, this project also raised additional questions about steps and analyses necessary for this method. I explore my results, and my resulting questions, below.

Prior to comparing my SPD with the available paleoenvironmental reconstructions, I took a moment to study my radiocarbon database, derived from tipi ring sites, against itself and radiocarbon data representing a broad sample of cultural sites throughout Wyoming and Montana, obtained from the CARD database. The site record data I used revealed a discrepancy between site ages calculated from radiocarbon samples and those deduced from diagnostic artifacts. A bar graph comparing the two standardized datasets revealed that the diagnostically derived cultural periods and the radiocarbon data have similar patterns that are, however, not temporally synched. The origin of this discrepancy is unclear, although likely factors are research biases in radiocarbon dating, the interpretation of diagnostic tools, or other subjective decisions when assigning cultural periods. Most valuable in these data is the visual representation of increasing frequencies through time across both datasets, which may reflect population growth and/or the effects of taphonomic bias. If the discrepancy arises from biases, it further justifies the corrections necessary prior to proxy comparisons.

Another important variable, elevation, merits further attention when discussing mobility and climatic variability in future research. Within the context of this project, statistical analyses failed to determine a significant pattern between site age and elevation. However, it is apparent that most tipi ring sites in this database were located between 4000 and 6000 ft. ASL. In some respects, this merely reflects Wyoming's geography; Montana's geography is considered secondary in this case, as only four tipi ring sites from the state contributed elevation data. Wyoming's average elevation is 6000 feet when its mountain ranges are excluded, with the northern portion of the state located at about 3500 feet ASL (Curtis and Grimes 2004). On the other hand, elevation data from the CARD database, filtered to reflect the same geographic areas, produced different results. This result further supports stating that 4000-6000 ft. elevations are more common locations for tipi ring habitation sites. However, other hereto unavailable variables, such as seasonality determined from pollen studies, or clustering of elevations by geographic region, may provide additional explanatory information about tipi ring elevations in the future. Elevation is a crucial environmental factor in the context of patch choice calculations and seasonal behaviors, and should be explored further.

Aside from data reflecting prehistoric behaviors, I also compared the frequency of radiocarbon dating itself across tipi ring sites. The resulting histogram makes it readily apparent that radiocarbon dating peaked in the 1980s and decreased in the 1990s and 2000s. This may reflect multiple factors, such as a continuing lack of interest in tipi ring research, increasing work by private cultural resource management firms and a lack of publicly available data, a decrease of tipi ring sites on the landscape due to their destruction or deterioration over time, or a shift toward other dating techniques. This could also result from issues with state data repositories, which may have outdated databases. Although radiocarbon dating techniques

have improved and become more widely available and affordable, the analysis dates for the tipi ring site radiocarbon database show that it has not benefitted from this technological progress, with a mean and median analysis age of 1992. Comparative data from CARD were not available for analysis, unfortunately, as it would have been interesting to determine whether this pattern is generalized across Wyoming and Montana, or limited to tipi ring sites.

On a similar note, I was able to study the radiocarbon sample material used for both tipi ring sites and across the CARD database. Results for both databases were strikingly similar. Both databases suffer from a lack of information for nearly a quarter of their dates, reflecting the poor state of this archaeological data. In order to use radiocarbon ages as a data category, we must ensure that current and future research includes all relevant variables for radiocarbon samples, and attempt to obtain these data for past radiocarbon ages, where possible.

The prevalence of charred material within both databases, over 60% in each case, highlights a potential issue with radiocarbon dating overall. Charred material, whether charcoal or otherwise, does not always have clear cultural origins. Crombé et al. (2013) explore the issue of open-air sites, similar to tipi ring sites. They recommend using charcoal from short-lived plant species located in hearths, calcined bone, and crusts on ceramics and other artifacts, concluding that to rely on radiocarbon ages from a single feature type, such as hearths, provides an incomplete and biased picture of the past (Crombé et al. 2013:599). This cannot be corrected in this particular study, but if we seek to maximize the value of this dating technique within the archaeological field, we must take heed.

Although the tipi ring site database provided some information about prehistoric behavior and current research practices, it required further manipulation to correct for the

potential biases of overrepresentation and taphonomic loss. For the former, Mann-Whitney U and Kolmogorov-Smirnov statistical tests determined that the original dataset and the dataset corrected for potential overrepresentation were not significantly statistically different. Overrepresentation among tipi ring sites is difficult to identify, as an area with 20 tipi rings could represent 20, 5 10, 2, or 1 target event due to reuse of favorable occupation areas creating archaeological palimpsests. Multiple radiocarbon ages within a tipi ring site could overlap temporally because they represent the same event or because the uncertainty of radiocarbon dating could not distinguish between occupation events taking place in different years or decades.

To truly address overrepresentation, researchers need to include detailed provenience and stratigraphic information for tipi ring sites, details which may be scarce at open-air sites. These results reveal that overrepresentation is less of an issue in this context than insufficient information and assumptions of contemporaneity applied uncritically. In the future, researchers must address these shortcomings, but in the short term it is more reasonable to assume that radiocarbon samples obtained from different features within the same site may represent different events and should be considered individually rather than statistically combined.

Just as overrepresentation is difficult to identify within the tipi ring context, so are the effects of taphonomic bias. It is difficult to argue that datable carbon materials at tipi ring sites have not been subject to taphonomic loss. These data do not show a consistent exponential growth pattern; however, they have the same drop off at 1000 years BP that was identified in the Surovell et al. (2009) data. Whether this results from taphonomic loss or other issues within the database, such as research bias favoring older sites and obscuring taphonomic effects, is

difficult to determine. As open-air sites, tipi rings may not be subject to the same taphonomic patterns identified in other contexts.

Researchers caution judicious use of techniques addressing overrepresentation and taphonomic loss, and the evidence in this case supports this. Statistical tests conducted for this research indicate that correcting for overrepresentation and taphonomic loss will not yield significantly different results for this database. However, as the paleoenvironmental proxies utilized in this study were subject to taphonomic correction, the corrected database was used for subsequent analyses. This is another instance of unquantifiable uncertainty necessary within this research. In order to ensure appropriate consideration for overrepresentation, a version of the database corrected for both overrepresentation and taphonomic bias was also analyzed in this study.

The tipi ring database had to be assessed, and wherever possible corrected, for biases arising from radiocarbon analyses, sampling issues, overrepresentation, taphonomic loss, patterns arising from the underlying calibration curve, and comparisons between proxies. While several methods are available to address the calibration curve, the one used in this study created two artificial datasets representing robust uniform and random distributions consisting of simulated radiocarbon dates summed over 10,000 MCMC iterations. This artificial dataset is meant to reveal the underlying radiocarbon calibration curve, but it should also represent unpatterned prehistoric occupation events on the landscape over the past 5000 years. While some researchers advocate the evenly distributed artificial dataset, others argue that a comparative dataset must be subjected to the same random sampling and taphonomic loss affecting datasets such as the tipi ring radiocarbon database (Contreras and Meadows 2014). The artificial dataset is meant to identify fluctuations within SPDs that arise from the

calibration curve; however, the different methods available yield different results and therefore differing interpretations. The difference between the two is important but the significance of using one over the other is unquantifiable in terms of results. A researcher's methodological preferences will inevitably affect results. This introduces further uncertainty when seeking to establish whether relationships exist between mobility and climatic change by using the available radiocarbon and paleoenvironmental data.

Despite these uncertainties, we can only utilize the information and tools at hand. The artificial dataset, despite its potential issues, is statistically strong because it represents the aggregate of 10,000 radiocarbon calibrations and averages these to reveal the underlying radiocarbon calibration curve. In this case, I chose the uniform distribution due to its higher correlation with the tipi ring site dataset as a conservative approach. Several methods also exist to compare the tipi ring site and artificial datasets; in this case I also opted for the more conservative running correlation method. There is a risk that these decisions ultimately obscured the relationships this research sought to identify.

Each paleoenvironmental reconstruction is expected to have an individual relationship with mobility, however, temperature and the moisture deficit are incontrovertibly linked, and similar correlation periods are expected. The hypothesis presented in this paper predicts that as temperature increases, resulting in drier and hotter periods and decreasing resource availability, mobility will decrease. This should present as a negative correlation. Temporal periods indicating a negative correlation between temperature and the tipi ring site SPD were identified over eight periods, between 2950-3249 years BP, at various lags and intervals, as well as at 4850-4999 years BP. However, contrary to expectations, temporal periods with a positive correlation between temperature and the SPD were also identified between 550-699

years BP, 2950-3099 years BP, and 4700-4849 years BP. The primary significant negative correlation periods between temperature and the tipi ring site SPD are continuous with significant *positive* correlation periods. This inconsistency casts doubt over the predicted relationship, at least at the 150- and 200-year scales with this data resolution. It is interesting to note that, within these periods with significant correlations, smaller periods of decades to centuries were identified that appear independent from the calibration curve (Table 9). However, it may be possible to identify periods of independence from the calibration curve in other 250- to 350-year periods independent of any correlations between temperature and the tipi ring site SPD.

When considering moisture deficit, the hypothesis would be that as the deficit increases, in this case decreasing in negative value, signaling drier conditions and subsequent decreasing resource availability, mobility should decrease. Due to the negative values used to calculate moisture deficit, this would result in a positive correlation. Of the six significant correlations identified, three were negative and three were positive. The correlation results between moisture deficit and the tipi ring site SPD are as inconsistent as those for temperature.

The fine-scale correlations between the paleoenvironmental reconstructions and the mobility proxy are inconsistent with our expectations, as well as within results for lag and the direction of correlation. Considering the numerous variables affecting mobility, perhaps it deviated from our expectations in the recent past due to reasons beyond climate change, such as increasing sedentism associated with increasing population (Binford 2001; Kelly 2013). Unfortunately, these results give little indication of the actual relationship between mobility and climate change and do not allow us to form predictions on a fine-grained scale.

On the larger scale, however, the tipi ring site SPD correlates with both temperature and moisture deficit and these correlations meet our expectations. Comparisons with the artificial datasets indicate either no or very weak correlations with the moisture deficit reconstructions. While significant correlations do occur between the artificial datasets and the temperature reconstruction, the correlation coefficient is always weaker than the tipi ring site SPD's correlation results. This increases confidence in the conclusion that, although fine resolution relationships could not be identified in this study, a larger relationship between past mobility and climate variability remains apparent even after corrections and considerations for biases are resolved.

Unfortunately, lagging the relationship 50 and 100 years did not yield different correlation values, particularly when considering the confidence intervals produced by bootstrapping the correlation tests. However, correcting for overrepresentation appears to increase the strength of the correlations when using nonparametric correlation tests, as seen in Figures 26 and 27. My primary concern with overrepresentation was that it might create a spurious pattern. In this case, the results are more conservative without correcting for overrepresentation. The most conservative correlations result from the Kendall's tau correlation tests, although the most *consistent* results between the original and overrepresentation corrections were produced by the Pearson's r correlation tests.

Ultimately, although the correlation test may slightly increase in strength depending on the correlation test used, these results remain consistent. These correlations are a first step to further research, and in this paper a theory-driven relationship between climatic change and mobility has been posited which appears supported by a statistical relationship in these data. Further refinement of the data, and the applied models, may clarify these results.

Most researchers using SPDs in archaeology use radiocarbon dates as proxies for prehistoric population change (Bamforth and Grund 2012:1769). However, the models used in demographic studies, such as exponential and logistic growth models (Brown 2017a; Williams 2012) are not directly applicable to mobility. Researchers studying demographics have yet to determine how to distinguish it from mobility (French and Collins 2015), and as is apparent in this case, the converse is the same. Perhaps once this has been resolved, the present research question will be easier to answer.

As methods improve, so should the underlying dataset. Williams (2012) suggests a minimum dataset size below which results should be considered provisional; operating with a dataset that is too small may minimize our ability to identify real patterns from spurious ones (McLaughlin 2018). This database can and should be expanded to at least 500 radiocarbon dates, preferably more, with continued attention given to chronometric hygiene and matching of the radiocarbon sample with the intended target event.

Future steps should also consider the study area's flora and fauna and the thresholds at which climatic changes affect their distribution and availability on the landscape (Rohling 2016), as well as the lag period between decreasing resources and decreasing mobility (Smith et al. 2008), examples of which may perhaps be present in ethnographic studies. Additional high-resolution proxies should be considered (Tallavaara and Pesonen 2018; Wang et al. 2014), and these should be binned at smaller periods to allow for greater statistical power when comparing data, as opposed to the available sample sizes of n=3 or n=4 when considering fine-grained temporal scales. This might also allow for identification of processes that occur over years, decades, or a century (Shennan 2013:302), such as changes in mobility patterns. If such fine-grained paleoenvironmental proxies are not available, Contreras et al. (2018) have

recently written about downscaling, the practice of using modern environmental data to supplement paleoenvironmental reconstructions and create a predictive model of environmental data at yearly or even monthly scales. Downscaling, in combination with a larger tipi ring site dataset, might allow for the identification of past human behavior change.

While numerous methods exist to determine whether the tipi ring site SPD reflects past human behavior rather than stochastic processes, taphonomic loss or the radiocarbon calibration curve, the crucial comparisons occur after these steps, when the SPD is compared to paleoenvironmental reconstruction. Beyond visual assessments, running correlations present one way of comparing time-series; however, as seen above, this increases the risk of Type II errors and leads to a much smaller alpha value when determining significance to mitigate this risk. Improved change point detection may provide a useful future alternate statistical test (Bevan 2015; Robinson et al. 2007), while methods such as kernel density estimation may provide alternate methods to SPDs yet answer similar questions (Brown 2017b; Chaput et al. 2015; McLaughlin 2018).

The first steps necessary to this process are ultimately increasing the size of the radiocarbon dataset and obtaining more proxies and fine-grained paleoenvironmental data, which may, when subjected to the same methods outlined in this research, present a first-order estimation of past mobility changes in the Wyoming and Montana region in relation to climate variability. Even with these improvements, the aforementioned biases and the difficulties associated with separating signal from noise will remain, particularly when using probabilistic proxies for both mobility and climate signals at the human scale. However, these attempts have merit and a wide and growing body of methods within archaeology and neighboring fields such as climatology and economics are available and will continue to advance. There is a

statistically significant correlation between prehistoric mobility, temperature and moisture deficit in Wyoming Montana; it remains to be seen how this correlation can be further refined and understood.

CHAPTER SIX:

CONCLUSION

Tipi ring sites are a widespread and understudied archaeological feature which may be easily and affordably radiocarbon dated. Existing radiocarbon analyses throughout Montana and Wyoming allowed for the creation of a large database dating tipi ring sites. Radiocarbon ages for these sites, although often the result of palimpsests, represent a sample of prehistoric behavior. While many archaeological projects using radiocarbon ages as samples of a larger population interpret these as representative of prehistoric demographics, limiting this database to tipi ring sites makes a stronger case for an alternate interpretation, that these represent prehistoric occupation events, and therefore a proxy for mobility.

The extensive availability of these data, as well as the availability of two regional paleoenvironmental reconstructions, allowed us to ask whether mobility might be subject to the predictions of the patch choice model. While the question, and ecological consequences, are fairly straightforward, the data and analyses necessary to answer it introduce uncertainty and bias nearly every step of the way. Previous research utilizing radiocarbon dates as data, creating SPDs, and comparing these to other proxies, necessitate explicit acknowledgement of constraints and biases. Overall, researchers call for judgement and caution (Contreras and Meadows 2014; Robinson et al. 2013; Surovell and Brantingham 2007).

Taking into account constraints, biases, and using a fair amount of caution, the results of a moving correlation between a tipi ring site SPD and two paleoenvironmental reconstructions were inconclusive and inconsistent. While some correlations met hypothesized expectations, others with the same statistical significance level directly

contradicted them. However, correlations between the reconstructions and the tipi ring site SPD across the 5000-year study period met hypothesized expectations. The relationships hypothesized in this study exist; they must be used as a foundation to further explore the relationship between climatic change and mobility at a fine-grained scale.

As the methods used above have been successful for researchers exploring similar questions, I believe that they may provide finer-grained, more statistically robust answers to this research question in the future. Subsequent projects must increase the size of the tipi ring radiocarbon database. Additional paleoenvironmental proxies should be compared with the tipi ring site SPD as these become available. As methods to identify the effects of the calibration curve are refined, these should be applied, but rather than choosing a singular method, the efficacy of each should be compared. Similarly, as statistical avenues that allow for better distinction of significant relationships among moving correlations are developed, these should be adopted and applied at multiple scales.

Finally, other avenues should also be utilized, such as taking into consideration site elevations and pollen analyses that can provide seasonality data for sites, or using data from thoroughly studied sites such that comparisons between large and small camps can be made. Although these methods could not offer a satisfying resolution to the question at hand, they highlight that as our information about tipi rings increases in quantity and quality, our ability to answer questions about prehistoric behaviors in these regions increases as well.

REFERENCES CITED

Baillie, M. G. L.
1991 Suck-in and Smear: Two Related Chronological Problems for the 90s. *Journal of Theoretical Archaeology* 2:12-16

Bamforth, Douglas B. and Brigid Grund.
2012 Radiocarbon Calibration Curves, Summed Probability Distributions, and Early Paleoindian Population Trends in North America. *Journal of Archaeological Science* 39:1768-1774.

Banks, Kimball M. and J. Signe Snortland
1995 Every Picture Tells a Story: Historic Images, Tipi Camps, and Archaeology. *Plains Anthropologist* 40:124-144.

Beardsley, Richard K., Preston Holder, Alex D. Krieger, Betty J. Meggers, John B. Rinaldo and Paul Kutsche
1956 Functional and Evolutionary Implications of Community Patterning. In *Seminars in Archaeology*, edited by Robert Wauchope, pp. 129-158. SAA, Memoir No. 11. Salt Lake City.

Bevan, Andrew
2015 The Data Deluge. *Antiquity* 89:1473-1484.

Binford, Lewis R.
1980 Willow Smoke and Dogs' Tails: Hunter-Gatherer Settlement Systems and Archaeological Site Formation. *American Antiquity* 45:4-20.

2001. *Constructing Frames of Reference: an Analytical Method for Archaeological Theory Building Using Ethnographic and Environmental Data Sets*. University of California Press, Berkeley.

Bird, Douglas W. and James F. O'Connell
2006 Behavioral Ecology and Archaeology. *Journal of Archaeological Research* 14:143-188.

Box-Steffensmeier, Janet M., Freeman, John R., Hitt, Matthew P., and Pevehouse, Jon C.W.
2014 *Time Series Analysis for the Social Sciences.* Cambridge University Press, Cambridge.

Bradtmöller, Marcel, Andreas Pastoors, Berhard Weninger, and Gerd-Christian Weniger.
2012 The Repeated Replacement Model – Rapid Climate Change and Population Dynamics in Late Pleistocene Europe. *Quaternary International* 247:38-49.

Brasser, Ted J.
1983 The Tipi as an Element in the Emergence of Historic Plains Indian Nomadism.

Plains Anthropologist 28:309-321.

Bronk Ramsey, Christopher
2009 Bayesian Analysis of Radiocarbon Dates. *Radiocarbon* 51:337-360.

Brown, William A.
2017a The Past and Future of Growth Rate Estimation in Demographic Temporal Frequency Analysis: Biodemographic Interpretability and the Ascendance of Dynamic Growth Models. *Journal of Archaeological Science* 80:96-108

2017b They Don't Look Different, but They're Not the Same: Formal Resemblance and Interpretive Disparity in the Construction of Temporal Frequency Distributions. Preprint available via arXiv:1708.00535.

2015 Through a Filter, Darkly: Population Size Estimation, Systematic Error, and Random Error in Radiocarbon-Supported Demographic Temporal Frequency Analysis. *Journal of Archaeological Science* 53: 133–147.

Chaput, Michelle A., Bjorn Kriesche, Matthews Betts, Andrew Martindale, Rafal Kulik, Volker Schmidt, and Konrad Gajewski.
2015 Spatiotemporal Distribution of Holocene Populations in North America. *Proceedings of the National Academy of Sciences* 112:12127-12132.

Charnov, Eric L.
1976 Optimal Foraging, the Marginal Value Theorem. *Theoretical Population Biology* 9:129-136.

Cobb, Charles R., Anthony M. Krus, and Dawnie W. Steadman.
2015 Bayesian Modeling of the Occupation Span of the Averbuch Site in the Middle Cumberland Drainage, Tennessee. *Southeastern Archaeology* 34:46-56.

Collard, Mark, Kevan Edinborough, Stephen Shennan, and Mark G. Thomas
2010 Radiocarbon Evidence Indicates that Migrants Introduced Farming to Britain. *Journal of Archaeological Science* 37(4): 866–870.

Contreras, Daniel A., and John Meadows
2014 Summed Radiocarbon Calibrations as a Population Proxy: a Critical Evaluation Using a Realistic Simulation Approach. *Journal of Archaeological Science* 52: 591–608.

Contreras, Daniel A., Joel Guiot, Romain Suarez, and Alan Kirman
2018 Reaching the Human Scale: A Spatial and Temporal Downscaling Approach to the Archaeological Implications of Paleoclimate Data. *Journal of Archaeological Science* 93:54-67.

Crema, Enrico R.

2012 Modelling Temporal Uncertainty in Archaeological Analysis. *Journal of Archaeological Method and Theory* 19(3): 440–461.

Crombé, Philippe, and Erick Robinson
2014 14C Dates as Demographic Proxies in Neolithisation Models of Northwestern Europe: a Critical Assessment Using Belgium and Northeast France as a Case-Study. *Journal of Archaeological Science* 52: 558–566.

Dooley, Mathew A.
2004 Long-Term Hunter-Gatherer Land Use in Central North Dakota: An Environmental Analysis. *Plains Anthropologist* 49(190): 105–127.

Finnigan, James T.
1983 Tipi to Tipi Ring: A Transformational Model. *Plains Anthropologist* 28:16-28.

French, Jennifer C., and Christina Collins
2015 Upper Palaeolithic Population Histories of Southwestern France: a Comparison of the Demographic Signatures of 14C Date Distributions and Archaeological Site Counts. *Journal of Archaeological Science* 55: 122–134.

Field, Andy
2013 *Discovering Statistics Using IBM SPSS Statistics*. Sage, Los Angeles.

Frison, George
1983 Stone Circles, Stone-Filled Firepits, Grinding Stones and High Plains Archaeology. *Plains Anthropologist* 28:81-92.

1991 *Prehistoric Hunters of the High Plains*. Academic Press, San Diego.

Gragson, Ted L.
1983 A Preliminary Look at Stone Circle Site Distribution in Montana. *Plains Anthropologist* 28:139-145.

Good, Kent N and Lawrence L. Loendorf
1974 *The Results of the Archaeological Survey in the Grapevine Creek Area, Bighorn Canyon National Recreation Area 1972 Field Season.* University of North Dakota. Submitted to USDI National Park Service, Contract No. 4970P20444.

Holdaway, Simon, Patricia Fanning, and Ed Rhodes
2008 Challenging Intensification: Human–Environment Interactions in The Holocene Geoarchaeological Record from Western New South Wales, Australia. *The Holocene* 3: 403–412.

Kehoe, Thomas F.
1958 Tipi Rings: The "Direct Ethnological" Approach Applied to an Archaeological Problem. *American Anthropologist* 60:861-873.

Kelly, Robert L.
1995 *The Foraging Spectrum. Diversity in Hunter-Gatherer Lifeways*. Smithsonian Institution Press, Washington.

Kelly, Robert L., Todd A. Surovell, Bryan N. Shuman, and Geoffrey M. Smith
2013 A Continuous Climatic Impact on Holocene Human Population in the Rocky Mountains. *Proceedings of the National Academy of Sciences* 110(2): 443–447.

Kerr, Thomas R., and Finbar McCormick
2014 Statistics, Sunspots and Settlement: Influences on Sum of Probability Curves. *Journal of Archaeological Science* 41: 493–501.

Lau, Robert
2018 Stationary and Differencing. In *Statistical Forecasting: Notes on Regression and Time Series Analysis.* Electronic document, https://people.duke.edu/~rnau/411diff.htm, accessed 7/29/2018.

Loendorf, Lawrence L.
1969 *The Results of the Archaeological Survey in the Pryor Mountain Bighorn Canyon Area 1968 Field Season*. University of Missouri. Submitted to USDI National Park Service and University of Missouri, Montana, Missoula.

1970 Prehistoric Patterns of Campsite Selection in the Pryor Mountains, Montana. *Archaeology in Montana* 11:17-44.

1974 *The Results of the Archaeological Survey in the Pryor Mountain Bighorn Canyon Area 1971 Field Season*. University of North Dakota. Submitted to USDI National Park Service, USDI Bureau of Land Management, and USDA Forest Service, and the University of Missouri. Contract No. 2 920 P1 0016.

Malouf, Carling
1961 The Tipi Rings of the High Plains. *American Antiquity* 26:381-389.

Martindale, Andrew, Richard Morlan, Matthew Betts, Michael Blake, Konrad Gajewski, Michelle Chaput, Andrew Mason, and Pierre Vermeersch
2017 *Canadian Archaeological Radiocarbon Database (CARD 2.1*). Electronic database, www.canadianarchaeology.ca, accessed 10/22/2017.

McLaughlin, T. Rowan
2018 On Applications of Space-Time Modelling with Open-Source 14C Age Calibration. *Journal of Archaeological Method and Theory* 1:23.

Mobley, Charles M.
1983 A Statistical Analysis of Tipi Ring Diameters at Sites Near Santa Rosa, New Mexico. *Plains Anthropologist* 28:101-112.

Montgomery, Douglass C., Peck, Elizabeth A., Vining, Geoffrey G.
2010 *Introduction to Linear Regression Analysis.* John Wiley and Sons, Hoboken, NJ.

Munoz, Samuel E., Konrad Gajewski, Matthew C. Peros, and H. E. Wright
2010 Synchronous Environmental and Cultural Change in the Prehistory of the Northeastern United States. *Proceedings of the National Academy of Sciences* 51:22008-22013.

Muscio, Hernán J. and Gabriel E.J. Lopez
2016 Radiocarbon Dates and Anthropogenic Signal in the South-Central Andes (12,500-600 cal. years BP). *Journal of Archaeological Science* 65:93-102.

Murdock, George F.
1967 Ethnographic Atlas, A Summary. *Ethnology* 6:109-236.

Naudinot, Nicolas, Antonin Tomasso, Carlo Tozzi, and Marco Peresani
2014 Changes in Mobility Patterns as a Factor of 14C Date Density Variation in the Late Epigravettian of Northern Italy and Southeastern France. *Journal of Archaeological Science* 52: 578–590.

Oetelaar, Gerald A.
2000 Beyond Activity Areas: Structure and Symbolism in the Organization and Use of Space Inside Tipis. *Plains Anthropologist* 45:35-61.

Peros, Matthew C., Samuel E. Munoz, Konrad Gajewski, and André E. Viau
2010 Prehistoric Demography of North America Inferred from Radiocarbon Data. *J Journal of Archaeological Science* 37(3): 656–664.

R Studio Team
2015 *RStudio: Integrated Development for R.* RStudio, Inc., Boston, MA. http://www.rstudio.com/.

Ramsey, Christopher Bronk
2008 Deposition Models for Chronological Records. *Quaternary Science Reviews* 27(1–2):42–60.

Riede, Felix, and Kevan Edinborough
2012 Bayesian Radiocarbon Models for the Cultural Transition During the Allerød in Southern Scandinavia. *Journal of Archaeological Science* 39(3): 744–756.

Rick, John W.
1987 Dates as Data: An Examination of the Peruvian Preceramic Radiocarbon Record. *American Antiquity* 52:55-73.

Robinson, Erick, Mark Van Strydonck, Vanessa Gelorini, and Philippe Crombé

2013 Radiocarbon Chronology and the Correlation of Hunter-Gatherer Sociocultural Change with Abrupt Palaeoclimate Change: the Middle Mesolithic in the Rhine-Meuse-Scheldt Area of Northwest Europe. *Journal of Archaeological Science* 40(1): 755–763.

Robinson, Lucy F., Victor H. de la Peña, and Yochanan Kushnir
2007 Detecting Shifts in Correlation and Variability with Application to ENSO-Monsoon Rainfall Relationships. *Theoretical and Applied Climatology* 94:3-4.

Rohling, Eelco J.
2016 Of Lakes and Fields: A Framework for Reconciling Palaeoclimatic Drought Inferences with Archaeological Impacts. *Journal of Archaeological Science* 73:17-24.

Scheiber, Laura L. and Judson B. Finley
2010 Domestic Campsites and Cyber Landscapes in the Rocky Mountains. *Antiquity* 84:114-130

Shennan, Stephen
2013 Demographic Continuities and Discontinuities in Neolithic Europe: Evidence, Methods and Implications. *Journal of Archaeological Method and Theory* 20(2): 300–311.

Shuman, Bryan
2012 Recent Wyoming Temperature Trends, Their Drivers, and Impacts in a 14,000-Year Context. *Climatic Change* 112(2): 429–447.

Shuman, Bryan, Paul Pribyl, Thomas A. Minckley, and Jacqueline J. Shinker
2010 Rapid Hydrologic Shifts and Prolonged Droughts in Rocky Mountain Headwaters during the Holocene. *Geophysical Research Letters* 37(6): 1–5.

Smith, Mike
2016 Comment. The Use of Summed-Probability Plots of Radiocarbon Data in Archaeology. *Archaeology in Oceania* 51:214-219.

Smith, Mike A., Alan N. Williams, Chris S. M. Turney, and Matthew L. Cupper
2008 Human-Environment Interactions in Australian Drylands: Exploratory Time-Series Analysis of Archaeological Records. *The Holocene* 18:389-401.

Surovell, Todd A., and P. Jeffrey Brantingham
2007 A Note on the Use of Temporal Frequency Distributions in Studies of Prehistoric Demography. *Journal of Archaeological Science* 34(11): 1868–1877.

Surovell, Todd A., Judson Byrd Finley, Geoffrey M. Smith, P. Jeffrey Brantingham, and Robert Kelly
2009 Correcting Temporal Frequency Distributions for Taphonomic Bias. *Journal of Archaeological Science* 36(8): 1715–1724.

Tallavaara, Miikka and Petro Pesonen
2018 Human Ecodynamics in the North-West Coast of Finland 10,000–2000 Years Ago. *Quaternary International*, in press.

Tallavaara, Miikka, Petro Pesonen, and Markku Oinonen
2010 Prehistoric Population History in Eastern Fennoscandia. *Journal of Archaeological Science* 37(2): 251–260.

Telford, Richard.
2013 Running Correlations – Running into Problems. *Musings on Quantitative Palaeoecology* (blog), April 1, 2013 https://quantpalaeo.wordpress.com/2013/01/04/running-correlations-running-into-problems/, accessed April 8, 2018.

Timpson, Adrian, Katie Manning, and Stephen Shennan
2015 Inferential Mistakes in Population Proxies: A Response to Torfing's "Neolithic Population and Summed Probability Distribution of 14C-dates." *Journal of Archaeological Science* 63:199-202.

Van West, Carla R.
1979 *Data Base and Assessment of Archaeological Resources in Bighorn Canyon National Recreation Area*. Midwest Archaeological Center. Submitted to USDI National Park Service, Lincoln, Nebraska.

Wang, Can, Houyuan Lu, Jianping Zhang, Zhaoyan Gu, and Keyang He.
2014 Prehistoric Demographic Fluctuations in China Inferred from Radiocarbon Dasta and their Linkage with Climate Change over the Past 50,000 Years. *Quaternary Science Reviews* 98:45-59.

Waterbolk, Harm T.
1971 Working with Radiocarbon Dates. *Proceedings of the Prehistoric Society* 37(2): 15–33.

Williams, Alan N.
2012 The Use of Summed Radiocarbon Probability Distributions in Archaeology: a Review of Methods. *Journal of Archaeological Science* 39(3): 578–589.

Zahid, H. Jabran, Erick Robinson, and Robert L. Kelly
2016 Agriculture, Population Growth, and Statistical Analysis of the Radiocarbon Record. *Proceedings of the National Academy of Sciences* 113(4): 931–935.

Zedeño, Maria Nieves, Jesse AM Ballenger, and John R. Murray
2014 Landscape Engineering and Organizational Complexity Among Late Prehistoric Bison Hunters of the Northwestern Plains. *Current Anthropology* 55: 23–58.

APPENDICES

APPENDIX A: 5000-YEAR CORRELATION RESULTS

Correlations

				Tipi Ring Site SPD	RCombine SPD	Temperature	Moisture Deficit
Tipi Ring Site SPD	Pearson Correlation			1	.976**	-.707**	.398**
	Sig. (2-tailed)				.000	.000	.000
	N			112	112	112	112
	Bootstrap[c]	Bias		0	.000	.004	-.001
		Std. Error		0	.005	.048	.062
		BCa 95% Confidence Interval	Lower	.	.963	-.791	.280
			Upper	.	.985	-.599	.527
RCombine SPD	Pearson Correlation			.976**	1	-.715**	.425**
	Sig. (2-tailed)			.000		.000	.000
	N			112	112	112	112
	Bootstrap[c]	Bias		.000	0	.004	-.001
		Std. Error		.005	0	.045	.061
		BCa 95% Confidence Interval	Lower	.963	.	-.799	.306
			Upper	.985	.	-.609	.548
			Upper	.527	.548	-.160	.

**. Correlation is significant at the 0.01 level (2-tailed).

c. Unless otherwise noted, bootstrap results are based on 1000 bootstrap samples

Correlations

					Tipi Ring Site SPD	RCombine SPD	Temperature	Moisture Deficit
Kendall's tau_b	Tipi Ring Site SPD	Correlation Coefficient			1.000	.822**	-.301**	.202**
		Sig. (2-tailed)			.	.000	.000	.002
		N			112	112	112	112
		Bootstrap[c]	Bias		.000	.000	.002	-.002
			Std. Error		.000	.025	.067	.073
			BCa 95% Confidence Interval	Lower	.	.767	-.414	.053
				Upper	.	.870	-.167	.346
	RCombine SPD	Correlation Coefficient			.822**	1.000	-.330**	.220**
		Sig. (2-tailed)			.000	.	.000	.001
		N			112	112	112	112
		Bootstrap[c]	Bias		.000	.000	.003	.000
			Std. Error		.025	.000	.064	.067
			BCa 95% Confidence Interval	Lower	.767	.	-.446	.072
				Upper	.870	.	-.197	.355

**. Correlation is significant at the 0.01 level (2-tailed).

*. Correlation is significant at the 0.05 level (2-tailed).

c. Unless otherwise noted, bootstrap results are based on 1000 bootstrap samples

Correlations

					Tipi Ring Site SPD	RCombine SPD	Temperature	Moisture Deficit
Spearman's rho	Tipi Ring Site SPD	Correlation Coefficient			1.000	.946**	-.468**	.271**
		Sig. (2-tailed)			.	.000	.000	.004
		N			112	112	112	112
		Bootstrap[c]	Bias		.000	-.004	.007	-.003
			Std. Error		.000	.016	.085	.103
			BCa 95% Confidence Interval	Lower	.	.917	-.630	.079
				Upper	.	.963	-.284	.457
	RCombine SPD	Correlation Coefficient			.946**	1.000	-.519**	.319**
		Sig. (2-tailed)			.000	.	.000	.001
		N			112	112	112	112
		Bootstrap[c]	Bias		-.004	.000	.007	-.004
			Std. Error		.016	.000	.079	.095
			BCa 95% Confidence Interval	Lower	.917	.	-.669	.135
				Upper	.963	.	-.336	.491

**. Correlation is significant at the 0.01 level (2-tailed).

*. Correlation is significant at the 0.05 level (2-tailed).

c. Unless otherwise noted, bootstrap results are based on 1000 bootstrap samples

Correlations

				Tipi Ring Site SPD 50-Year Lag	RCombine SPD 50-Year Lag	Temperature	Moisture Deficit
Tipi Ring Site SPD 50-Year Lag	Pearson Correlation			1	.976**	-.674**	.415**
	Sig. (2-tailed)				.000	.000	.000
	N			112	112	112	112
	Bootstrap[c]	Bias		0	.000	.001	.001
		Std. Error		0	.005	.053	.060
		BCa 95% Confidence Interval	Lower	.	.965	-.768	.291
			Upper	.	.985	-.569	.537
RCombine SPD 50-Year Lag	Pearson Correlation			.976**	1	-.681**	.437**
	Sig. (2-tailed)			.000		.000	.000
	N			112	112	112	112
	Bootstrap[c]	Bias		.000	0	.001	.001
		Std. Error		.005	0	.050	.060
		BCa 95% Confidence Interval	Lower	.965	.	-.769	.320
			Upper	.985	.	-.580	.557

**. Correlation is significant at the 0.01 level (2-tailed).

c. Unless otherwise noted, bootstrap results are based on 1000 bootstrap samples

Correlations

					Tipi Ring Site SPD 50-Year Lag	RCombine SPD 50-Year Lag	Temperature	Moisture Deficit
Kendall's tau_b	Tipi Ring Site SPD 50-Year Lag	Correlation Coefficient			1.000	.822**	-.295**	.226**
		Sig. (2-tailed)			.	.000	.000	.000
		N			112	112	112	112
		Bootstrap[c]	Bias		.000	-.001	.000	.001
			Std. Error		.000	.026	.063	.067
			BCa 95% Confidence Interval	Lower	.	.763	-.410	.091
				Upper	.	.871	-.169	.358
	RCombine SPD 50-Year Lag	Correlation Coefficient			.822**	1.000	-.326**	.237**
		Sig. (2-tailed)			.000	.	.000	.000
		N			112	112	112	112
		Bootstrap[c]	Bias		-.001	.000	.001	.001
			Std. Error		.026	.000	.060	.060
			BCa 95% Confidence Interval	Lower	.763	.	-.431	.119
				Upper	.871	.	-.203	.358
				Upper	.358	.358	-.033	.

**. Correlation is significant at the 0.01 level (2-tailed).

*. Correlation is significant at the 0.05 level (2-tailed).

c. Unless otherwise noted, bootstrap results are based on 1000 bootstrap samples

Correlations

					Tipi Ring Site SPD 50-Year Lag	RCombine SPD 50-Year Lag	Temperature	Moisture Deficit
Spearman's rho	Tipi Ring Site SPD 50-Year Lag	Correlation Coefficient			1.000	.946**	-.456**	.320**
		Sig. (2-tailed)			.	.000	.000	.001
		N			112	112	112	112
		Bootstrap[c]	Bias		.000	-.003	.004	-.001
			Std. Error		.000	.016	.083	.103
			BCa 95% Confidence Interval	Lower	.	.911	-.603	.121
				Upper	.	.967	-.275	.516
	RCombine SPD 50-Year Lag	Correlation Coefficient			.946**	1.000	-.512**	.352**
		Sig. (2-tailed)			.000	.	.000	.000
		N			112	112	112	112
		Bootstrap[c]	Bias		-.003	.000	.006	-.001
			Std. Error		.016	.000	.078	.093
			BCa 95% Confidence Interval	Lower	.911	.	-.656	.176
				Upper	.967	.	-.337	.521

**. Correlation is significant at the 0.01 level (2-tailed).

*. Correlation is significant at the 0.05 level (2-tailed).

c. Unless otherwise noted, bootstrap results are based on 1000 bootstrap samples

Correlations

				Tipi Ring Site SPD 100-Year Lag	RCombine SPD 100-Year Lag	Temperature	Moisture Deficit
Tipi Ring Site SPD 100-Year Lag	Pearson Correlation			1	.976**	-.628**	.433**
	Sig. (2-tailed)				.000	.000	.000
	N			111	111	111	111
	Bootstrap[c]	Bias		0	.000	.003	.002
		Std. Error		0	.005	.061	.062
		BCa 95% Confidence Interval	Lower	.	.965	-.731	.306
			Upper	.	.984	-.500	.554
RCombine SPD 100-Year Lag	Pearson Correlation			.976**	1	-.635**	.451**
	Sig. (2-tailed)			.000		.000	.000
	N			111	111	111	111
	Bootstrap[c]	Bias		.000	0	.003	.002
		Std. Error		.005	0	.057	.060
		BCa 95% Confidence Interval	Lower	.965	.	-.737	.327
			Upper	.984	.	-.512	.568

**. Correlation is significant at the 0.01 level (2-tailed).

c. Unless otherwise noted, bootstrap results are based on 1000 bootstrap samples

Correlations

					Tipi Ring Site SPD 100-Year Lag	RCombine SPD 100-Year Lag	Temperature	Moisture Deficit
Kendall's tau_b	Tipi Ring Site SPD 100-Year Lag	Correlation Coefficient			1.000	.819**	-.287**	.249**
		Sig. (2-tailed)			.	.000	.000	.000
		N			111	111	111	111
		Bootstrap[c]	Bias		.000	.000	.002	-.002
			Std. Error		.000	.025	.064	.069
			BCa 95% Confidence Interval	Lower	.	.767	-.408	.119
				Upper	.	.867	-.147	.379
	RCombine SPD 100-Year Lag	Correlation Coefficient			.819**	1.000	-.324**	.253**
		Sig. (2-tailed)			.000	.	.000	.000
		N			111	111	111	111
		Bootstrap[c]	Bias		.000	.000	.001	-.002
			Std. Error		.025	.000	.061	.059
			BCa 95% Confidence Interval	Lower	.767	.	-.431	.138
				Upper	.867	.	-.208	.366

**. Correlation is significant at the 0.01 level (2-tailed).

*. Correlation is significant at the 0.05 level (2-tailed).

c. Unless otherwise noted, bootstrap results are based on 1000 bootstrap samples

Correlations

					Tipi Ring Site SPD 100-Year Lag	RCombine SPD 100-Year Lag	Temperature	Moisture Deficit
Spearman's rho	Tipi Ring Site SPD 100-Year Lag	Correlation Coefficient			1.000	.945**	-.436**	.356**
		Sig. (2-tailed)			.	.000	.000	.000
		N			111	111	111	111
		Bootstrap[c]	Bias		.000	-.004	.007	-.006
			Std. Error		.000	.017	.087	.096
			BCa 95% Confidence Interval	Lower	.	.913	-.590	.166
				Upper	.	.963	-.208	.522
	RCombine SPD 100-Year Lag	Correlation Coefficient			.945**	1.000	-.495**	.379**
		Sig. (2-tailed)			.000	.	.000	.000
		N			111	111	111	111
		Bootstrap[c]	Bias		-.004	.000	.006	-.006
			Std. Error		.017	.000	.082	.084
			BCa 95% Confidence Interval	Lower	.913	.	-.643	.204
				Upper	.963	.	-.288	.525

**. Correlation is significant at the 0.01 level (2-tailed).

*. Correlation is significant at the 0.05 level (2-tailed).

c. Unless otherwise noted, bootstrap results are based on 1000 bootstrap samples

APPENDIX B: PEARSON RUNNING CORRELATION RESULTS

Moisture - 150-Year Interval								
Period	**Direct**	**P Value**	**Period**	**50 Year Lag**	**P Value**	**Period**	**100 Year Lag**	**P Value**
0-149	-0.998	0.037	50-199	-1.000	-	100-249	-	-
50-199	-0.997	0.047	100-249	-0.946	0.211	150-299	-1.000	-
100-249	-0.999	0.025	150-299	-0.657	0.544	200-349	-0.827	0.380
150-299	0.850	0.353	200-349	-0.876	0.320	250-399	-0.925	0.249
200-349	0.920	0.257	250-399	-0.999	0.029	300-449	0.452	0.701
250-399	0.993	0.078	300-449	-0.030	0.981	350-499	-0.406	0.734
300-449	-0.998	0.039	350-499	-0.888	0.304	400-549	-0.538	0.638
350-499	-0.999	0.034	400-549	-0.998	0.039	450-599	-0.888	0.304
400-549	0.679	0.525	450-599	-0.999	0.034	500-649	-0.998	0.039
450-599	-0.768	0.443	500-649	0.679	0.525	550-699	-0.999	0.034
500-649	-0.814	0.394	550-699	-0.926	0.246	600-749	0.870	0.328
550-699	-0.992	0.080	600-749	-0.944	0.215	650-799	-0.785	0.426
600-749	-0.939	0.224	650-799	-0.992	0.081	700-849	-0.944	0.213
650-799	-0.962	0.176	700-849	-0.840	0.365	750-899	-0.940	0.222
700-849	0.189	0.879	750-899	-0.890	0.301	800-949	-0.930	0.240
750-899	0.306	0.802	800-949	0.610	0.582	850-999	-0.591	0.597
800-949	-0.968	0.162	850-999	0.695	0.511	900-1049	0.197	0.874
850-999	-1.000	0.012	900-1049	-1.000	0.004	950-1099	0.499	0.668
900-1049	-0.713	0.495	950-1099	-0.757	0.453	1000-1149	-0.740	0.469
950-1099	-0.740	0.470	1000-1149	-0.987	0.104	1050-1199	-0.974	0.146
1000-1149	-0.695	0.511	1050-1199	-0.975	0.142	1100-1249	-0.698	0.508
1050-1199	-0.893	0.297	1100-1249	-0.979	0.130	1150-1299	-0.930	0.239
1100-1249	0.984	0.115	1150-1299	0.599	0.591	1200-1349	0.967	0.165
1150-1299	0.918	0.260	1200-1349	0.943	0.216	1250-1399	0.917	0.261

1200-1349	-0.648	0.551	1250-1399	0.993	0.074	1300-1449	0.808	0.401
1250-1399	-0.957	0.188	1300-1449	-0.775	0.435	1350-1499	0.956	0.190
1300-1449	-0.399	0.739	1350-1499	-0.980	0.126	1400-1549	-0.383	0.750
1350-1499	-0.989	0.093	1400-1549	-0.146	0.907	1450-1599	0.936	0.228
1400-1549	-0.918	0.260	1450-1599	-0.989	0.093	1500-1649	-0.146	0.907
1450-1599	-0.875	0.322	1500-1649	-0.918	0.260	1550-1699	-0.989	0.093
1500-1649	-0.902	0.285	1550-1699	-0.875	0.322	1600-1749	-0.918	0.260
1550-1699	-0.249	0.840	1600-1749	-0.902	0.285	1650-1799	-0.875	0.322
1600-1749	0.948	0.205	1650-1799	-0.249	0.840	1700-1849	-0.902	0.285
1650-1799	0.967	0.163	1700-1849	0.948	0.205	1750-1899	-0.249	0.840
1700-1849	0.914	0.266	1750-1899	0.967	0.163	1800-1949	0.948	0.205
1750-1899	0.998	0.043	1800-1949	0.911	0.270	1850-1999	0.969	0.159
1800-1949	-0.679	0.525	1850-1999	0.997	0.046	1900-2049	0.909	0.273
1850-1999	0.735	0.474	1900-2049	-0.678	0.526	1950-2099	0.997	0.046
1900-2049	0.088	0.944	1950-2099	0.966	0.166	2000-2149	-0.942	0.217
1950-2099	-0.996	0.060	2000-2149	0.496	0.670	2050-2199	0.770	0.440
2000-2149	-0.497	0.669	2050-2199	-0.990	0.092	2100-2249	0.452	0.702
2050-2199	0.924	0.249	2100-2249	-0.568	0.615	2150-2299	-0.998	0.038
2100-2249	0.968	0.162	2150-2299	0.898	0.290	2200-2349	-0.620	0.575
2150-2299	0.729	0.480	2200-2349	0.936	0.229	2250-2399	0.940	0.222
2200-2349	-0.718	0.490	2250-2399	0.972	0.150	2300-2449	0.988	0.100
2250-2399	0.932	0.236	2300-2449	0.949	0.205	2350-2499	-0.241	0.845
2300-2449	-0.597	0.593	2350-2499	0.994	0.070	2400-2549	0.988	0.101
2350-2499	-0.997	0.046	2400-2549	0.119	0.924	2450-2599	0.646	0.553
2400-2549	-0.956	0.191	2450-2599	0.587	0.600	2500-2649	0.781	0.429
2450-2599	-0.894	0.296	2500-2649	-0.444	0.707	2550-2699	0.991	0.084
2500-2649	0.318	0.794	2550-2699	0.836	0.370	2600-2749	0.998	0.041
2550-2699	-0.949	0.204	2600-2749	0.777	0.433	2650-2799	1.000	0.009
2600-2749	0.556	0.625	2650-2799	-0.798	0.412	2700-2849	0.938	0.225

2650-2799	0.918	0.259	2700-2849	0.691	0.515	2750-2899	-0.890	0.302
2700-2849	0.126	0.919	2750-2899	-0.393	0.743	2800-2949	-0.721	0.487
2750-2899	-0.913	0.267	2800-2949	-0.970	0.157	2850-2999	-0.960	0.180
2800-2949	0.220	0.859	2850-2999	-0.937	0.228	2900-3049	-0.983	0.118
2850-2999	0.808	0.401	2900-3049	-0.135	0.914	2950-3099	-1.000	0.000
2900-3049	0.856	0.345	2950-3099	0.751	0.459	3000-3149	-0.224	0.856
2950-3099	0.981	0.125	3000-3149	0.995	0.062	3050-3199	0.963	0.175
3000-3149	0.931	0.238	3050-3199	0.759	0.451	3100-3249	0.915	0.265
3050-3199	0.921	0.255	3100-3249	1.000	0.005	3150-3299	0.947	0.208
3100-3249	0.986	0.106	3150-3299	0.958	0.186	3200-3349	0.993	0.074
3150-3299	0.964	0.172	3200-3349	0.946	0.210	3250-3399	0.992	0.081
3200-3349	0.506	0.662	3250-3399	0.969	0.158	3300-3449	0.939	0.224
3250-3399	-0.865	0.335	3300-3449	0.498	0.668	3350-3499	0.967	0.164
3300-3449	-0.741	0.469	3350-3499	-0.671	0.532	3400-3549	0.738	0.471
3350-3499	0.544	0.634	3400-3549	0.888	0.304	3450-3599	0.929	0.241
3400-3549	0.163	0.896	3450-3599	0.866	0.334	3500-3649	1.000	0.004
3450-3599	-0.946	0.210	3500-3649	0.209	0.866	3550-3699	0.888	0.304
3500-3649	-0.916	0.263	3550-3699	-0.995	0.064	3600-3749	0.426	0.720
3550-3699	-0.958	0.185	3600-3749	-0.779	0.432	3650-3799	-0.986	0.105
3600-3749	0.096	0.939	3650-3799	-0.829	0.378	3700-3849	-0.009	0.995
3650-3799	0.190	0.878	3700-3849	-0.797	0.413	3750-3899	0.973	0.148
3700-3849	0.251	0.838	3750-3899	-0.996	0.054	3800-3949	0.799	0.411
3750-3899	-0.875	0.321	3800-3949	-0.325	0.789	3850-3999	-0.784	0.427
3800-3949	-0.107	0.932	3850-3999	-0.576	0.609	3900-4049	-0.706	0.501
3850-3999	0.991	0.086	3900-4049	0.186	0.881	3950-4099	-0.789	0.422
3900-4049	0.898	0.290	3950-4099	0.968	0.162	4000-4149	-0.201	0.871
3950-4099	0.844	0.360	4000-4149	0.957	0.188	4050-4199	0.996	0.060
4000-4149	0.434	0.714	4050-4199	1.000	0.015	4100-4249	0.670	0.533
4050-4199	-0.903	0.282	4100-4249	-0.836	0.369	4150-4299	-0.844	0.360

4100-4249	-0.945	0.211	4150-4299	-0.903	0.282	4200-4349	-0.836	0.369
4150-4299	0.829	0.378	4200-4349	-0.668	0.534	4250-4399	-0.581	0.605
4200-4349	-0.310	0.800	4250-4399	-0.036	0.977	4300-4449	-0.985	0.111
4250-4399	-0.973	0.148	4300-4449	-0.757	0.453	4350-4499	0.486	0.677
4300-4449	0.956	0.190	4350-4499	0.738	0.471	4400-4549	0.979	0.130
4350-4499	0.800	0.410	4400-4549	0.922	0.253	4450-4599	0.999	0.028
4400-4549	-0.206	0.868	4450-4599	0.700	0.506	4500-4649	0.970	0.156
4450-4599	-0.850	0.353	4500-4649	-0.208	0.866	4550-4699	0.701	0.505
4500-4649	-0.943	0.217	4550-4699	-0.426	0.720	4600-4749	-0.708	0.500
4550-4699	0.908	0.276	4600-4749	0.980	0.128	4650-4799	0.831	0.375
4600-4749	-0.171	0.891	4650-4799	0.926	0.247	4700-4849	0.988	0.099
4650-4799	-0.994	0.067	4700-4849	-0.167	0.893	4750-4899	0.927	0.245
4700-4849	-0.998	0.042	4750-4899	-1.000	0.013	4800-4949	-0.250	0.839
4750-4899	0.849	0.355	4800-4949	-0.998	0.040	4850-4999	-1.000	0.015
4800-4949	0.993	0.076	4850-4999	0.830	0.377	4900-5049	-1.000	0.018
4850-4999	0.894	0.296	4900-5049	0.994	0.072	4950-5099	0.827	0.380
4900-5049	0.869	0.329	4950-5099	0.895	0.294	5000-5149	0.994	0.071
4950-5099	0.972	0.151	5000-5149	0.891	0.300	5050-5199	0.874	0.324
5000-5149	0.950	0.202	5050-5199	0.972	0.151	5100-5249	0.891	0.300
5050-5199	-0.201	0.871	5100-5249	0.950	0.202	5150-5299	0.972	0.151
5100-5249	-0.526	0.647	5150-5299	-0.201	0.871	5200-5349	0.950	0.202
5150-5299	-0.057	0.964	5200-5349	-0.009	0.994	5250-5399	0.693	0.512
5200-5349	0.469	0.690	5250-5399	-0.926	0.246	5300-5449	0.899	0.288
5250-5399	-0.962	0.177	5300-5449	-0.868	0.331	5350-5499	0.581	0.605
5300-5449	-0.963	0.173	5350-5499	-0.720	0.488	5400-5549	-1.000	0.020
5350-5499	-0.341	0.779	5400-5549	-1.000	0.013	5450-5599	-0.870	0.329
5400-5549	0.994	0.070	5450-5599	-0.553	0.627	5500-5649	-0.977	0.138
5450-5599	0.980	0.128	5500-5649	0.935	0.230	-	-0.328	0.787

Moisture - 200-Year Interval								
Period	**Direct**	**P Value**	**Period**	**50 Year Lag**	**P Value**	**Period**	**100 Year Lag**	**P Value**
0-199	-0.9940	0.0495	50-249	-0.9456	0.1520	100-299	-	-
50-249	-0.9977	0.0308	100-299	-0.7464	0.3581	150-349	-0.8274	0.2849
100-299	-0.7071	0.3919	150-349	-0.7290	0.3731	200-399	-0.5562	0.5175
150-349	0.9088	0.1998	200-399	-0.4613	0.5964	250-449	0.4702	0.5890
200-399	0.9421	0.1569	250-449	0.0010	0.9991	300-499	0.1820	0.8371
250-449	0.9747	0.1023	300-499	0.0955	0.9141	350-549	-0.0284	0.9745
300-499	-0.9992	0.0177	350-549	-0.8214	0.2905	400-599	-0.7219	0.3793
350-549	0.3129	0.7224	400-599	-0.9992	0.0177	450-649	-0.8214	0.2905
400-599	-0.6916	0.4049	450-649	0.3129	0.7224	500-699	-0.9992	0.0177
450-649	-0.8563	0.2567	500-699	-0.8871	0.2244	550-749	0.6076	0.4750
500-699	-0.8886	0.2228	550-749	-0.9456	0.1519	600-799	-0.7736	0.3342
550-749	-0.9033	0.2062	600-799	-0.9593	0.1306	650-849	-0.9015	0.2083
600-799	-0.9591	0.1309	650-849	-0.8167	0.2950	700-899	-0.9701	0.1115
650-849	-0.8739	0.2386	700-899	-0.9019	0.2079	750-949	-0.8067	0.3043
700-899	0.1612	0.8555	750-949	-0.3807	0.6644	800-999	-0.6787	0.4158
750-949	-0.3837	0.6618	800-999	0.4221	0.6293	850-1049	-0.5339	0.5360
800-999	-0.9930	0.0535	850-1049	-0.3043	0.7299	900-1099	0.2091	0.8130
850-1049	-0.7892	0.3203	900-1099	-0.8278	0.2845	950-1149	-0.0170	0.9847
900-1099	-0.8671	0.2456	950-1149	-0.8783	0.2339	1000-1199	-0.8889	0.2225
950-1149	-0.8226	0.2894	1000-1199	-0.9811	0.0882	1050-1249	-0.7868	0.3224
1000-1199	-0.7370	0.3663	1050-1249	-0.8141	0.2974	1100-1299	-0.7287	0.3734
1050-1249	0.8085	0.3026	1100-1299	0.6071	0.4754	1150-1349	0.8019	0.3087
1100-1299	0.9270	0.1773	1150-1349	0.8980	0.2123	1200-1399	0.9159	0.1913
1150-1349	-0.1440	0.8708	1200-1399	0.9684	0.1146	1250-1449	0.9288	0.1750
1200-1399	-0.7936	0.3162	1250-1449	-0.0465	0.9581	1300-1499	0.8849	0.2268
1200-1449	-0.9155	0.1918	1300-1499	-0.8295	0.2829	1350-1549	0.0793	0.9287

1250-1499	-0.0459	0.9587	1350-1549	-0.9786	0.0939	1400-1599	-0.4603	0.5972
1300-1549	-0.9399	0.1601	1400-1599	-0.6386	0.4492	1450-1649	0.7391	0.3644
1350-1599	-0.8492	0.2638	1450-1649	-0.9399	0.1601	1500-1699	-0.6386	0.4492
1400-1649	-0.9167	0.1904	1500-1699	-0.8492	0.2638	1550-1749	-0.9399	0.1601
1450-1699	-0.7842	0.3247	1550-1749	-0.9167	0.1904	1600-1799	-0.8492	0.2638
1500-1749	0.7007	0.3972	1600-1799	-0.7842	0.3247	1650-1849	-0.9167	0.1904
1550-1799	0.9201	0.1862	1650-1849	0.7007	0.3972	1700-1899	-0.7842	0.3247
1600-1849	0.9609	0.1280	1700-1899	0.9201	0.1862	1750-1949	0.7007	0.3972
1650-1899	0.8689	0.2438	1750-1949	0.9598	0.1298	1800-1999	0.9222	0.1836
1700-1949	-0.1817	0.8373	1800-1999	0.8645	0.2483	1850-2049	0.9589	0.1314
1750-1999	0.6694	0.4236	1850-2049	-0.1845	0.8348	1900-2099	0.8623	0.2506
1800-2049	0.1968	0.8239	1900-2099	0.9651	0.1208	1950-2149	-0.7191	0.3817
1850-2099	-0.3330	0.7051	1950-2149	0.5676	0.5080	2000-2199	0.7777	0.3306
1900-2149	-0.7783	0.3301	2000-2199	-0.1187	0.8934	2050-2249	0.5305	0.5388
1950-2199	0.7288	0.3733	2050-2249	-0.8091	0.3020	2100-2299	-0.1073	0.9036
2000-2249	0.9631	0.1241	2100-2299	0.6518	0.4382	2150-2349	-0.8653	0.2475
2050-2299	0.8516	0.2614	2150-2349	0.9486	0.1475	2200-2399	0.6842	0.4112
2100-2349	0.2928	0.7398	2200-2399	0.9324	0.1703	2250-2449	0.9483	0.1479
2150-2399	0.0983	0.9116	2250-2449	0.9672	0.1168	2300-2499	0.7390	0.3645
2200-2449	-0.4070	0.6420	2300-2499	0.9932	0.0526	2350-2549	0.3291	0.7085
2250-2499	-0.7040	0.3945	2350-2549	0.2724	0.7576	2400-2599	0.7347	0.3682
2300-2549	-0.7799	0.3286	2400-2599	0.2752	0.7551	2450-2649	0.6809	0.4140
2350-2599	-0.8960	0.2146	2450-2649	0.6251	0.4605	2500-2699	0.8429	0.2699
2400-2649	-0.3361	0.7025	2500-2699	0.3775	0.6671	2550-2749	0.5892	0.4902
2450-2699	-0.1047	0.9059	2550-2749	0.7544	0.3511	2600-2799	0.9996	0.0124
2500-2749	0.4699	0.5892	2600-2799	0.3783	0.6664	2650-2849	0.9756	0.1004
2550-2799	0.6883	0.4077	2650-2849	0.4301	0.6225	2700-2899	0.5548	0.5187
2600-2849	0.5993	0.4818	2700-2899	0.1237	0.8889	2750-2949	-0.2364	0.7891
2650-2899	-0.4073	0.6418	2750-2949	-0.7876	0.3217	2800-2999	-0.9168	0.1902

2700-2949	-0.6894	0.4068	2800-2999	-0.9197	0.1866	2850-3049	-0.9829	0.0838
2750-2999	0.6229	0.4623	2850-3049	-0.8476	0.2653	2900-3099	-0.9850	0.0785
2800-3049	0.7155	0.3847	2900-3099	0.3816	0.6636	2950-3149	-0.9675	0.1163
2850-3099	0.8574	0.2555	2950-3149	0.7050	0.3936	3000-3199	0.3796	0.6653
2900-3149	0.7746	0.3334	3000-3199	0.7179	0.3826	3050-3249	0.8952	0.2155
2950-3199	0.8895	0.2218	3050-3249	0.8930	0.2179	3100-3299	0.9007	0.2093
3000-3249	0.9609	0.1280	3100-3299	0.9747	0.1023	3150-3349	0.9755	0.1008
3050-3299	0.9844	0.0799	3150-3349	0.9788	0.0935	3200-3399	0.9955	0.0426
3100-3349	0.9097	0.1988	3200-3399	0.9667	0.1178	3250-3449	0.9837	0.0817
3150-3399	-0.5085	0.5570	3250-3449	0.9169	0.1901	3300-3499	0.9619	0.1262
3200-3449	-0.6917	0.4049	3300-3499	-0.3853	0.6604	3350-3549	0.9518	0.1426
3250-3499	-0.5733	0.5033	3350-3549	-0.2654	0.7637	3400-3599	0.0965	0.9132
3300-3549	0.4147	0.6355	3400-3599	0.8422	0.2706	3450-3649	0.9943	0.0483
3350-3599	-0.4054	0.6434	3450-3649	0.5632	0.5117	3500-3699	0.9107	0.1976
3400-3649	-0.9317	0.1712	3500-3699	-0.3025	0.7314	3550-3749	0.7172	0.3832
3450-3699	-0.9407	0.1589	3550-3749	-0.7978	0.3125	3600-3799	-0.0225	0.9798
3500-3749	-0.9533	0.1403	3600-3799	-0.7844	0.3245	3650-3849	-0.5058	0.5593
3550-3799	0.2510	0.7763	3650-3849	-0.7420	0.3619	3700-3899	0.1342	0.8795
3600-3849	0.1662	0.8510	3700-3899	-0.5992	0.4819	3750-3949	0.9355	0.1662
3650-3899	-0.7473	0.3573	3750-3949	-0.3251	0.7119	3800-3999	-0.6697	0.4234
3700-3949	-0.0756	0.9320	3800-3999	-0.7560	0.3497	3850-4049	-0.5980	0.4829
3750-3999	0.7420	0.3619	3850-4049	0.1457	0.8693	3900-4099	-0.8934	0.2175
3800-4049	0.9235	0.1819	3900-4099	0.7162	0.3841	3950-4149	-0.1314	0.8821
3850-4099	0.9182	0.1884	3950-4149	0.8862	0.2254	4000-4199	0.5395	0.5313
3900-4149	0.8646	0.2483	4000-4199	0.9683	0.1148	4050-4249	0.7623	0.3442
3950-4199	0.5133	0.5530	4050-4249	0.8584	0.2546	4100-4299	0.7012	0.3969
4000-4249	-0.8292	0.2832	4100-4299	-0.8990	0.2112	4150-4349	-0.9342	0.1678
4050-4299	-0.0667	0.9400	4150-4349	-0.4178	0.6329	4200-4399	-0.6504	0.4394
4100-4349	-0.4337	0.6195	4200-4399	-0.5616	0.5130	4250-4449	-0.6631	0.4289

4150-4399	-0.4630	0.5950	4250-4449	-0.3610	0.6811	4300-4499	-0.9309	0.1723
4200-4449	0.8166	0.2951	4300-4499	0.7653	0.3416	4350-4549	0.9806	0.0894
4250-4499	0.8492	0.2638	4350-4549	0.9117	0.1963	4400-4599	0.9919	0.0576
4300-4549	0.8009	0.3096	4400-4599	0.8832	0.2286	4450-4649	0.9778	0.0957
4350-4599	-0.7778	0.3305	4450-4649	0.7147	0.3854	4500-4699	0.8756	0.2368
4400-4649	-0.8599	0.2530	4500-4699	-0.5043	0.5605	4550-4749	0.7559	0.3498
4450-4699	-0.9235	0.1819	4550-4749	-0.4609	0.5967	4600-4799	-0.2770	0.7535
4500-4749	0.8106	0.3007	4600-4799	0.9401	0.1598	4650-4849	0.9212	0.1847
4550-4799	-0.6656	0.4267	4650-4849	0.8353	0.2773	4700-4899	0.9535	0.1400
4600-4849	-0.9974	0.0322	4700-4899	-0.6984	0.3992	4750-4949	0.8088	0.3023
4650-4899	0.7297	0.3725	4750-4949	-0.9991	0.0190	4800-4999	-0.7505	0.3546
4700-4949	0.9376	0.1633	4800-4999	0.7087	0.3905	4850-5049	-0.9998	0.0081
4750-4999	0.9450	0.1528	4850-5049	0.9263	0.1783	4900-5099	0.6912	0.4053
4800-5049	0.9114	0.1968	4900-5099	0.9471	0.1497	4950-5149	0.9240	0.1812
4850-5099	0.9432	0.1554	4950-5149	0.9053	0.2039	5000-5199	0.9358	0.1657
4900-5149	0.9273	0.1770	5000-5199	0.9534	0.1401	5050-5249	0.8881	0.2234
4950-5199	0.7114	0.3881	5050-5249	0.9273	0.1770	5100-5299	0.9534	0.1401
5000-5249	-0.0645	0.9420	5100-5299	0.7114	0.3881	5150-5349	0.9273	0.1770
5050-5299	0.2141	0.8087	5150-5349	-0.0956	0.9140	5200-5399	-0.0790	0.9289
5100-5349	0.5489	0.5235	5200-5399	0.1321	0.8814	5250-5449	0.5333	0.5365
5150-5399	0.5053	0.5597	5250-5449	0.2610	0.7675	5300-5499	0.9060	0.2031
5200-5449	-0.7959	0.3142	5300-5499	-0.7659	0.3410	5350-5549	-0.9975	0.0319
5250-5499	-0.5500	0.5226	5350-5549	-0.8616	0.2512	5400-5599	-0.8978	0.2126
5300-5549	0.0821	0.9261	5400-5599	-0.7686	0.3386	5450-5649	-0.9445	0.1535
5350-5599	0.9574	0.1338	5450-5649	0.0664	0.9403	5500-5699	-0.6513	0.4387

Temperature - 150-Year Interval								
Period	**Direct**	**P Value**	**Period**	**50 Year Lag**	**P Value**	**Period**	**100 Year Lag**	**P Value**
0-149	-0.9989	0.0301	50-199	-1.0000	-	100-249	-	-
50-199	0.6682	0.5341	100-249	0.4564	0.6983	150-299	1.0000	-
100-249	0.8350	0.3710	150-299	0.9522	0.1977	200-349	0.9986	0.0335
150-299	-0.9063	0.2778	200-349	0.8135	0.3951	250-399	0.9631	0.1736
200-349	0.4412	0.7091	250-399	-0.7865	0.4237	300-449	0.9244	0.2491
250-399	0.8609	0.3398	300-449	0.5855	0.6018	350-499	-0.8790	0.3164
300-449	0.7490	0.4611	350-499	0.9529	0.1963	400-549	-0.2149	0.8621
350-499	0.5216	0.6507	400-549	0.4206	0.7236	450-599	0.0181	0.9885
400-549	-0.4956	0.6699	450-599	0.9608	0.1789	500-649	0.9862	0.1060
450-599	0.8374	0.3681	500-649	-0.7600	0.4504	550-699	0.9980	0.0406
500-649	0.9993	0.0238	550-699	0.5665	0.6166	600-749	-0.4555	0.6989
550-699	1.0000	0.0028	600-749	0.8967	0.2919	650-799	0.8539	0.3485
600-749	0.7522	0.4580	650-799	0.8797	0.3154	700-849	0.9995	0.0207
650-799	-0.3664	0.7612	700-849	-0.9405	0.2206	750-899	-0.8417	0.3632
700-849	0.3736	0.7562	750-899	-0.7869	0.4234	800-949	-0.9831	0.1171
750-899	0.5648	0.6179	800-949	0.3588	0.7664	850-999	-0.7966	0.4132
800-949	-0.9724	0.1500	850-999	0.6820	0.5222	900-1049	0.2150	0.8621
850-999	-0.9825	0.1193	900-1049	-0.9774	0.1355	950-1099	0.6651	0.5368
900-1049	-0.9629	0.1739	950-1099	-0.9785	0.1323	1000-1149	-0.9729	0.1484
950-1099	-0.9302	0.2392	1000-1149	-0.9804	0.1263	1050-1199	-0.9912	0.0846
1000-1149	-0.9343	0.2321	1050-1199	-0.9771	0.1364	1100-1249	-0.9359	0.2291
1050-1199	-0.9437	0.2147	1100-1249	-0.9452	0.2117	1150-1299	-0.9698	0.1568
1100-1249	-0.9100	0.2722	1150-1299	-0.9489	0.2044	1200-1349	-0.9398	0.2220
1150-1299	-0.9061	0.2781	1200-1349	-0.9523	0.1974	1250-1399	-0.9053	0.2793
1200-1349	0.8050	0.4044	1250-1399	-0.9404	0.2210	1300-1449	-0.9212	0.2544
1250-1399	0.9551	0.1915	1300-1449	0.7783	0.4321	1350-1499	-0.9543	0.1932
1300-1449	-0.1532	0.9021	1350-1499	0.9339	0.2328	1400-1549	0.8174	0.3909

1350-1499	-0.9912	0.0844	1400-1549	-0.1330	0.9150	1450-1599	0.9410	0.2198
1400-1549	-0.8776	0.3183	1450-1599	-0.9719	0.1512	1500-1649	-0.2361	0.8482
1450-1599	-0.5210	0.6511	1500-1649	-0.9940	0.0697	1550-1699	-0.9316	0.2368
1500-1649	-0.6196	0.5746	1550-1699	-0.9988	0.0318	1600-1749	-0.6499	0.5496
1550-1699	0.1192	0.9240	1600-1749	-0.6831	0.5212	1650-1799	-0.9911	0.0851
1600-1749	-0.5520	0.6278	1650-1799	-0.8708	0.3272	1700-1849	-0.1844	0.8819
1650-1799	-0.7741	0.4364	1700-1849	-0.7307	0.4784	1750-1899	0.6292	0.5667
1700-1849	-0.8134	0.3952	1750-1899	-0.2723	0.8244	1800-1949	-0.2083	0.8664
1750-1899	-0.5663	0.6167	1800-1949	-0.2430	0.8437	1850-1999	-0.7954	0.4145
1800-1949	-0.5071	0.6615	1850-1999	-0.3581	0.7668	1900-2049	-0.6615	0.5398
1850-1999	0.8811	0.3136	1900-2049	-0.8402	0.3648	1950-2099	0.9477	0.2069
1900-2049	0.9928	0.0767	1950-2099	-0.0521	0.9668	2000-2149	0.1322	0.9156
1950-2099	0.9376	0.2260	2000-2149	-0.2556	0.8355	2050-2199	-0.9086	0.2744
2000-2149	0.9438	0.2145	2050-2199	0.8423	0.3624	2100-2249	-0.9256	0.2471
2050-2199	-0.9916	0.0827	2100-2249	0.0828	0.9473	2150-2299	0.8355	0.3703
2100-2249	-0.9989	0.0295	2150-2299	-0.7279	0.4810	2200-2349	0.8239	0.3836
2150-2299	-0.5053	0.6628	2200-2349	-0.7975	0.4123	2250-2399	-0.9981	0.0393
2200-2349	0.8633	0.3368	2250-2399	-0.8886	0.3033	2300-2449	-0.9966	0.0528
2250-2399	0.9975	0.0450	2300-2449	0.9929	0.0760	2350-2499	-0.6323	0.5642
2300-2449	-0.5330	0.6421	2350-2499	0.9826	0.1188	2400-2549	0.9724	0.1498
2350-2499	-0.8760	0.3204	2400-2549	-0.4410	0.7092	2450-2599	0.9577	0.1859
2400-2549	0.6769	0.5267	2450-2599	-0.9151	0.2642	2500-2649	-0.3602	0.7654
2450-2599	0.9572	0.1869	2500-2649	0.5904	0.5979	2550-2699	-0.9544	0.1930
2500-2649	0.9337	0.2331	2550-2699	0.9554	0.1909	2600-2749	0.5854	0.6019
2550-2699	0.7358	0.4737	2600-2749	0.1728	0.8895	2650-2799	-0.4727	0.6866
2600-2749	0.6925	0.5130	2650-2799	-0.4172	0.7260	2700-2849	-0.5397	0.6371
2650-2799	0.9635	0.1724	2700-2849	0.7825	0.4279	2750-2899	-0.9436	0.2148
2700-2849	0.9942	0.0684	2750-2899	0.9119	0.2692	2800-2949	0.6792	0.5246
2750-2899	0.8924	0.2980	2800-2949	0.9565	0.1885	2850-2999	0.9727	0.1491

2800-2949	0.1463	0.9065	2850-2999	0.9999	0.0069	2900-3049	0.9833	0.1164
2850-2999	-0.9954	0.0614	2900-3049	-0.3880	0.7463	2950-3099	0.8605	0.3403
2900-3049	-0.9833	0.1165	2950-3099	-1.0000	0.0032	3000-3149	-0.4793	0.6818
2950-3099	-0.9089	0.2738	3000-3149	-0.9905	0.0876	3050-3199	-0.9992	0.0257
3000-3149	-0.9998	0.0127	3050-3199	-0.9510	0.2002	3100-3249	-0.9998	0.0140
3050-3199	-0.9999	0.0078	3100-3249	-0.9224	0.2525	3150-3299	-0.9981	0.0396
3100-3249	-0.9577	0.1859	3150-3299	-0.9863	0.1056	3200-3349	-0.9706	0.1547
3150-3299	-0.9584	0.1842	3200-3349	-0.9521	0.1979	3250-3399	-0.9892	0.0936
3200-3349	-0.9938	0.0712	3250-3399	-0.7774	0.4331	3300-3449	-0.2862	0.8152
3250-3399	-0.5366	0.6394	3300-3449	0.8413	0.3636	3350-3499	0.9757	0.1407
3300-3449	0.9769	0.1370	3350-3499	0.9933	0.0739	3400-3549	0.1205	0.9231
3350-3499	0.9944	0.0672	3400-3549	0.9161	0.2627	3450-3599	0.8719	0.3258
3400-3549	0.8042	0.4051	3450-3599	0.9698	0.1569	3500-3649	0.7217	0.4867
3450-3599	0.7739	0.4366	3500-3649	0.1447	0.9075	3550-3699	-0.6725	0.5305
3500-3649	0.1671	0.8931	3550-3699	0.6293	0.5667	3600-3749	-0.9902	0.0892
3550-3699	0.3522	0.7708	3600-3749	0.9709	0.1540	3650-3799	0.7285	0.4804
3600-3749	-0.9652	0.1684	3650-3799	0.8156	0.3928	3700-3849	0.9387	0.2240
3650-3799	0.4955	0.6699	3700-3849	-0.9488	0.2045	3750-3899	0.8471	0.3567
3700-3849	0.6459	0.5530	3750-3899	0.5051	0.6629	3800-3949	-0.9523	0.1975
3750-3899	0.0003	0.9998	3800-3949	0.9850	0.1106	3850-3999	-0.1647	0.8947
3800-3949	0.2312	0.8515	3850-3999	-0.8159	0.3925	3900-4049	-0.4288	0.7179
3850-3999	0.9984	0.0365	3900-4049	-0.0050	0.9968	3950-4099	-0.6564	0.5442
3900-4049	0.9994	0.0226	3950-4099	0.9863	0.1056	4000-4149	0.2165	0.8611
3950-4099	0.8815	0.3130	4000-4149	0.9326	0.2350	4050-4199	0.9860	0.1067
4000-4149	0.7852	0.4251	4050-4199	0.8881	0.3041	4100-4249	0.9275	0.2439
4050-4199	0.9097	0.2727	4100-4249	0.8280	0.3790	4150-4299	0.8525	0.3502
4100-4249	0.9533	0.1954	4150-4299	0.9138	0.2663	4200-4349	0.8223	0.3853
4150-4299	-0.3526	0.7706	4200-4349	0.9753	0.1417	4250-4399	0.9448	0.2126
4200-4349	0.6203	0.5741	4250-4399	-0.3127	0.7975	4300-4449	0.9838	0.1147

4250-4399	0.9863	0.1054	4300-4449	0.7110	0.4965	4350-4499	-0.4258	0.7200
4300-4449	0.8490	0.3545	4350-4499	0.9933	0.0736	4400-4549	0.4880	0.6754
4350-4499	0.0075	0.9952	4400-4549	-0.8592	0.3419	4450-4599	-0.5585	0.6228
4400-4549	0.3958	0.7409	4450-4599	-0.8273	0.3798	4500-4649	-0.9028	0.2831
4450-4599	0.9188	0.2583	4500-4649	0.0609	0.9612	4550-4699	-0.5877	0.6001
4500-4649	0.9543	0.1931	4550-4699	0.8836	0.3102	4600-4749	0.1421	0.9093
4550-4699	0.8444	0.3600	4600-4749	0.9449	0.2123	4650-4799	0.8973	0.2910
4600-4749	-0.0299	0.9810	4650-4799	0.9697	0.1570	4700-4849	0.9999	0.0094
4650-4799	-0.9995	0.0204	4700-4849	-0.2386	0.8466	4750-4899	0.8971	0.2914
4700-4849	-0.9823	0.1199	4750-4899	-0.9947	0.0655	4800-4949	-0.3670	0.7607
4750-4899	0.8660	0.3333	4800-4949	-0.9954	0.0610	4850-4999	-0.9999	0.0066
4800-4949	0.9550	0.1916	4850-4999	0.9173	0.2607	4900-5049	-0.9781	0.1336
4850-4999	0.9549	0.1918	4900-5049	0.7943	0.4156	4950-5099	0.2059	0.8680
4900-5049	-0.6962	0.5097	4950-5099	-0.9841	0.1137	5000-5149	-0.9851	0.1101
4950-5099	0.6849	0.5197	5000-5149	0.9942	0.0687	5050-5199	0.4650	0.6921
5000-5149	0.3231	0.7905	5050-5199	0.2462	0.8416	5100-5249	-0.4437	0.7074
5050-5199	-0.4633	0.6933	5100-5249	-0.9336	0.2333	5150-5299	-0.9019	0.2844
5100-5249	-0.0945	0.9398	5150-5299	0.7522	0.4580	5200-5349	-0.5680	0.6154
5150-5299	-0.5016	0.6655	5200-5349	0.4433	0.7076	5250-5399	0.2931	0.8106
5200-5349	0.8840	0.3097	5250-5399	-0.5543	0.6260	5300-5449	0.4980	0.6681
5250-5399	0.9445	0.2130	5300-5449	0.8947	0.2948	5350-5499	-0.5347	0.6409
5300-5449	0.9933	0.0738	5350-5499	0.9288	0.2416	5400-5549	0.9138	0.2662
5350-5499	0.6444	0.5542	5400-5549	0.9456	0.2110	5450-5599	0.9866	0.1044
5400-5549	-0.9773	0.1360	5450-5599	0.4634	0.6933	5500-5649	0.9936	0.0720
5450-5599	-0.9985	0.0345	5500-5649	-0.9944	0.0675	-	0.5558	0.6248

Temperature – 200-Year Interval								
Period	**Direct**	**P Value**	**Period**	**50 Year Lag**	**P Value**	**Period**	**100 Year Lag**	**P Value**
0-199	0.2940	0.7388	50-249	0.4564	0.6005	100-299	-	-
50-249	0.7610	0.3454	100-299	0.9256	0.1792	150-349	0.9986	0.0237
100-299	0.1027	0.9077	150-349	0.8974	0.2130	200-399	0.9424	0.1565
150-349	0.3307	0.7071	200-399	0.2435	0.7828	250-449	0.9549	0.1377
200-399	0.6693	0.4237	250-449	0.3803	0.6646	300-499	0.3034	0.7306
250-449	0.8833	0.2286	300-499	0.6731	0.4205	350-549	-0.0673	0.9395
300-499	0.8505	0.2624	350-549	0.9318	0.1711	400-599	0.2144	0.8084
350-549	-0.4438	0.6110	400-599	0.7583	0.3478	450-649	0.3054	0.7289
400-599	0.6595	0.4319	450-649	-0.2575	0.7706	500-699	0.9907	0.0616
450-649	0.9138	0.1938	500-699	0.5664	0.5090	550-749	-0.1667	0.8506
500-699	0.9986	0.0237	550-749	0.7871	0.3221	600-799	0.6470	0.4423
550-749	0.7861	0.3230	600-799	0.9407	0.1590	650-849	0.9168	0.1903
600-799	0.2061	0.8157	650-849	-0.3452	0.6946	700-899	0.2840	0.7475
650-849	-0.3876	0.6585	700-899	-0.8081	0.3030	750-949	-0.9837	0.0819
700-899	0.2829	0.7484	750-949	-0.5785	0.4990	800-999	-0.8747	0.2377
750-949	-0.2368	0.7887	800-999	0.3134	0.7220	850-1049	-0.6618	0.4300
800-999	-0.9548	0.1379	850-1049	-0.1471	0.8680	900-1099	0.2401	0.7858
850-1049	-0.9349	0.1670	900-1099	-0.9540	0.1392	950-1149	-0.1502	0.8653
900-1099	-0.9638	0.1229	950-1149	-0.9535	0.1400	1000-1199	-0.9688	0.1140
950-1149	-0.9705	0.1107	1000-1199	-0.9860	0.0756	1050-1249	-0.9184	0.1883
1000-1199	-0.9606	0.1285	1050-1249	-0.9780	0.0952	1100-1299	-0.9686	0.1144
1050-1249	-0.9658	0.1194	1100-1299	-0.9656	0.1198	1150-1349	-0.9765	0.0985
1100-1299	-0.9412	0.1583	1150-1349	-0.9807	0.0892	1200-1399	-0.9513	0.1434
1150-1349	0.3236	0.7132	1200-1399	-0.9624	0.1255	1250-1449	-0.9648	0.1212
1200-1399	0.9014	0.2085	1250-1449	0.2342	0.7910	1300-1499	-0.9559	0.1363
1200-1449	0.7675	0.3397	1300-1499	0.8892	0.2222	1350-1549	0.2535	0.7740
1250-1499	-0.6388	0.4491	1350-1549	0.7416	0.3623	1400-1599	0.9075	0.2014

1300-1549	-0.9141	0.1935	1400-1599	-0.6616	0.4301	1450-1649	0.6959	0.4013
1350-1599	-0.6424	0.4461	1450-1649	-0.9798	0.0913	1500-1699	-0.5369	0.5334
1400-1649	-0.6260	0.4597	1500-1699	-0.5321	0.5375	1550-1749	-0.9378	0.1630
1450-1699	-0.4068	0.6422	1550-1749	-0.7471	0.3575	1600-1799	-0.9914	0.0591
1500-1749	-0.4702	0.5889	1600-1799	-0.3921	0.6547	1650-1849	-0.3355	0.7029
1550-1799	-0.6536	0.4368	1650-1849	-0.7199	0.3809	1700-1899	0.0209	0.9812
1600-1849	-0.7785	0.3298	1700-1899	-0.5261	0.5424	1750-1949	-0.1556	0.8605
1650-1899	-0.7745	0.3334	1750-1949	-0.6407	0.4476	1800-1999	-0.8413	0.2714
1700-1949	-0.5027	0.5618	1800-1999	-0.1283	0.8848	1850-2049	-0.4998	0.5642
1750-1999	0.8575	0.2554	1850-2049	-0.7860	0.3231	1900-2099	0.2053	0.8164
1800-2049	0.8691	0.2436	1900-2099	0.1739	0.8442	1950-2149	0.3100	0.7249
1850-2099	0.8534	0.2595	1950-2149	-0.1614	0.8553	2000-2199	-0.7836	0.3253
1900-2149	0.9302	0.1733	2000-2199	0.0178	0.9840	2050-2249	-0.8476	0.2653
1950-2199	-0.8493	0.2636	2050-2249	0.5703	0.5058	2100-2299	0.1337	0.8800
2000-2249	-0.9955	0.0428	2100-2299	-0.6617	0.4301	2150-2349	0.8021	0.3085
2050-2299	-0.8305	0.2819	2150-2349	-0.8768	0.2355	2200-2399	-0.7056	0.3931
2100-2349	0.0227	0.9795	2200-2399	-0.7832	0.3257	2250-2449	-0.9976	0.0313
2150-2399	0.9161	0.1911	2250-2449	-0.1334	0.8803	2300-2499	-0.8663	0.2465
2200-2449	-0.2374	0.7882	2300-2499	0.9744	0.1031	2350-2549	0.0957	0.9139
2250-2499	-0.6864	0.4093	2350-2549	-0.1037	0.9068	2400-2599	0.9293	0.1743
2300-2549	-0.8050	0.3059	2400-2599	-0.6323	0.4545	2450-2649	0.0053	0.9952
2350-2599	0.7858	0.3233	2450-2649	-0.8741	0.2384	2500-2699	-0.5623	0.5124
2400-2649	0.9672	0.1169	2500-2699	0.7156	0.3846	2550-2749	-0.9242	0.1810
2450-2699	0.9232	0.1822	2550-2749	0.7734	0.3344	2600-2799	0.1558	0.8603
2500-2749	0.7028	0.3954	2600-2799	-0.0006	0.9994	2650-2849	-0.0550	0.9505
2550-2799	0.9149	0.1925	2650-2849	0.7804	0.3281	2700-2899	-0.4757	0.5844
2600-2849	0.9846	0.0795	2700-2899	0.8349	0.2777	2750-2949	0.5635	0.5115
2650-2899	0.9255	0.1793	2750-2949	0.9636	0.1233	2800-2999	0.8640	0.2488
2700-2949	0.8010	0.3095	2800-2999	0.9648	0.1212	2850-3049	0.9672	0.1169

2750-2999	-0.5803	0.4976	2850-3049	0.8796	0.2326	2900-3099	0.9817	0.0868
2800-3049	-0.9864	0.0748	2900-3099	-0.9497	0.1459	2950-3149	0.4397	0.6145
2850-3099	-0.8974	0.2130	2950-3149	-0.9903	0.0628	3000-3199	-0.9524	0.1417
2900-3149	-0.9464	0.1507	3000-3199	-0.9470	0.1499	3050-3249	-0.9998	0.0092
2950-3199	-0.9999	0.0067	3050-3249	-0.9693	0.1129	3100-3299	-0.9992	0.0176
3000-3249	-0.9785	0.0942	3100-3299	-0.9469	0.1500	3150-3349	-0.9704	0.1109
3050-3299	-0.9727	0.1064	3150-3349	-0.9877	0.0711	3200-3399	-0.9838	0.0816
3100-3349	-0.9620	0.1261	3200-3399	-0.8986	0.2117	3250-3449	-0.8524	0.2606
3150-3399	-0.1919	0.8283	3250-3449	-0.7516	0.3536	3300-3499	-0.2544	0.7733
3200-3449	0.8544	0.2585	3300-3499	0.9823	0.0854	3350-3549	0.0126	0.9886
3250-3499	0.9821	0.0857	3350-3549	0.9349	0.1670	3400-3599	0.7944	0.3156
3300-3549	0.9725	0.1067	3400-3599	0.9106	0.1977	3450-3649	0.6889	0.4072
3350-3599	0.7725	0.3352	3450-3649	0.8646	0.2482	3500-3699	0.3821	0.6632
3400-3649	0.3744	0.6697	3500-3699	0.2242	0.7998	3550-3749	-0.6898	0.4065
3450-3699	0.5723	0.5042	3550-3749	0.9788	0.0934	3600-3799	0.2518	0.7755
3500-3749	0.3135	0.7219	3600-3799	0.8480	0.2649	3650-3849	0.9507	0.1444
3550-3799	0.2048	0.8169	3650-3849	0.6294	0.4569	3700-3899	0.9138	0.1939
3600-3849	0.4587	0.5985	3700-3899	0.1919	0.8282	3750-3949	0.6592	0.4321
3650-3899	0.7174	0.3831	3750-3949	0.5321	0.5374	3800-3999	-0.2254	0.7987
3700-3949	0.1262	0.8867	3800-3999	0.3772	0.6673	3850-4049	-0.2119	0.8105
3750-3999	0.8062	0.3047	3850-4049	0.0063	0.9943	3900-4099	-0.8042	0.3066
3800-4049	0.9975	0.0320	3900-4099	0.8017	0.3088	3950-4149	0.1806	0.8382
3850-4099	0.9357	0.1659	3950-4149	0.9501	0.1452	4000-4199	0.7629	0.3436
3900-4149	0.9412	0.1583	4000-4199	0.9397	0.1604	4050-4249	0.8889	0.2225
3950-4199	0.8768	0.2355	4050-4249	0.9490	0.1468	4100-4299	0.9286	0.1754
4000-4249	0.8444	0.2684	4100-4299	0.8974	0.2130	4150-4349	0.9361	0.1653
4050-4299	0.6995	0.3983	4150-4349	0.8714	0.2412	4200-4399	0.8972	0.2133
4100-4349	0.5790	0.4986	4200-4399	0.7646	0.3422	4250-4449	0.9152	0.1922
4150-4399	0.8195	0.2924	4250-4449	0.6262	0.4596	4300-4499	0.7375	0.3658

4200-4449	0.9373	0.1636	4300-4499	0.8273	0.2850	4350-4549	0.5231	0.5449
4250-4499	0.5138	0.5527	4350-4549	0.1126	0.8988	4400-4599	-0.0781	0.9297
4300-4549	-0.3067	0.7278	4400-4599	-0.8068	0.3042	4450-4649	-0.8450	0.2679
4350-4599	0.7744	0.3335	4450-4649	-0.7928	0.3169	4500-4699	-0.8413	0.2715
4400-4649	0.9588	0.1315	4500-4699	0.8505	0.2624	4550-4749	-0.6222	0.4629
4450-4699	0.8475	0.2654	4550-4749	0.9473	0.1494	4600-4799	0.8479	0.2650
4500-4749	0.7825	0.3263	4600-4799	0.9284	0.1756	4650-4849	0.9469	0.1501
4550-4799	-0.5803	0.4975	4650-4849	0.8891	0.2222	4700-4899	0.9751	0.1016
4600-4849	-0.9887	0.0681	4700-4899	-0.7926	0.3172	4750-4949	0.7084	0.3907
4650-4899	0.7888	0.3206	4750-4949	-0.9896	0.0653	4800-4999	-0.8208	0.2911
4700-4949	0.9523	0.1419	4800-4999	0.8270	0.2853	4850-5049	-0.9809	0.0887
4750-4999	0.9593	0.1306	4850-5049	0.8263	0.2859	4900-5099	0.3405	0.6987
4800-5049	0.8371	0.2756	4900-5099	0.7296	0.3726	4950-5149	0.1859	0.8336
4850-5099	0.5844	0.4942	4950-5149	0.2938	0.7390	5000-5199	0.2206	0.8029
4900-5149	0.3675	0.6755	5000-5199	0.3573	0.6842	5050-5249	0.1709	0.8469
4950-5199	0.2901	0.7422	5050-5249	0.1225	0.8900	5100-5299	-0.4133	0.6367
5000-5249	-0.3039	0.7302	5100-5299	-0.5997	0.4815	5150-5349	-0.8386	0.2742
5050-5299	0.1959	0.8247	5150-5349	0.2279	0.7965	5200-5399	-0.3648	0.6779
5100-5349	0.8185	0.2933	5200-5399	0.4533	0.6031	5250-5449	0.1007	0.9095
5150-5399	0.9446	0.1533	5250-5449	0.8128	0.2986	5300-5499	0.4858	0.5759
5200-5449	0.9693	0.1129	5300-5499	0.9431	0.1555	5350-5549	0.8437	0.2692
5250-5499	0.8498	0.2632	5350-5549	0.9690	0.1136	5400-5599	0.9604	0.1288
5300-5549	0.1347	0.8791	5400-5599	0.7888	0.3206	5450-5649	0.9935	0.0514
5350-5599	-0.9882	0.0694	5450-5649	0.0114	0.9897	5500-5699	0.7990	0.3113